



**Synthetic Approaches and Structural Studies of Metal Complexes of
Macrocyclic Ligands Using Sodium Template**

Wanida Wongratchasee

Master of Science Thesis in Organic Chemistry

Prince of Songkla University

2002


T

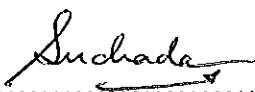
เลขที่	GD79.CA537 W95 2002
Bib Key	292286
	194 D.O. 2547

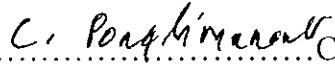
(1)

Thesis Title Synthetic Approaches and Structural Studies of Metal
 Complexes of Macrocyclic Ligands Using Sodium
 Template
Author Miss Wanida Wongratchasee
Major Program Organic Chemistry


Advisory committee

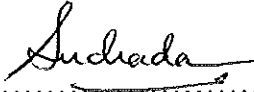

.....Chairman
(Asst. Prof. Dr. Chatchanok Karalai)

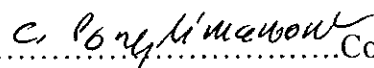

.....Committee
(Asst. Prof. Suchada Chantrapromma)

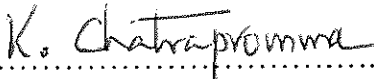

.....Committee
(Asst. Prof. Chanita Ponglimanont)

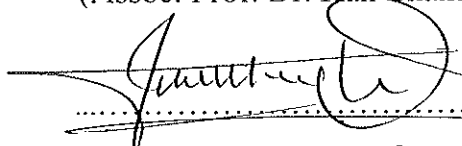
Examining committee


.....Chairman
(Asst. Prof. Dr. Chatchanok Karalai)

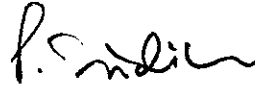

.....Committee
(Asst. Prof. Suchada Chantrapromma)


.....Committee
(Asst. Prof. Chanita Ponglimanont)


.....Committee
(Assoc. Prof. Dr. Kan Chantrapromma)


.....Committee
(Prof. Dr. Hoong-Kun Fun)

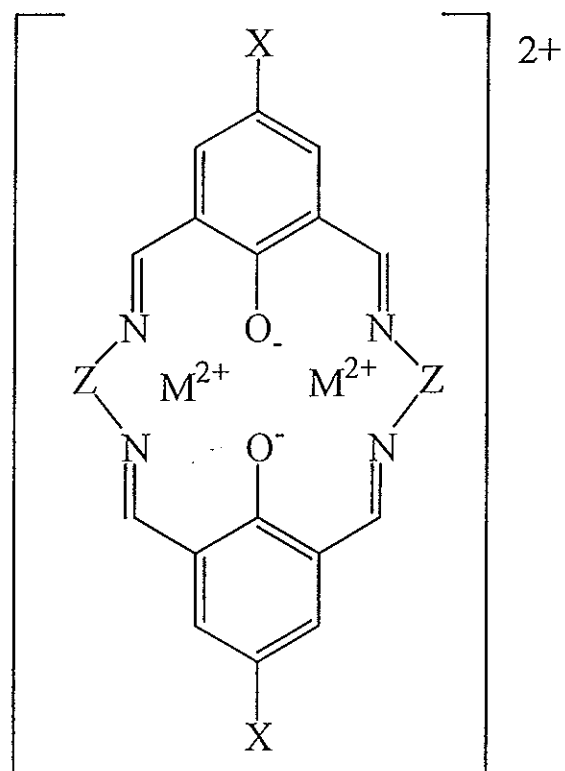
The Graduate School, Prince of Songkla University, has approved this thesis as partial fulfillment of the requirement for the Master of Science degree in Organic Chemistry.


.....
(Piti Trisdikoon, Ph. D.)
Associate Professor and Dean
Graduate School

ชื่อวิทยานิพนธ์ การสังเคราะห์และการศึกษาโครงสร้างของสารประกอบ
 เชิงซ้อนลิแกนด์วงแหวนขนาดใหญ่ โดยอาศัยโซเดียมเป็นต้นแบบ
 ผู้เขียน นางสาวนิตา วงศ์ราชสีห์
 สาขาวิชา เคมีอินทรีย์
 ปีการศึกษา 2545

บทคัดย่อ

ปฏิกิริยา [2+2] cyclocondensation ระหว่างสารประกอบ sodium 4-substituted-2,6-diformylphenoxide และสารประกอบ polyamines ได้แก่ ethylenediamine 1,3-diaminopropane และ 1,4-diaminobutane ได้สารประกอบลิแกนด์วงแหวนขนาด 18 20 และ 22 อะตอม (L^{8-10}) เป็นผลิตภัณฑ์ตามลำดับ แต่อย่างไรก็ตาม เมื่อให้สารประกอบ sodium 4-chloro-2,6-diformylphenoxide ทำปฏิกิริยากับสารประกอบ N^3 -(benzyl)diethylenetriamine-trihydrochloride จะได้สารประกอบ ลิแกนด์วงแหวนขนาด 18 อะตอม (L^{13}) เป็นผลิตภัณฑ์ แทนที่จะได้สารประกอบลิแกนด์วงแหวนขนาด 24 อะตอม (L^{12}) ทั้งนี้เนื่องจากผลของการเกิด ring contraction ของสารประกอบลิแกนด์วงแหวนขนาด 24 อะตอม ลิแกนด์วงแหวนที่สังเคราะห์ได้ทั้งหมดนี้ นำไปทำปฏิกิริยา transmetallation กับไอออนของโลหะหนักของ Cu^{2+} Fe^{2+} Co^{2+} Ni^{2+} Zn^{2+} Pb^{2+} Cd^{2+} หรือ Hg^{2+} ได้ผลึกของสารประกอบเชิงซ้อน binuclear ของโลหะหนักเหล่านี้หลายสาร แต่มีเฉพาะบางตัวเท่านั้นที่สามารถนำไปวิเคราะห์เพื่อยืนยันโครงสร้างโดยอาศัยข้อมูลการเลี้ยวเบนของรังสีเอกซ์ (X-ray) ซึ่งได้แก่สารประกอบเชิงซ้อนของ Cu_2L^8 Ni_2L^8 Cu_2L^{9a} Co_2L^{9a} Cu_2L^9 Cu_2L^{10} Zn_2L^{13} Cd_2L^{13} และ Hg_2L^{13}



Cu_2L^8 X=CH₃ Z=CH₂CH₂ M²⁺ = Cu²⁺ (18-membered ring)

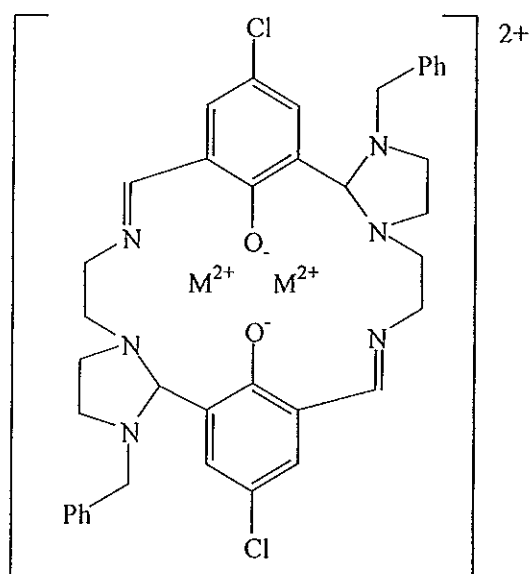
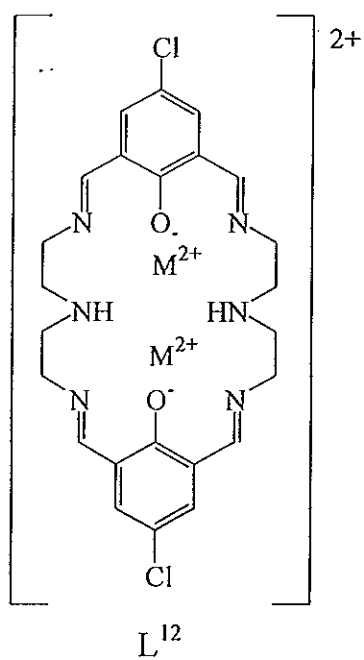
Ni_2L^8 X=CH₃ Z=CH₂CH₂ M²⁺ = Ni²⁺ (18-membered ring)

Cu_2L^{9a} X=CH₃ Z=CH₂CH₂CH₂ M²⁺ = Cu²⁺ (20-membered ring)

Co_2L^{9a} X=CH₃ Z=CH₂CH₂CH₂ M²⁺ = Co²⁺ (20-membered ring)

Cu_2L^{9b} X=Cl Z=CH₂CH₂CH₂ M²⁺ = Cu²⁺ (20-membered ring)

Cu_2L^{10} X=CH₃ Z=CH₂CH₂CH₂CH₂ M²⁺ = Cu²⁺ (22-membered ring)



Zn_2L^{13} $M^{2+} = Zn^{2+}$ (unexpected 18-membered ring)

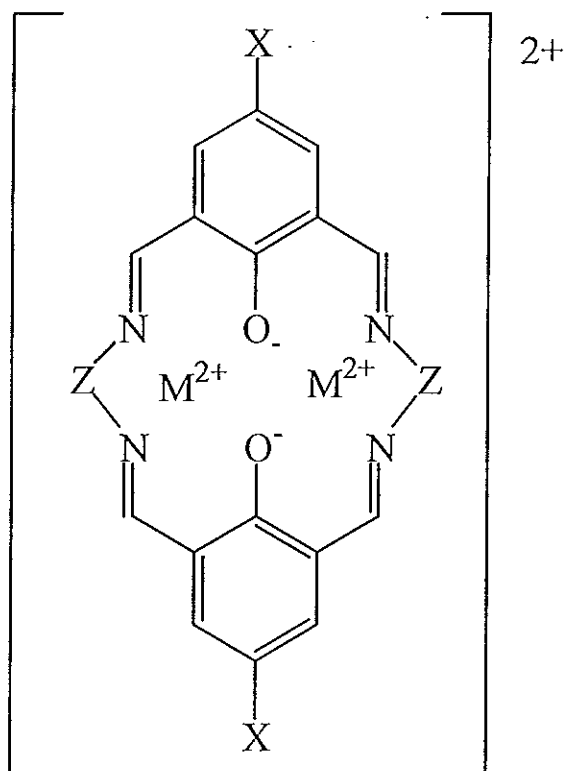
Cd_2L^{13} $M^{2+} = Cd^{2+}$ (unexpected 18-membered ring)

Hg_2L^{13} $M^{2+} = Hg^{2+}$ (unexpected 18-membered ring)

Thesis Title Synthetic Approaches and Structural Studies of Metal
 Complexes of Macrocyclic Ligands Using Sodium
 Template
Author Miss Wanida Wongratchasee
Major Program Organic Chemistry
Academic Year 2002

Abstract

The [2+2] cyclocondensation reaction between sodium 4-substituted-2,6-diformylphenoxide and polyamines gave 18-, 20- and 22-membered ring macrocyclic ligands (L^{8-10}) when polyamine were ethylenediamine, 1,3-diaminopropane, and 1,4-diaminobutane, respectively. However, the reaction between sodium 4-chloro-2,6-diformylphenoxide with N^3 -(benzyl)diethylene triamine-trihydrochloride yielded an unexpected 18-membered ring (L^{13}) macrocyclic ligand instead of a predicted 24-membered ring macrocyclic ligand (L^{12}). The formation of a smaller ring (L^{13}) was proposed to result from a ring contraction of the initial product (L^{12}). All of these compounds were transmetallated with heavy metals such as Cu^{2+} , Fe^{2+} , Co^{2+} , Ni^{2+} , Zn^{2+} , Pb^{2+} , Cd^{2+} or Hg^{2+} to give binuclear metal complex crystals of these macrocyclic ligands. Only some crystals were suitable for confirmation of the structures by X-ray diffraction technique. These crystals are Cu_2L^8 , Ni_2L^8 , Cu_2L^{9a} , Co_2L^{9a} , Cu_2L^{9b} , Cu_2L^{10} , Zn_2L^{13} , Cd_2L^{13} and Hg_2L^{13} .



Cu_2L^8 X=CH₃ Z=CH₂CH₂ M²⁺ = Cu²⁺ (18-membered ring)

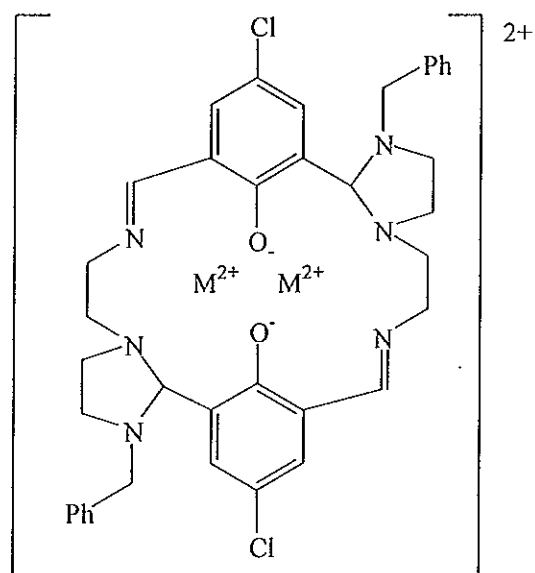
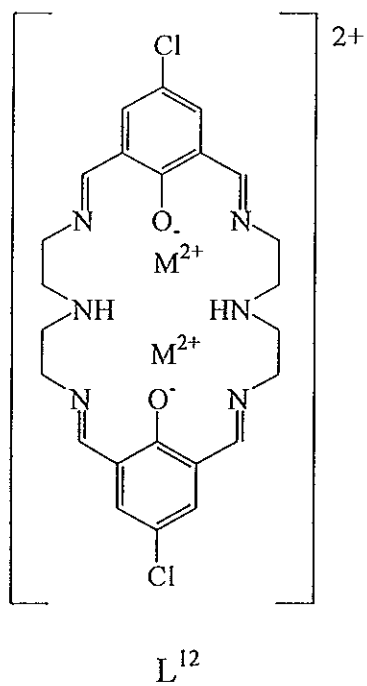
Ni_2L^8 X=CH₃ Z=CH₂CH₂ M²⁺ = Ni²⁺ (18-membered ring)

Cu_2L^{9a} X=CH₃ Z=CH₂CH₂CH₂ M²⁺ = Cu²⁺ (20-membered ring)

Co_2L^{9a} X=CH₃ Z=CH₂CH₂CH₂ M²⁺ = Co²⁺ (20-membered ring)

Cu_2L^{9b} X=Cl Z=CH₂CH₂CH₂ M²⁺ = Cu²⁺ (20-membered ring)

Cu_2L^{10} X=CH₃ Z=CH₂CH₂CH₂CH₂ M²⁺ = Cu²⁺ (22-membered ring)



Zn_2L^{13} $M^{2+} = Zn^{2+}$ (unexpected 18-membered ring)

Cd_2L^{13} $M^{2+} = Cd^{2+}$ (unexpected 18-membered ring)

Hg_2L^{13} $M^{2+} = Hg^{2+}$ (unexpected 18-membered ring)

ACKNOWLEDGEMENT

I wish to express my deepest and sincere gratitude to my supervisor, Assistant Professor Dr. Chatchanok Karalai, for his valuable instructions, expert guidance, excellent suggestions and kindness.

My sincere thanks are expressed to Assistant Professor Suchada Chantrapromma and Assistant Professor Chanita Ponglimanont co-advisors and also to Associate Professor Dr. Kan Chantrapromma for their kindness and valuable advices. Special thanks are addressed to Professor Dr. Hoong-Kun Fun, X-ray Crystallography Unit, School of Physics, Universiti Sains Malaysia, Malaysia for structure determination by single crystal X-ray diffraction.

I would like to extend my appreciation to Mr. Bunsit Watanathai for recording some 60 MHz NMR spectral data.

This research was made possible by a scholarship from Postgraduate Education and Research Program in Chemistry, funded by The Royal Thai Government (PERCH) and the Graduate School, Prince of Songkla University for supporting materials.

Wanida Wongratchasee

CONTENTS

	Page
ABSTRACT (in Thai).....	(3)
ABSTRACT (in English).....	(6)
ACKNOWLEDGEMENT.....	(9)
CONTENTS.....	(10)
LIST OF TABLES.....	(11)
LIST OF ILLUSTRATIONS.....	(12)
LIST OF SCHEMES.....	(16)
CHAPTER	
1 INTRODUCTION.....	1
2 EXPERIMENT.....	27
3 RESULTS AND DISCUSSION.....	51
1. Synthesis of sodium 4-substituted-2,6-diformylphenoxide.....	51
2. Synthesis of disodium macrocyclic ligands.....	56
3. Conclusion.....	98
BIBLIOGRAPHY.....	99
APPENDIX.....	103
VITAE.....	138

LIST OF TABLES

Table	Page
1 Crystal structure data for $\text{Cu}_2\text{L}^8(\text{ClO}_4)_2$	59
2 Crystal structure data for $[\text{Ni}_2\text{L}^8].2\text{ClO}_4$	62
3 Crystal structure data for $[\text{Co}_2\text{L}^{9a}(\text{NO}_3)(\text{CH}_3\text{OH})(\text{H}_2\text{O})].\text{NO}_3$	66
4 Crystal structure data for $[\text{Cu}_2\text{L}^{9a}(\text{H}_2\text{O})_2].2\text{ClO}_4$	69
5 Crystal structure data for $[\text{Cu}_2\text{L}^{9b}(\text{H}_2\text{O})_2].2\text{ClO}_4$	73
6 Crystal structure data for $[\text{Cu}_2\text{L}^{10}].2\text{ClO}_4$	77
7 Crystal structure data for $[\text{Zn}_2\text{L}^{13}(\text{CH}_3\text{COO})_2].1.75(\text{C}_2\text{H}_6\text{O}).0.25\text{H}_2\text{O}$	87
8 Crystal structure data for $\text{Cd}_2\text{L}^{13}(\text{CH}_3\text{COO})_2$	90
9 Crystal structure data for $[\text{Hg}_2\text{L}^{13}(\text{CH}_3\text{COO})_4].4\text{H}_2\text{O}.2\text{CH}_3\text{CH}_2\text{OH}$	93

LIST OF ILLUSTRATIONS

Figure	Page
1 Amphotericin B	2
2 γ -cyclodextrin	2
3 (a) Lunarine and (b) Chaksine	3
4 Bolaamphiphile	4
5 (a) Amphidinolide, (b) and (c) are macrocycles from red algae <i>Phacelocaspus Labillardieri</i>	5
6 Phalloidin	5
7 Schematic representation of the bulkiness of some heteroatoms and the methylene group	10
8 Reaction of 2,6-diacetylpyridine with diethylenetriamine in the presence of a metal cation, the ligands formed depending on the molar ratio of the reactants, the reaction condition and the nature of the cations	18
9 Structure of macrocycle L ⁴ and L ⁵	20
10 Structure of macrocycle L ⁶ and L ⁷	21
11 Crystal structure and conformation of (a) uncomplexed dibenzo-18-crown-6, (b) its complex with rubidium thiocyanate	23
12 Crystal structure and conformation of (a) dibenzo-30-crown-10, (b) its complex with potassium iodide	24
13 Structure of the complex benzo-15-crown-5/Na ⁺ /H ₂ O	24
14 Structure of 2/1 complex formed between benzo-15-crown-5 and potassium iodide	25

LIST OF ILLUSTRATIONS (continued)

Figure	Page
15 Crystal structure of $\text{Cu}_2\text{L}^8(\text{ClO}_4)_2$ ClO_4^- counter ions are not shown	61
16 Crystal structure of $[\text{Ni}_2\text{L}^8].2\text{ClO}_4$ ClO_4^- counter ions are not shown	64
17 Crystal structure of $[\text{Co}_2\text{L}^{9a}(\text{NO}_3)(\text{CH}_3\text{OH})(\text{H}_2\text{O})].\text{NO}_3$ NO_3^- counter ion is not shown	68
18 Crystal structure of $[\text{Cu}_2\text{L}^{9a}(\text{H}_2\text{O})_2].2\text{ClO}_4$ ClO_4^- counter ions are not shown	71
19 Crystal structure of $[\text{Cu}_2\text{L}^{9b}(\text{H}_2\text{O})_2].2\text{ClO}_4$ ClO_4^- counter ions are not shown	75
20 Crystal structure of $[\text{Cu}_2\text{L}^{10}].2\text{ClO}_4$ ClO_4^- counter ions are not shown	79
21 Crystal structure of $[\text{Zn}_2\text{L}^{13}(\text{CH}_3\text{COO})_2].1.75(\text{C}_2\text{H}_6\text{O}).0.25\text{H}_2\text{O}$ Disordered water and ethanol not shown	89
22 Crystal structure of $\text{Cd}_2\text{L}^{13}(\text{CH}_3\text{COO})_2$	92
23 Crystal structure of $[\text{Hg}_2\text{L}^{13}(\text{CH}_3\text{COO})_4].4\text{H}_2\text{O}.2\text{CH}_3\text{CH}_2\text{OH}$ Water and ethanol not shown	95
24 FTIR spectrum (KBr pellets) of 4-chloro-2,6-bis(hydroxymethyl)phenol (9a)	104
25 ^1H NMR spectrum (CD_3Cl) of 4-chloro-2,6-bis(hydroxymethyl)phenol (9a)	105
26 FTIR spectrum (KBr pellets) of 4-chloro-2,6-diformylphenol (10a)	106
27 ^1H NMR spectrum (CDCl_3) of 4-chloro-2,6-diformylphenol (10a)	107

LIST OF ILLUSTRATIONS (continued)

Figure	Page
28 FTIR spectrum (KBr pellets) of 4-chloro-2,6-diformylphenoxide (11a)	108
29 ¹ H NMR spectrum (D ₂ O+CD ₃ COCD ₃) of 4-chloro-2,6-diformylphenoxide (11a)	109
30 FTIR spectrum (KBr pellets) of 4-methyl-2,6-bis(hydroxymethyl)phenol (9b)	110
31 ¹ H NMR spectrum (CDCl ₃) of 4-methyl-2,6-bis(hydroxymethyl)phenol (9b)	111
32 FTIR spectrum (KBr pellets) of 4-methyl-2,6-diformylphenol (10b)	112
33 ¹ H NMR spectrum (CDCl ₃) of 4-methyl-2,6-diformylphenol (10b)	113
34 FTIR spectrum (KBr pellets) of 4-methyl-2,6-diformylphenoxide (11b)	114
35 ¹ H NMR spectrum (D ₂ O) of 4-methyl-2,6-diformylphenoxide (11b)	115
36 FTIR spectrum (KBr pellets) of disodium complexes of macrocyclic ligand L ⁸	116
37 ¹ H NMR spectrum (CDCl ₃ +CD ₃ OD) of disodium complexes of macrocyclic ligand L ⁸	117
38 FTIR spectrum (KBr pellets) of disodium complexes of macrocyclic ligand L ^{9a}	118
39 ¹ H NMR spectrum (CDCl ₃) of disodium complexes of macrocyclic ligand L ^{9a}	119
40 FTIR spectrum (neat) of disodium complexes of macrocyclic ligand L ^{9b}	120

LIST OF ILLUSTRATIONS (continued)

Figure	Page
41 ^1H NMR spectrum (CDCl_3) of disodium complexes of macrocyclic ligand $\text{L}^{9\text{b}}$	121
42 UV spectrum (CHCl_3) of disodium complexes of macrocyclic ligand L^{10}	122
43 FTIR spectrum (neat) of disodium complexes of macrocyclic ligand L^{10}	123
44 ^1H NMR spectrum (CDCl_3) of disodium complexes of macrocyclic ligand L^{10}	124
45 UV spectrum (CHCl_3) of disodium complexes of macrocyclic ligand $\text{L}^{11\text{a}}$	125
46 FTIR spectrum (neat) of disodium complexes of macrocyclic ligand $\text{L}^{11\text{a}}$	126
47 ^1H NMR spectrum (CDCl_3) of disodium complexes of macrocyclic ligand $\text{L}^{11\text{a}}$	127
48 UV spectrum (CHCl_3) of disodium complexes of macrocyclic ligand $\text{L}^{11\text{b}}$	128
49 FTIR spectrum (neat) of disodium complexes of macrocyclic ligand $\text{L}^{11\text{b}}$	129
50 ^1H NMR spectrum (CDCl_3) of disodium complexes of macrocyclic ligand $\text{L}^{11\text{b}}$	130
51 UV spectrum (CH_3OH) of N^3 -(benzyl)diethylenetriamine-trihydrochloride (14)	131

LIST OF ILLUSTRATIONS (continued)

Figure	Page
52 FTIR spectrum (KBr pellets) of N ³ -(benzyl)diethylenetriamine-trihydrochloride (14)	132
53 ¹ H NMR spectrum (D ₂ O) of N ³ -(benzyl)diethylenetriamine-trihydrochloride (14)	133
54 ¹ H NMR spectrum (CDCl ₃) of N ³ -(benzyl)diethylenetriamine (14')	134
55 UV spectrum (CHCl ₃) of disodium complexes of macrocyclic ligand L ¹²	135
56 FTIR spectrum (neat) of disodium complexes of macrocyclic ligand L ¹²	136
57 ¹ H NMR spectrum (CDCl ₃) of disodium complexes of macrocyclic ligand L ¹²	137

LIST OF SCHEMES

Scheme	Page
1 Cyclization	7
2 [1+1] cyclocondensation	8
3 [2+2] cyclocondensation	9
4 Cyclic monomer and cyclic dimer afforded by depolymerization	12
5 Conversion of lactam into an amino-amide with ring enlargement (KAPA reagent = potassium aminopropylamide in 1,3-propanediamine	13
6 Synthesis of cyclic aminoalcohols by electrolytic reduction of bicyclic α -aminoketones	13
7 Some examples of many possibilities for metal-templated cyclization using several structural units	15
8 Condensation of a dicarbonyl (1) with a diamine (2) compound, the macrocyclic products formed depending on the relative overall proportion of (1) and (2), the nature of the reactants (chain length) and the cation used	16
9 Mechanism of ring expansion and contraction for L^2 and L^3	19
10 Mechanism for the formation of $[BaL_8][ClO_4]_2$	22
11 Synthetic diagram of 4-substituted-2,6-diformylphenoxide (a, X = Cl and b, X = CH ₃)	55
12 Synthetic diagram of disodium macrocyclic complexes L^{8-10}	57
13 Synthetic diagram of disodium macrocyclic complexes of L^{11a-12}	80

LIST OF SCHEMES (continued)

Scheme	Page
14 Synthetic diagram of N ³ -(benzyl)diethylenetriamine-trihydrochloride (14)	85
15 Reaction of (14) with aqueous sodium hydroxide	86
16 The formation of 18-membered ring (L ¹³) (pathway I)	96
17 The formation of 18-membered ring (L ¹³) (pathway II)	97

ABBREVIATIONS AND SYMBOLS

<i>s</i>	=	<i>singlet</i>
<i>d</i>	=	<i>doublet</i>
<i>t</i>	=	<i>triplet</i>
<i>q</i>	=	<i>quartet</i>
<i>m</i>	=	<i>multiplet</i>
<i>br s</i>	=	<i>broad singlet</i>
<i>br m</i>	=	<i>broad multiplet</i>
δ	=	<i>chemical shift relative to TMS</i>
<i>J</i>	=	<i>coupling constant</i>
λ_{max}	=	<i>maximum wavelength</i>
ν	=	<i>absorption frequencies</i>
ϵ	=	<i>molar extinction coefficient</i>
MHz	=	Megahertz
ppm	=	parts per million
g	=	gram
$^{\circ}\text{C}$	=	degree Celcius
mp.	=	melting point
cm^{-1}	=	reciprocal centimeter (wave number)
s	=	strong
m	=	medium
w	=	weak
UV	=	Ultraviolet-Visible
IR	=	Infrared
NMR	=	Nuclear Magnetic Resonance

ABBREVIATIONS AND SYMBOLS (continued)

Å	=	angstrom
h	=	hour
TMS	=	tetramethylsilane
CDCl ₃	=	deuteriochloroform
CD ₃ COCD ₃	=	deuteroacetone
CD ₃ OD	=	deuteromethanol
DMSO	=	dimethyl sulphoxide

CHAPTER 1

INTRODUCTION

Macrocyclic ligands have long been the focus of research with interest in the recognition of particular metal ions and for modeling of metallo-biosites. Based on the bonding strength of the ligating group and the cavity of the ring, macrocyclic ligands can combine with metal ions optionally (Gou, *et al.*, 1994). These ligands are more stable than the noncyclic ligands which has a similar sequence of chelate rings. This large increase in stability can be attributed to translational entropy and have been termed as the macrocyclic effect (Cabbiness, *et al.*, 1969). The stability of the complexes is greatly increased despite the more restricted geometry.

Ring system, cyclo (CH₂)_n, can be classified into four groups:

1. small rings n = 3, 4
2. normal rings n = 5, 6, 7
3. medium rings n = 8-11
4. large rings n ≥ 12

The persistent fascination in small rings could be seen in relation to the development of bonding theories. The synthesis of “strained” ring has been a constant challenge for existing theories. Normal rings dated back to the beginning of organic chemistry have been very widely studied. The synthesis of medium and large ring was quite well studied about 50 years ago and certain basic rules in this area were established at that time.

The second half of the 1960s marked the beginning of current macrocyclic chemistry with the realization that macrocyclic structures could give rise to particularly effective and selective complexing agents. This is the case for various natural macrocycles. Many natural substances have a macrocyclic structure whether or not they exhibit complexing properties. A few examples will illustrate its varieties.

Cyclic antibiotics constitute an important class containing an impressive number of members (Figure 1).

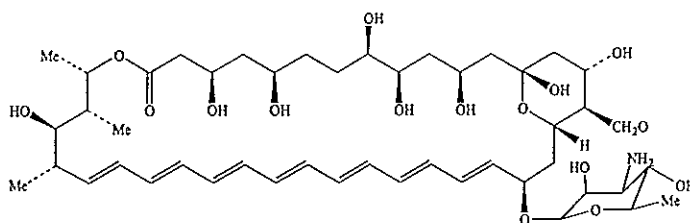


Figure 1 Amphotericin B

Cyclodextrins and certain cyclodextrin derivatives can bind various molecular substrates thus giving rise to reactions which serve as models for certain enzymatic processes (Figure 2)

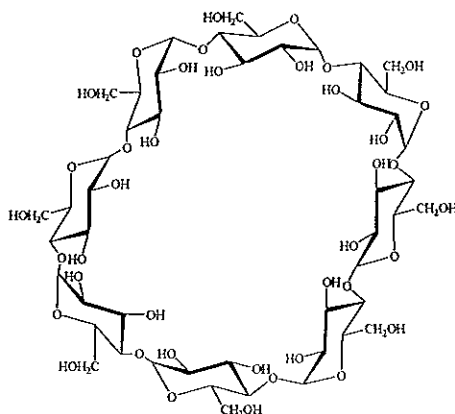
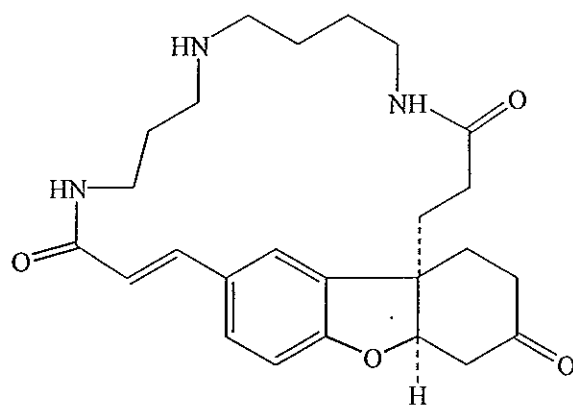
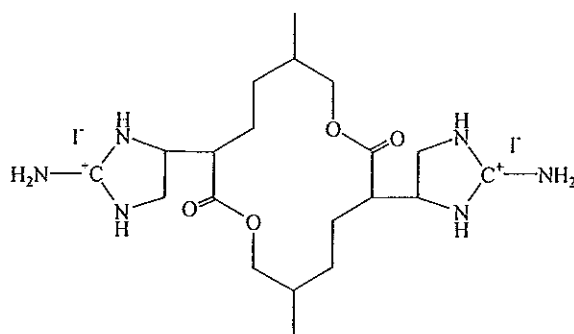


Figure 2 γ -cyclodextrin

Many macrocycles found in living systems are alkaloids, e.g. lunarine, chaksine.



(a)



(b)

Figure 3 (a) Lunarine

(b) Chaksine

Very large macrocycles with bolaamphiphile properties are found in lipidic membranes of bacteria (Figure 4).

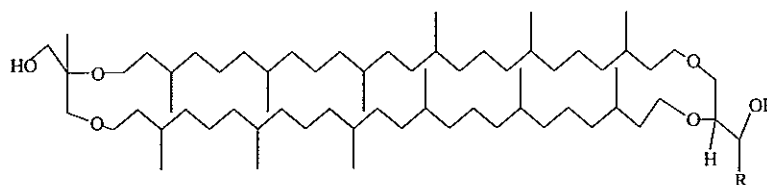
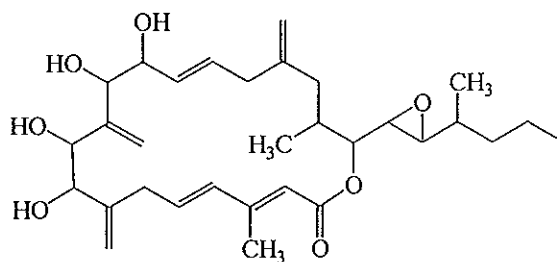
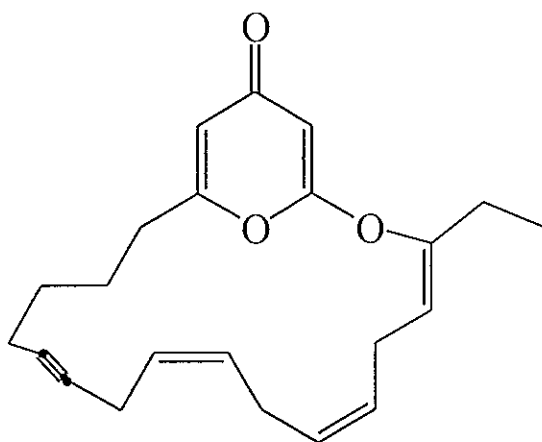


Figure 4 Bolaamphiphile

Marine chemistry has revealed a large number of macrocycles, some of which show interesting antineoplastics. Their structures are sometimes quite surprising (Figure 5).



(a)



(b)

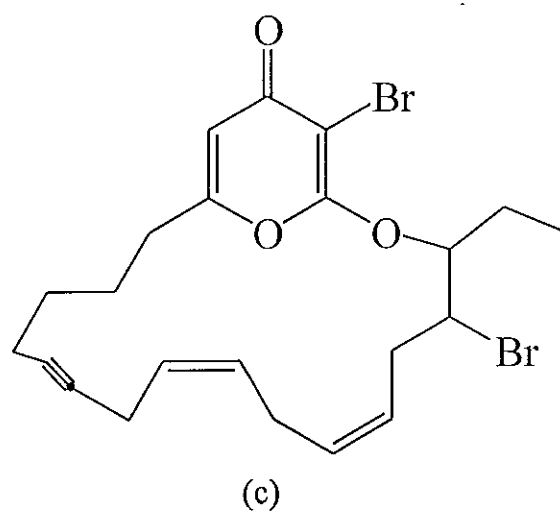


Figure 5 (a) Amphidinolide

(b) and (c) are macrocycles from red algae

Phacelocarpus labillardieri

Some natural macrocycles also exist such as phalloidin obtained from the poisonous toadstool, *Amanita phalloides* (Figure 6).

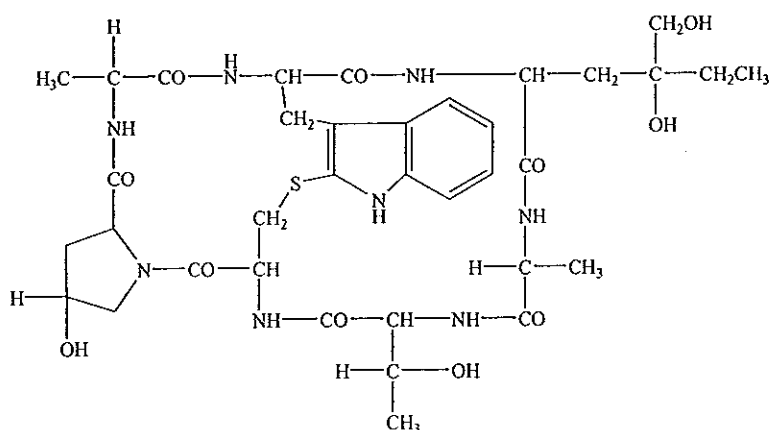


Figure 6 Phalloidin

Because of the rapid increase in the number of known macrocyclic compounds both natural and synthetic, the difficult problem of nomenclature of these substances has arisen.

In the case of natural macrocycles, proposed name often reflects either the natural origin of the product (e.g., phalloidin come from *Amanita phalloides*) or the structural characteristic (e.g., valinomycin contains only one type of amino acid, valine, and is extracted from *Streptomyces fulvissimus*).

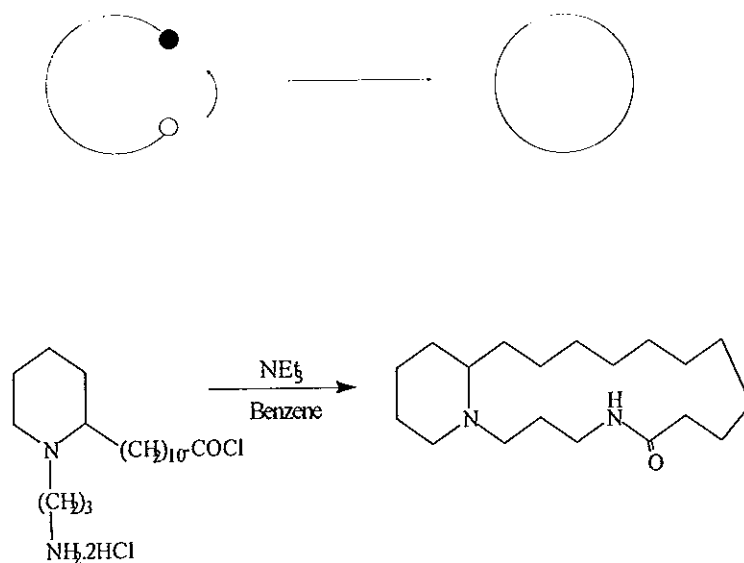
The situation is more delicate for synthetic macrocyclic and macropolycyclic systems. The complexity of the compounds makes official nomenclature (IUPAC) unusable in practice. Simplified nomenclature used in publication, varies according to authors (e.g., [18]crown-6, [18]C-6, [18]<O₆coronand-6>, 18-0-6, etc.).

Macrocycle Synthesis

Formation of macrocycles can be carried out starting from a chain or a group of linear fragments. Whatever the nature of the starting materials or the methods used, the last step is almost invariably connection of the two ends of a chain. However, this chain can either be the starting material itself or result from the *in situ* assembly of bifunctional units.

Several ways of obtaining macrocycles can be envisaged:

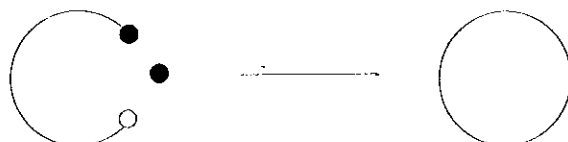
1. simple cyclization (Scheme 1)



Scheme 1 Cyclization

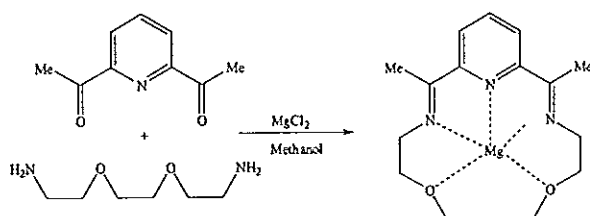
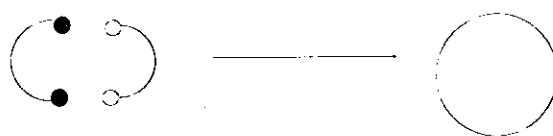
2. cyclization in conjunction with another molecule

(capping)



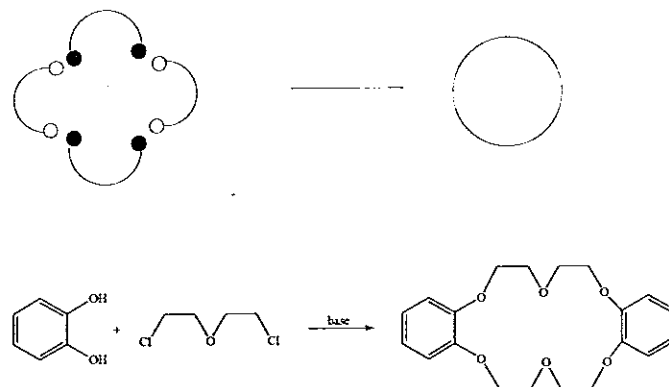
3. condensation

[1+1] condensation (Scheme 2)



Scheme 2 [1+1] cyclocondensation

[2+2] condensation (Scheme 3)



Scheme 3 [2+2] cyclocondensation

The fundamental problem in the synthesis of macrocycles from chains is the cyclization, arising from the intramolecular reaction over end to end linking giving polycondensation. It is therefore necessary to analyse the factors favoring intramolecular reaction: chain length; nature of the atoms and groups from which the chain is made up; type of cyclization, and hence the nature of end groups and experimental techniques.

1. Effect of chain length. The tendency towards cyclization depends on interactions and on the ensuing entropy change $\Delta S < 0$, $\Delta S^\ddagger < 0$ (Liebman, *et al.*, 1976).

2. Effect of the nature of the chain atoms and group on ring formation can be examined in terms of heteroatom and rigid group. The presence of heteroatoms decreases transannular interaction: -O-, -S- and -N-H are groups which are less bulky than CH_2 (Figure 7). Heteroatoms favor formation of rings. Thus, the minimum in the yield profile vs. ring size for cycloalkane formation almost disappears for oxygen-containing medium rings. However, in

large rings the effect of heteroatoms is much less clear-cut since even in their absences, transannular interaction are weak or non existent (Simmons, *et al.*, 1968 and Dietrich, *et al.*, 1969).

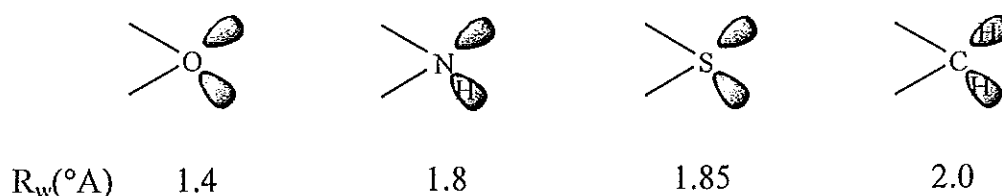


Figure 7 Schematic representation of the bulkiness of some heteroatoms and the methylene group

For rigid group, because of the flexibility of the chains and the greater number of possible conformations with increasing chain length, the probability of intramolecular encounter of the two chain ends decreases as chain length and internal entropy increase. Decrease in internal entropy should therefore favor ring closure, hence come the idea of incorporating rigid groups in order to increase the probability of intramolecular reaction. This principle was initially proposed by Baker's group (Dietrich, *et al.*, 1993), and a more quantitative study has been carried out by Illuminati's group (Illuminati, *et al.*, 1974).

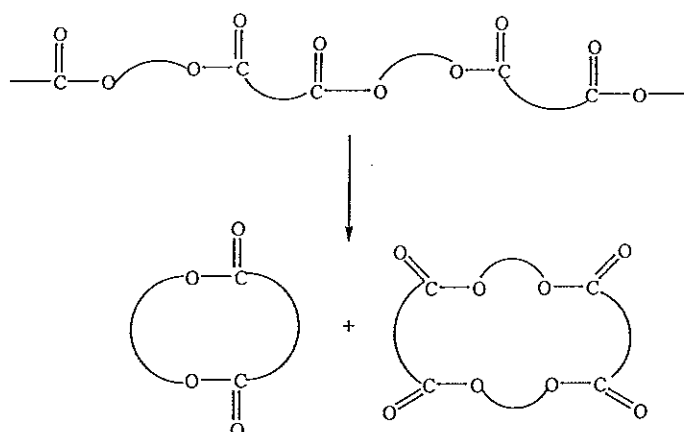
3. Type of cyclization. This type of reaction also affects ring closure yield since the stereochemistry as well as particular reaction features (reactant nature, temperature) are involved. The term cyclization taken in its broadest sense defines any interaction or reaction taking place between two ends of a chain (Winnik, *et al.*, 1981). It depends on chain end proximity. However, the definition of "proximity" depends on the ability of the two to undergo the process envisaged and thus varies with the type of reaction. Cyclization may

occur over a short distance (bond formation and therefore ring closure), a medium distance up to 10 Å (electron transfer), or long distance up to 100 Å (energy transfer).

4. Experimental method for ring closure. Some methods for the formation of macrocycles.

4.1 High dilution technique. A high cyclization yield, must be favored at the expense of polycondensation. The intramolecular ring closure reaction is of first order its rate being proportional to concentration. The intermolecular condensation reaction is second order and therefore its rate is proportional to the square of the concentration. It follows that dilution should favor the intramolecular reaction.

4.2 Depolymerization, the principle of this method has been known for a long time (Hill, *et al.*, 1933), and is used to obtain cyclic products from linear polymers. The method has been principally applied to depolymerization of polyesters prepared by condensation of an ω -hydroxyacid or of an acid with a diol (Scheme 4).

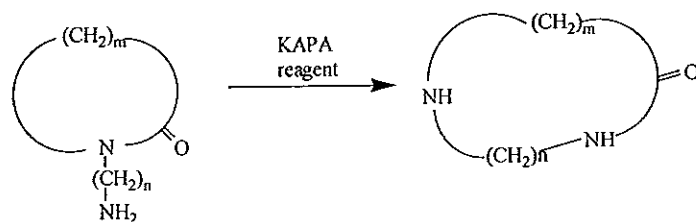


Scheme 4 Cyclic monomer and cyclic dimer
afforded by depolymerization

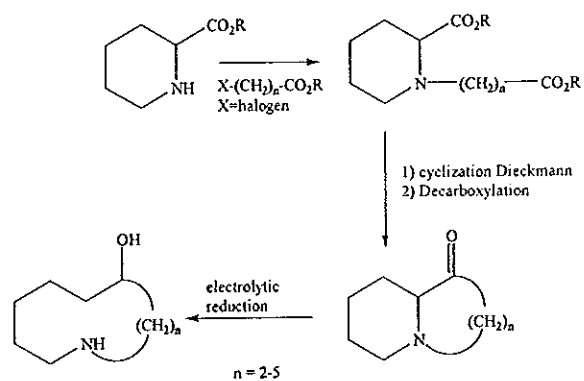
4.3 Templated technique, many cyclization methods are based on the use of a temporary or permanent template, and on specific reactions which depend on the nature of the reacting groups between which the bond leading to ring closure is formed. Cyclization may take place using either an internal or external template (endo- or exo-template). This method can be classified into two groups.

4.3.1 Endo-template

When the formation of a macrocycle is based on a smaller ring which is then ring-enlarged to include all the pre-existing parts of the molecule, the process can be described as occurring by the use of an endo-support. The cyclization on endo-template can be classified into two modes: the “zip” reaction which is a ring expansion by the process of sliding along a side chain (Scheme 5), and cleavage reactions in a bicyclic system (Scheme 6).



Scheme 5 Conversion of a lactam into an amino-amide with ring enlargement (KAPA reagent = potassium aminopropylamide in 1,3- propanediamine)



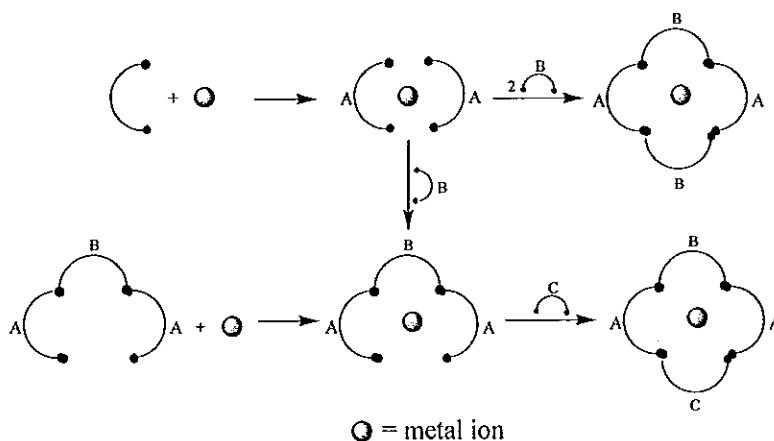
Scheme 6 Synthesis of cyclic aminoalcohols by electrolytic reduction of bicyclic α -aminoketones

4.3.2 Exo-template

A temporary center or group, which may be either ionic or covalent, may be used in cyclization reaction. This serves as a template on which the macrocycle is assembled, and which is subsequently eliminated. Metal cations are by far the oldest-known and most used templates. The metal ion guided the reactants into proper orientation for macrocyclization, this being the "template effect". This method has both advantages and drawbacks. One of the advantages is the increase yield as a result of partial or total inhibition of the competing reaction, polymerization and formation of non-cyclic products. Another advantage is the possibility of selective cyclization. By judicious choice of the metal ion, formation of a desired macrocycle may be encouraged. However, one of the disadvantages is that the macrocycle is generally coordinated to the metal ion and it is sometimes difficult to separate them. Also, the method is often specific for a certain metal ion and cannot be generalized. However, it has proved very useful in spite of these limitation. Two types of processes can be envisaged:

4.3.2.1 The molecules are assembled and become bonded to each other around the cation in a single step.

4.3.2.2 The assembly of one type of unit around the ion followed by bridging by another structural unit (Scheme 7). This method offers more possibilities for synthesis than the first since numerous variants are possible depending on the nature of the end groups.

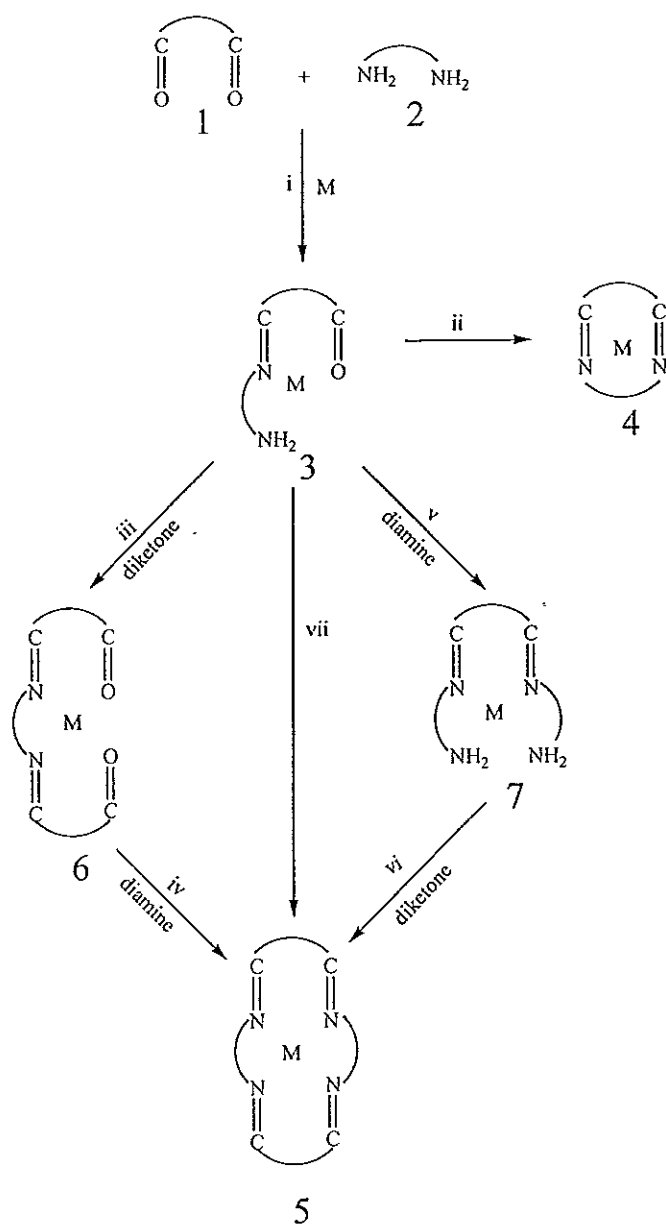


Scheme 7 Some examples of many possibilities for metal-templated cyclization using several structural units

The type of macrocyclic product obtained depends on:

- the constituent molecules: size, reactivity of end groups, rigidity, and geometry,
- the metal cation: size, favored coordination sites, and coordination geometry.

In order to study the mechanisms for formation of Schiff's base and to isolate reaction intermediates, Neson's group (Neson, *et al.*, 1981) undertook a very detailed study of a homologous series for the synthesis of [2+2] macrocyclic ligands between diamine and dicarbonyl compounds. The first aspect covered was the orientation of condensation (Scheme 8).



Scheme 8 Condensation of a dicarbonyl (1) with a diamine (2) compound, the macrocyclic products formed depending on the relative overall proportions of 1 and 2, the nature of the reactants (chain length) and the cations used

From scheme 8, product orientation resulting from condensation either of one molecule of diamine with one of dicarbonyl compound, [1+1], or two molecules of each of the two components, [2+2], depended on the reactants and the template metal (Neson, *et al.*, 1981). The initial step led in all cases to product 3 resulting from the reaction between one molecule of diamine and one molecule of dicarbonyl compound in the presence of metal cation.

Possible routes from 3 were the following:

- Intramolecular condensation leading to the [1+1] product 4.
- If the diamine had insufficient chain length to span the two carbonyl groups, or if it were too rigid to fit by folding, the [2+2] macrocyclic 5 was obtained.
- If the template cation was large in relation to the cavity size of the [1+1] ring, then again the [2+2] compound was formed.

An example of [2+2] macrocyclic ligand is the reaction in methanol between 2,6-diacetylpyridine (1 equivalent) and diethylenetriamine (2 equivalent) in the presence of the salt of an alkaline-earth cation (1 equivalent) which gave at room temperature the complexes $[ML^1]X_2 \cdot xH_2O$ ($X = ClO_4^-$ or NO_3^- , $x = 0$ or 1 and $M = Ba^{2+}$, Sr^{2+} , Ca^{2+} or Mg^{2+}) (Figure 8). When this same reaction was carried out with 1:1:1 reactant mole ratio (and the same cations apart from Mg^{2+}) under reflux, complexes of the L^3 macrocycle were obtained (Drew, *et al.*, 1981).

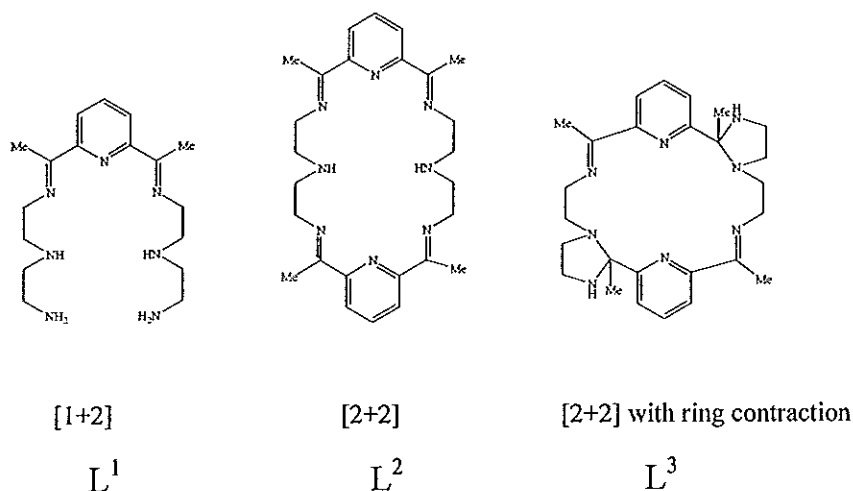
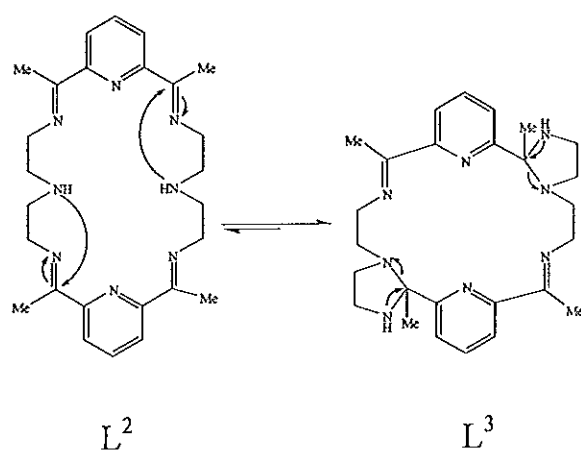


Figure 8 Reaction of 2,6-diacetylpyridine with diethylenetriamine in the presence of a metal cation, the ligands formed depending on the molar ratio of the reactants, the reaction condition and the nature of the cation

The surprising result was the formation of an 18-membered ring (L^3) rather than the expected 24-membered ring (L^2). The structure of the L^3 ligand has been confirmed by X-ray diffraction study of its complex with barium ion. Various experiments have also furnished an explanation for the formation of the L^3 macrocycle and at the same time have enabled the determination of some properties. Heating L^1 complexes (excepting those of Mg^{2+}) in methanol under reflux afforded the macrocycle L^3 complexes and this was in the absence of any other reactant. The L^1 complexes were thus an intermediate in the formation of L^3 .

The L^3 ring cloud was considered as resulting from nucleophilic addition of each of the two secondary amine functional groups in L^2 across a C=N bond at each end of the macrocycle. Then, the two imidazolidine rings were formed and expelled outside the ring which size decreased from being 24- to being 18-membered. The ring expansion and contraction mechanisms are shown in Scheme 9 (Dietrich, *et al.*, 1993.).



Scheme 9 Mechanisms of ring expansion and contraction
for L^2 and L^3

The other example of the ring contraction product was reaction between of 1,3-diamino-2-hydroxypropane and 2,6-diacetylpyridine in the presence of Ba^{2+} (2:2:1 molar ratio) which led to the precipitation of a white powder. Recrystallisation from acetonitrile afforded colorless crystal of the mononuclear complex of the macrocycle L^4 . But the reaction of 1,3-diamino-2-hydroxypropane with 2,6-diacetylpyridine in the presence of Pb^{2+} led to the precipitation of the mononuclear complex of the macrocycle L^5 (Figure 9) (Adams, *et al.*, 1987).

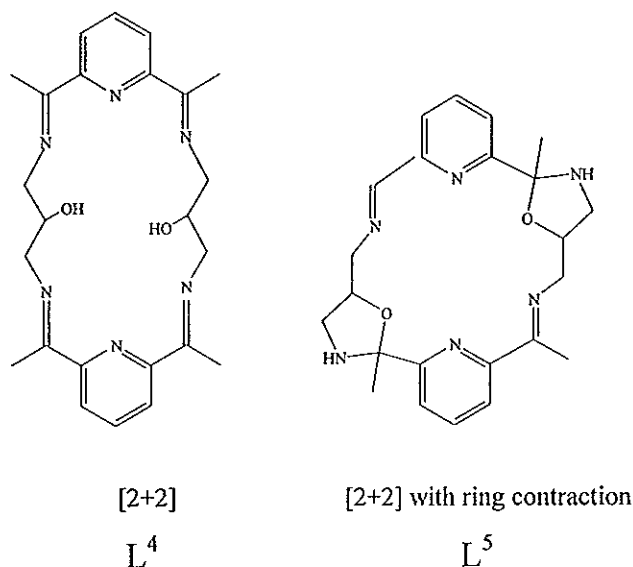


Figure 9 Structure of macrocycle L^4 and L^5

Direct [2+2] condensation of isophthalaldehyde with diethylenetriamine produced an 18-membered macrocycle L^6 , rather than the expected 24-membered macrocycle L^7 . The macrocycle L^6 contained an 18-membered inner ring, two imine bonds, and two 5-membered imidazolidine outer rings (Figure 10) (Menif, *et al.*, 1990).

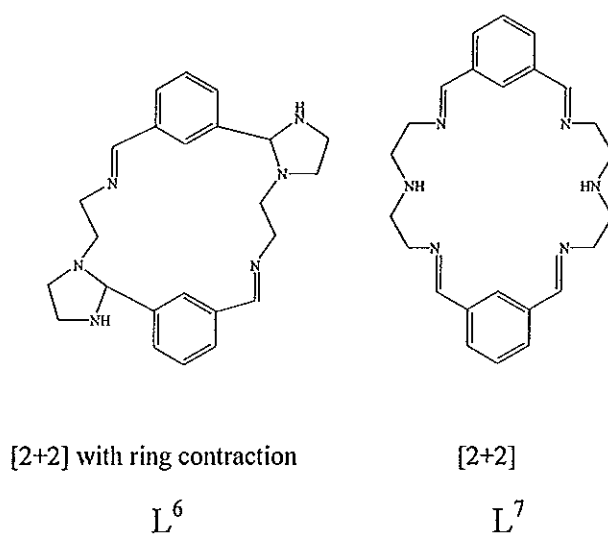
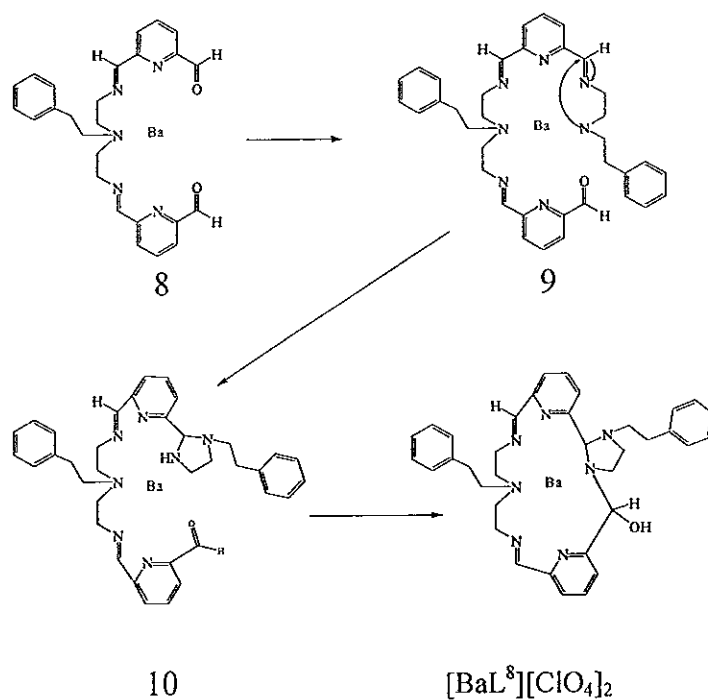


Figure 10 Structure of macrocycle L^6 and L^7

The cyclocondensation reaction between *N,N*-bis(2-aminoethyl)-2-phenylethylamine and 2,6-diformylpyridine in the presence of a barium template gave an unexpected 18-membered macrocyclic product in which a ring contraction at one side-arm had occurred to produce an imidazolidine ring. A mechanism was suggested in Scheme 10. It was assumed that the first condensation reaction was between 2,6-diformylpyridine and *N,N*-bis(2-aminoethyl)-2-phenylethylamine and led to a [2+1] diformyl product 8. This product could then undergo a condensation reaction with *N*-(2-aminoethyl)-2-phenylethylamine to form intermediate 9 which subsequently undergo an intramolecular addition of the secondary amine across the adjacent imine bond to yield the imidazolidine 10. An internal cyclisation via reaction of the imidazolidine NH with the carbonyl group would then yield $[BaL^8][ClO_4]_2$ (Adams, *et al.*, 1996).



Scheme 10 Mechanism for the formation of $[\text{BaL}^8][\text{ClO}_4]_2$

Synthetic Macrocyclic Complexes

Cation complexation is governed by coordination chemistry. The selection of the cation is ensured by a cavity of adequate size, and the bond to the macrocycle arises through the presence of polar interaction sites lining the cavity. The complementarity of the macrocycle cavity (shape, size, number of binding site) and the cationic substrate determine the type of complex.

1. Conformation of the macrocycle

1.1 “Key” and “lock” type complementarity

In this case, the size of the cation and the preformed cavity in the macrocycle are very similar. The cation sits in the center of the cavity. The cation and the cavity correspond like a key and lock. However, the cation

remains accessible from both sides of the macrocycle thus leading to formation of an anion pair. This is so for the complex of dibenzo-18-crown-6 with rubidium thiocyanate (Figure 11). The thiocyanate ion is bound to Rb^+ by its most highly charged site, this being the nitrogen atom (Bright, *et al.*, 1970).

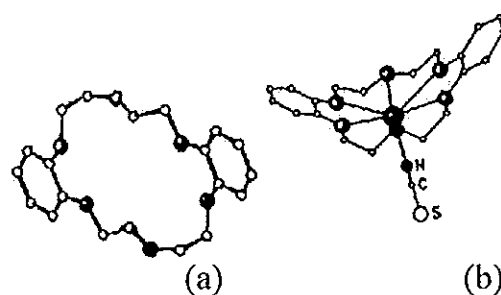


Figure 11 Crystal structure and conformation of
(a) uncomplexed dibenzo-18-crown-6,
(b) its complex with rubidium thiocyanate

1.2 Induced conformational adjustment

In this case, the macrocycle, which is too large for the cation, is extensively reorganized in the latter's dibenzo-30-crown-10 with the potassium iodide. The ligand wraps itself round the cation so forming a three dimensional cavity (Figure 12). The conformation is therefore completely different from that for the free ligand. No ion pair is formed (Bush, *et al.*, 1972).

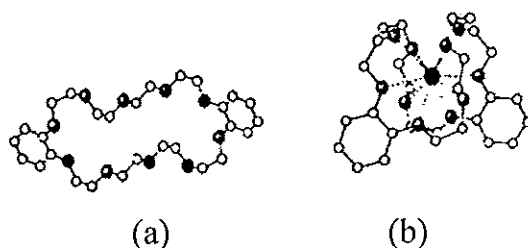


Figure 12 Crystal structure and conformation of
 (a) dibenzo-30-crown-10,
 (b) its complex with potassium iodide

2. Relative sizes of the cation and cavity

Two types of complexes have been observed with the cyclic pentaether benzo-15-O-5 depending on cation sizes:

2.1 The Na^+ cation fits the cavity giving rise to formation of 1/1 complex which crystallizes with one molecule of water. The cation, sitting slightly above the mean plane of the cavity, is coordinated to the five macrocycle oxygen atoms and one molecule of water (w) (Figure 13). The water molecule forms a hydrogen bond with the I^- anion.

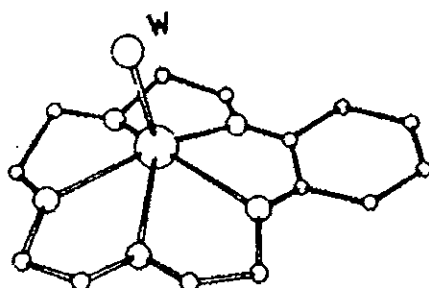


Figure 13 Structure of the complex benzo-15-crown-5/ Na^+ / H_2O

2.2 The K^+ cation is too large to fit the cavity and so a 2/1 sandwich-type complex is formed (Truter *et al.*, 1972) (Figure 14). There is no interaction between the I^- anion and the complexed cation.

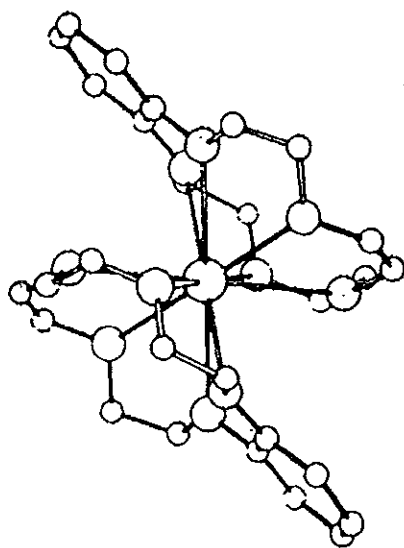


Figure 14 Structure of 2/1 complex formed between benzo-15-crown-5 and potassium iodide

Objectives of this thesis

1. To synthesize the binuclear macrocyclic complexes via Na-template.
2. To synthesize the other metal macrocyclic complexes by transmetallation technique.
3. To determine the structure by spectroscopic technique and confirm by X-ray diffraction.

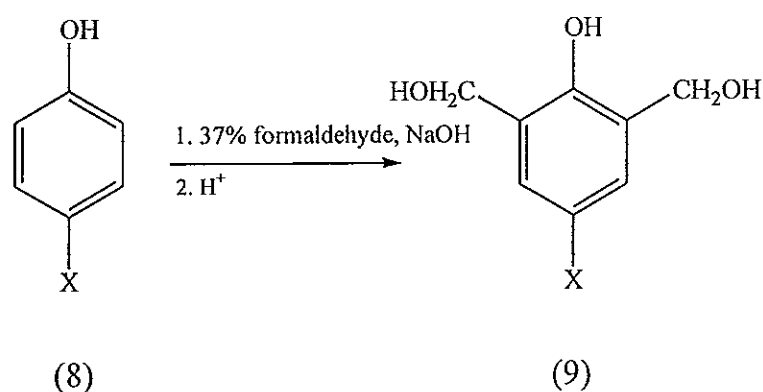
CHAPTER 2

EXPERIMENT

Melting point was recorded in °C and was measured on an Electrothermal melting point apparatus. Proton nuclear magnetic resonance spectra were recorded on a JEOL-PM_x 60 spectrometer with tetramethylsilane (TMS) as internal standard. Chemical shifts were expressed in ppm (δ); multiplicity, *s*=singlet, *d*=doublet, *t*=triplet, *q*=quartet, *quint*=quintet, *m*=multiplet, *br*=broad. Infrared spectra were recorded on a Perkin Elmer GX FTIR spectrophotometer and major bands (ν) were recorded in wave number (cm^{-1}). Ultraviolet (UV) absorption spectra were recorded using UV-160A spectrophotometer (SHIMADZU) and principle bands (λ_{max}) were recorded as wavelengths (nm) and $\log \epsilon$ in methanol and chloroform solution. Single crystal x-ray diffraction measurements were collected using SMART 1-K CCD diffractometer with monochromated Mo-K α radiation ($\lambda=0.71073 \text{ \AA}$) using ω -scan mode and SHELXTL for structural solution and refinement. The yields were reported as percentage of crude products except the yield of dinuclear zinc, cadmium and mercuric complexes were reported as percentage of crystals.

1. Synthesis of sodium 4-substituted-2,6-diformylphenoxide (11a, 11b)

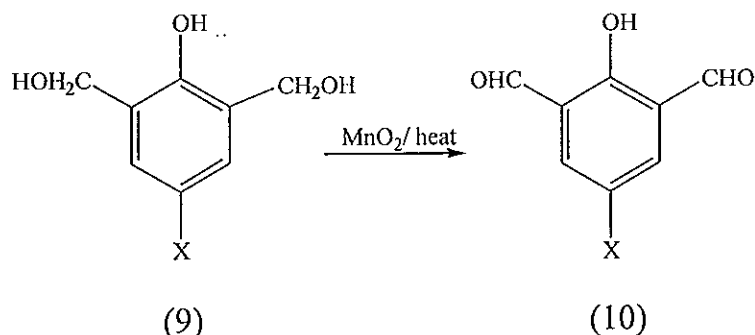
1.1 4-Substituted-2,6-bis(hydroxymethyl)phenol (9a, 9b)



To a mixture of compound (8) (0.30 mol) in 75% aqueous NaOH (20 cm³, 0.37 mol) was added 37% formaldehyde (39 g, 1.90 mol). The mixture was kept and stirred at room temperature for three days. The resulting solids were filtered, washed with saturated aqueous NaCl, dried in vacuum and dissolved in hot water (500 cm³). Then the resulting solution was acidified to pH ~ 4 with 1:2 acetic acid to give the precipitate which was collected and dried (37.40% for X=Cl (9a)). ¹H NMR (CDCl₃) δ: 7.10 (*s*, 2H, *Ar*); 4.80 (*s*, 4H, 2×O-CH₂-); 2.73 (*br s*, OH). IR (KBr pellets, cm⁻¹): 3413s, ν(O-H); 1476s, 1445s, ν(C=C); 1070s, ν(C-O). mp=162-164 °C.

The yield was 55%, for X=CH₃, (9b). ¹H NMR (CDCl₃+CD₃OD) δ: 6.80 (*s*, 2H, *Ar*); 4.67 (*s*, 4H, 2×O-CH₂-); 2.26 (*s*, 3H, CH₃-Ar). IR (KBr pellets, cm⁻¹): 3394s, ν(O-H); 1465s, ν(C=C); 1061s, ν(C-O). mp=127-129 °C.

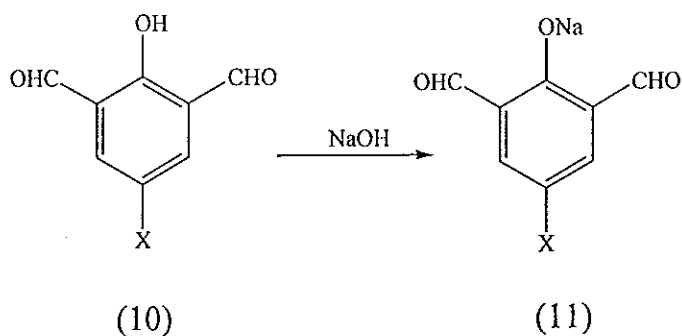
1.2 4-Substituted-2,6-diformylphenol (10a, 10b)



The suspension of freshly activated MnO_2 (90 g) and compound (9) (53.00 mmole) in CHCl_3 (300 cm^3) was stirred under reflux at 60-70 $^\circ\text{C}$ for three days, then MnO_2 was filtered out and washed with CHCl_3 ($3 \times 100 \text{ cm}^3$). The filtrate and the washing solvent were combined. After removing the solvent by rotary evaporator, a yellow product was obtained and kept in a vacuum dessicator (55.08% for $\text{X}=\text{Cl}$ (10a)). $^1\text{H NMR}$ (CDCl_3) δ : 11.63 (*s*, 1H, chelate *OH*, disappear when shake with D_2O); 10.30 (*s*, 2H, $2 \times \text{CHO}$); 7.83 (*s*, 2H, *Ar*). IR (KBr pellets, cm^{-1}): 2840w, $\nu(\text{C-H}$ of aldehyde); 1686s, $\nu(\text{C=O})$; 1579m, 1439m, $\nu(\text{C=C})$. UV (CH_3OH) λ_{max} nm (log ϵ): 226 (4.27), 346 (3.44), 439 (3.20). mp=108-112 $^\circ\text{C}$.

The yield was 34.4% for $\text{X}=\text{CH}_3$ (10b). $^1\text{H NMR}$ (CDCl_3) δ : 11.39 (*s*, 1H, chelate *OH*, disappear when shake with D_2O); 10.10 (*s*, 2H, $2 \times \text{CHO}$); 7.66 (*s*, 2H, *Ar*); 2.36 (*s*, 3H, $\text{CH}_3\text{-Ar}$). IR (KBr pellets, cm^{-1}): 2835w, $\nu(\text{C-H}$ of aldehyde); 1677s, $\nu(\text{C=O})$; 1600s, 1458s, $\nu(\text{C=C})$. UV (CH_3OH) λ_{max} nm (log ϵ): 232 (4.32). mp=98-110 $^\circ\text{C}$.

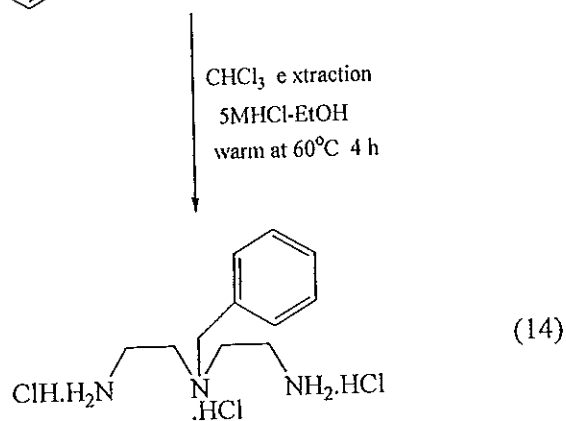
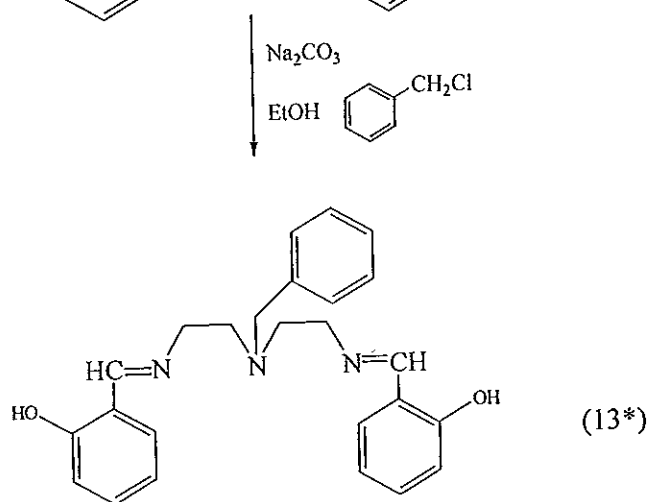
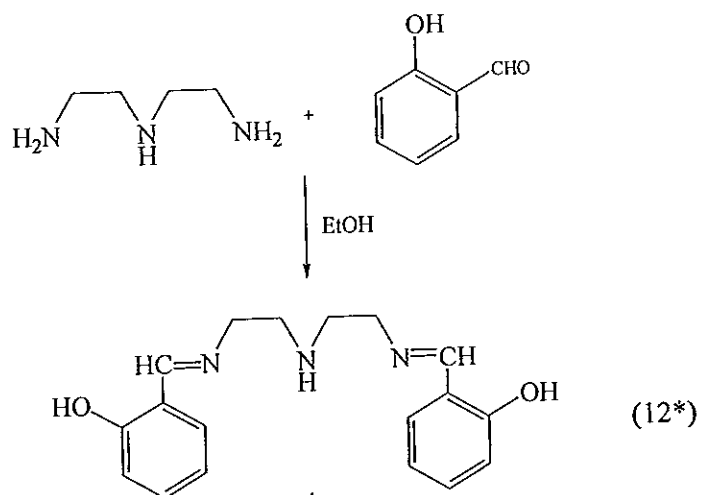
1.3 Sodium 4-substituted-2,6-diformylphenoxide (11a, 11b)



To a solution of compound (10) (38 mmol) in ethanol was added dropwise a solution of 39% aqueous NaOH (4 cm³, 39 mmol). During the addition the color of the mixture was changed from light yellow to dark yellow. The solid product was collected and dried in vacuum (91.80% for X=Cl (11a)). ¹H NMR (D₂O+CD₃COCD₃) δ: 10.00 (*s*, 2H, 2×CHO); 7.60 (*s*, 2H, *Ar*). IR (KBr pellets, cm⁻¹): 2840w, ν(C-H of aldehyde); 1686s, ν(C=O); 1439m, ν(C=C). UV (CH₃OH) λ_{max} nm (log ε): 228 (4.34), 441 (3.79). mp>300 °C.

The yield was 34.4% for X=CH₃ (11b). ¹H NMR (D₂O) δ: 9.90 (*s*, 2H, 2×CHO); 7.43 (*s*, 2H, *Ar*); 2.10 (*s*, 3H, 2×CH₃-Ar). IR (KBr pellets, cm⁻¹): 2838w, ν(C-H of aldehyde); 1674s, ν(C=O); 1515s, ν(C=C). UV (CH₃OH) λ_{max} nm (log ε): 233 (4.28); 347 (3.61), 436 (3.47). mp>300 °C.

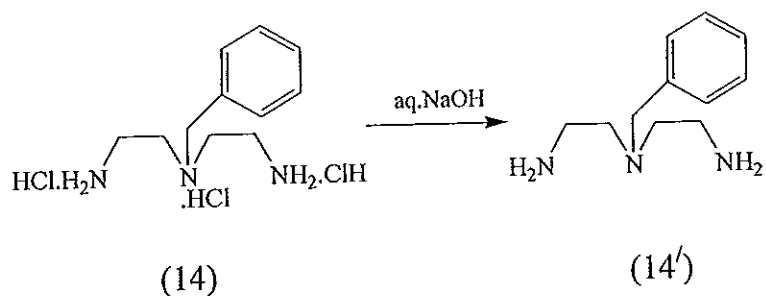
2. Synthesis of N³-(benzyl)diethylenetriamine-trichloride (14)



* unisolated product

A mixture of diethylenetriamine (20 mmol) and salicylaldehyde (40 mmol) in absolute ethanol (200 cm³) was refluxed 40 min. The golden yellow solution was cooled to room temperature, and benzyl chloride (20 mmol) and Na₂CO₃ (28.3 mmol) were added. The solution was refluxed for 36 h. Upon cooling to room temperature, the excess Na₂CO₃ was filtered off and the filtrate was evaporated to dryness under vacuum to give a residue (red oil), which was dissolved in CHCl₃ (50 cm³). The resulting solution was washed with water (3×50 cm³), dried over anhydrous Na₂SO₄ and filtered. After the solvent was evaporated under reduced pressure, the residue was acidified with 5 M HCl–EtOH (60 cm³) and the resulting mixture was warmed at 60 °C for 4 h. The mixture was filtered and the precipitate was recrystallized from aqueous ethanol to give trihydrochloride salt of compound (14) as plate crystals (11.17%). ¹H NMR (D₂O) δ: 7.70 (*s*, 5H, *Ar*); 4.30 (*s*, 2H, CH₂-*Ar*); 3.60 and 3.53 (*s* and *m*, 8H, 2×N-CH₂-CH₂-NH₂). IR (KBr pellets, cm⁻¹): 2939s-2896s, ν(-⁺NH₃); 2754s-2674s, ν(-⁺NH); 1539m, 1478, ν(C=C). UV (CH₃OH) λ_{max} nm(log ε): 208 (3.35). mp=264-270 °C.

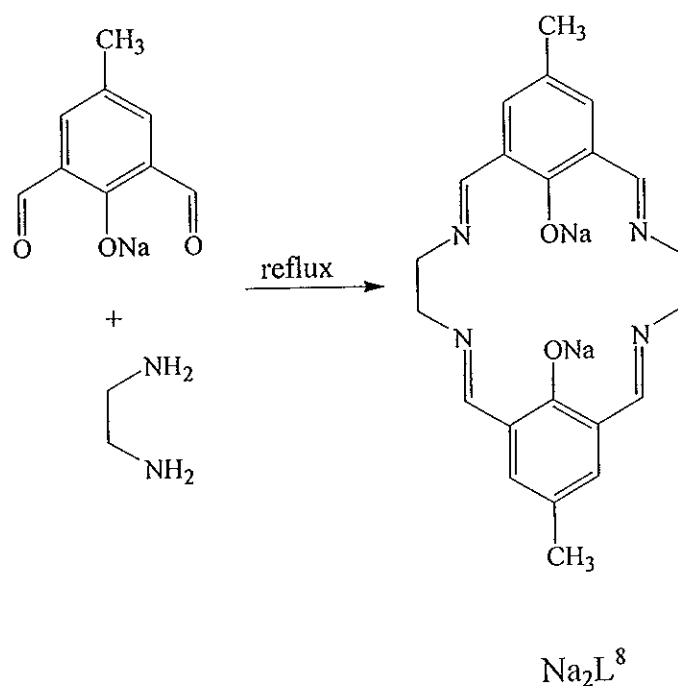
N³-(benzyl)diethylenetriamine (14')



Compound (14) was dissolved in water and basified with aqueous NaOH. The mixture was extracted with ethyl acetate. The organic solvent was removed to yield liquid N³-(benzyl)diethylenetriamine compound (14'). ¹H NMR (CHCl₃) δ: 7.20 (*s*, 5H, *Ar*); 3.70 (*s*, 2H, CH₂-*Ar*); 2.60 (*m*, 8H, N-CH₂-CH₂-NH₂); 1.80 (*s*, 4H, -NH). IR (neat, cm⁻¹): 3303s, ν(N-H); 2936s, ν(C-H); 1586m, 1495, ν(C=C).

3. Synthesis of dinuclear complexes of macrocyclic ligands

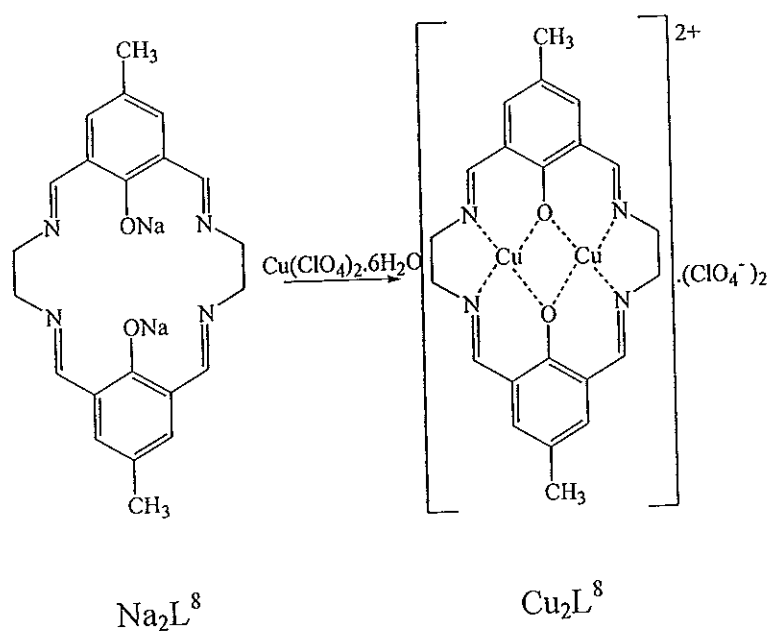
3.1 Disodium complex of macrocyclic ligand L⁸



A solution of ethylenediamine (1 mmol) in ethanol (4 cm³) was added slowly to a suspension of sodium 4-methyl-2,6-diformylphenoxide (1 mmol) in ethanol (30 cm³). The mixture was stirred under reflux for 1 h under nitrogen. The resulting yellow solid was filtered out and dried under vacuum (59%). ¹H NMR (CDCl₃+CD₃OD) δ: 8.36 (s, 4H, 4×CH=N), 7.33 (s, 4H, 4×Ar), 3.96 (s, 8H, 2×N-CH₂-CH₂-N), 2.20 (s, 6H, 2×CH₃-Ar). IR (KBr pellets, cm⁻¹): 3421s, ν(O-H); 2912w, ν(C-H); 1639s, ν(C=N); 1527m, 1458m, ν(C=C). mp>250 °C.

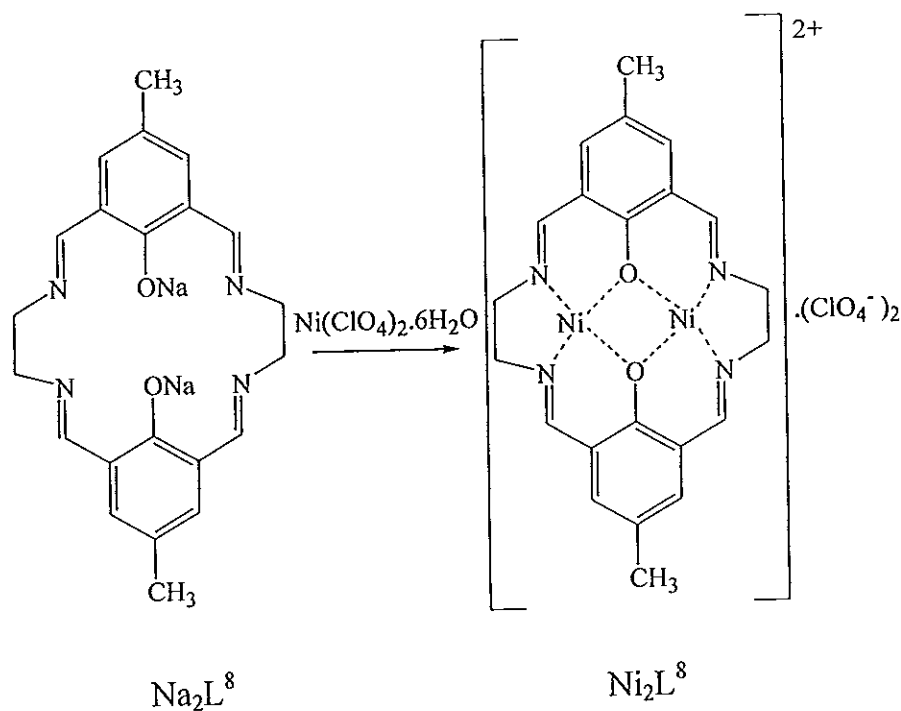
3.1.1 Transmetalation (Na-metal exchange) of Na_2L^8

3.1.1.1 Dinuclear copper (II) macrocyclic complex of L^8



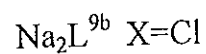
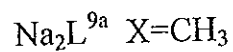
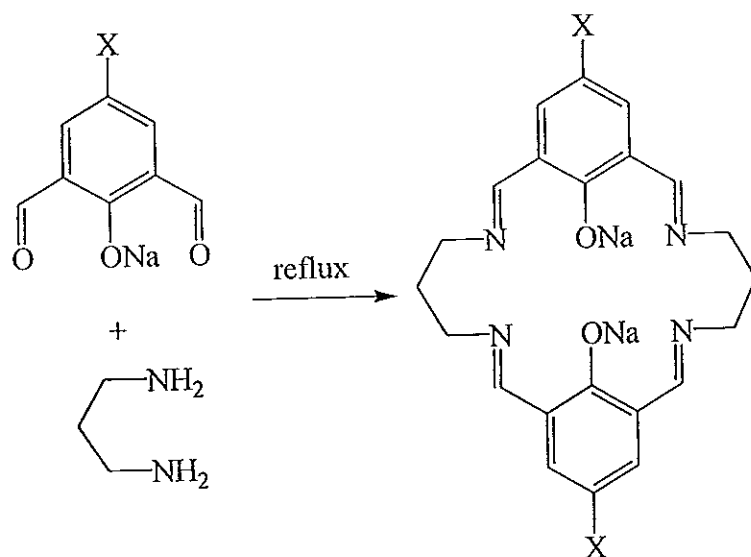
The mixture of Na_2L^8 (0.24 mmol) and copper perchlorate (0.50 mmol) in ethanol (25 cm^3) was refluxed and stirred for 1 h under nitrogen and the resulting suspension was then filtered. The crude solid obtained (25.81%) was further purified by recrystallisation using CH_3CN - MeOH as mixed solvent to give crystallized solid: mp=188-198 °C, IR (KBr pellets, cm^{-1}): 1624s, $\nu(\text{C}=\text{N})$; 1544m, 1442m, $\nu(\text{C}=\text{C})$. A reddish-brown cubic-shaped crystal was selected for X-ray structure determination.

3.1.1.2 Dinuclear nickel (II) macrocyclic complex of L⁸



The mixture of Na_2L^8 (0.28 mmol) and nickel perchlorate (0.58 mmol) in ethanol (25 cm^3) was refluxed with stirring for 1 h in an inert atmosphere. After the reaction was complete, the resulting suspension was filtered. The crude solid obtained (70.43%) was purified by recrystallisation using H_2O - MeOH as mixed solvent to yield crystallized solid as reddish brown needle: mp=198-204 °C, IR (KBr pellets, cm^{-1}): 3404m, $\nu(\text{O-H})$; 1638s, $\nu(\text{C=N})$; 1459s, $\nu(\text{C=C})$. A reddish-brown needle-shaped crystal was used for the X-ray crystallographic study.

3.2 Disodium complex of macrocyclic ligand L^{9a-9b}



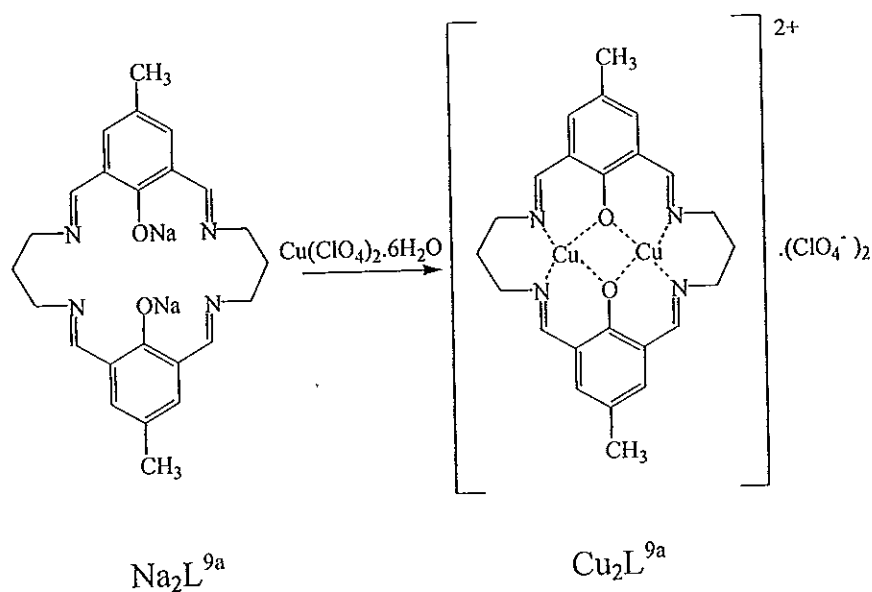
A solution of 1,3-diaminopropane (1 mmol) in ethanol (4 cm³) was added slowly to a suspension of sodium 4-substituted-2,6-diformylphenoxide (1 mmol) in ethanol (30 cm³). The mixture was stirred under reflux for 1 h under nitrogen. The resulting yellow solid was filtered and dried under vacuum.

The yield was 80% for Na₂L^{9a}. ¹H NMR (CDCl₃) δ: 8.40 (s, 4H, 4×CH=N), 7.30 (s, 4H, 4×Ar), 3.66 (t, J=6 Hz, 8H, 2×N-CH₂-CH₂-CH₂-N), 2.20 (s, 6H, 2×CH₃-Ar), 2.33-1.80 (m, 4H, 2×N-CH₂-CH₂-CH₂-N). IR (KBr pellets, cm⁻¹): 1630s, ν(C=N); 1518s, 1459m, ν(C=C). mp>210 °C (decompose).

The yield was 54% for Na₂L^{9b}. ¹H NMR (CDCl₃) δ: 8.36 (s, 4H, 4×CH=N), 7.46 (s, 4H, 4×Ar), 3.74 (t, 8H, J=6 Hz, 8H, 2×N-CH₂-CH₂-CH₂-N), 2.40-1.86 (m, 4H, 2×N-CH₂-CH₂-CH₂-N). IR (neat, cm⁻¹)δ: 1638s, ν(C=N); 1435m, ν(C=C). mp=160-170 °C.

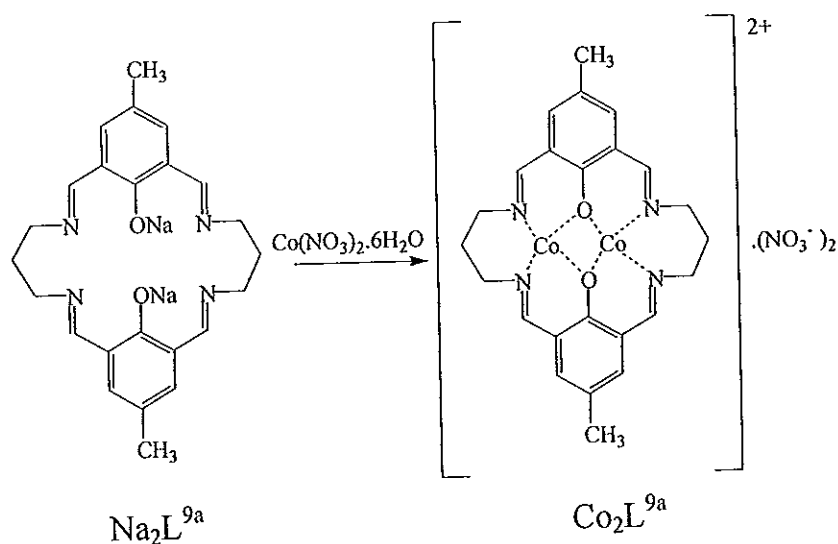
3.2.1 Transmetallation (Na-metal exchange) of Na_2L^{9a}

3.2.1.1 Dinuclear copper (II) macrocyclic complex of L^{9a}



The mixture of Na_2L^{9a} (0.20 mmol) and copper perchlorate (0.41 mmol) in ethanol (25 cm³) was refluxed under nitrogen for 1 h, then the resulting suspension was filtered. The crude solid obtained (76.70%) was purified by recrystallisation using H₂O-MeOH as mixed solvent to give crystals mixed with its powder: mp > 300 °C, IR (KBr pellets, cm⁻¹): 1639s, ν(C=N); 1571m ν(C=C). A green needle-shaped crystal was selected for X-ray structure determination.

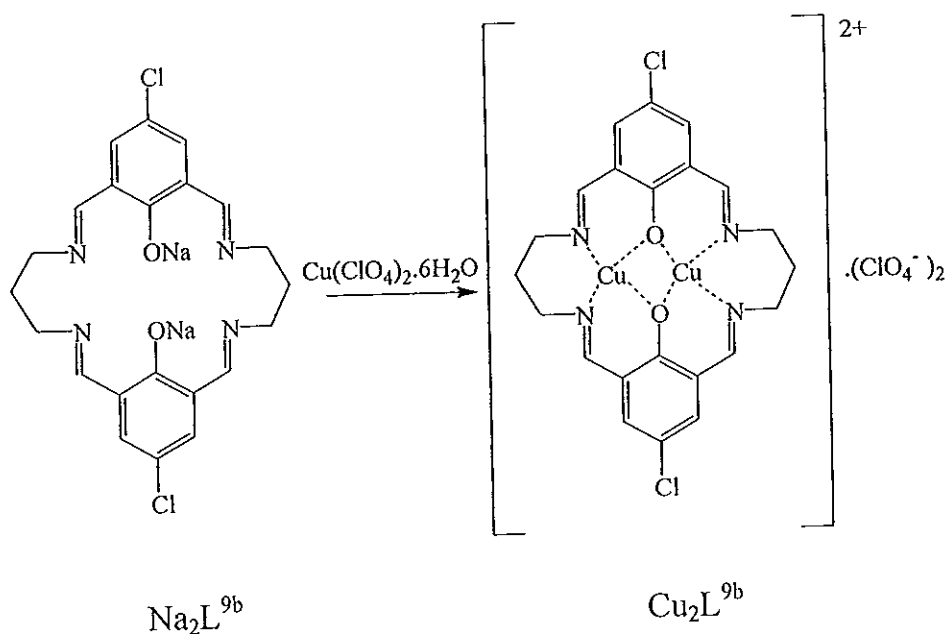
3.2.1.2 Dinuclear cobalt (II) macrocyclic complex of L^{9a}



The mixture of Na_2L^{9a} (0.24 mmol) and cobalt nitrate (0.47 mmol) in ethanol (25 cm³) was refluxed for 1 h under nitrogen. After the reaction was completed, the resulting suspension was filtered to give a crude solid (21.45%) which was further recrystallized from EtOH-MeOH. The product obtained has mp=118-120 °C, IR (KBr pellets, cm⁻¹): 3420m, $\nu(\text{O-H})$; 2916w, $\nu(\text{C-H})$; 1630s, $\nu(\text{C=N})$; 1547m $\nu(\text{C=C})$. A reddish-brown cubic-shaped crystal was used for X-ray structure determination.

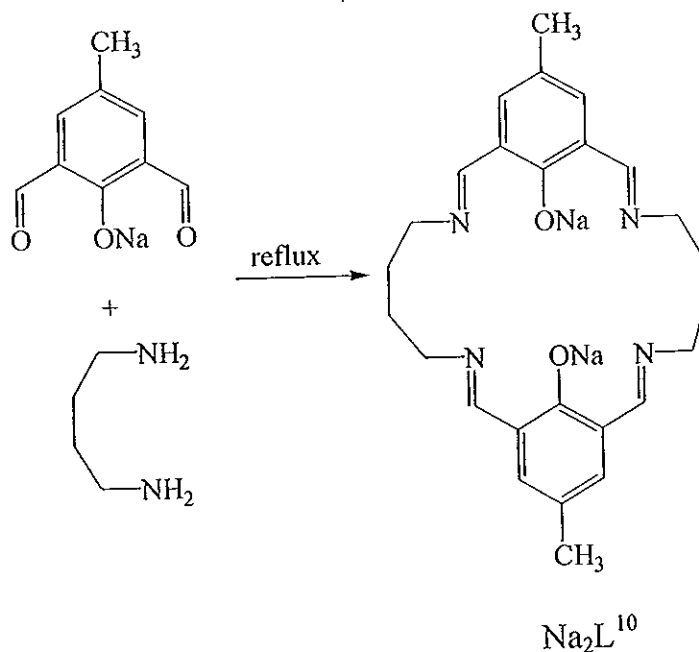
3.2.2 Transmetalation (Na-metal exchange) of Na_2L^{9b}

3.2.2.1 Dinuclear copper (II) macrocyclic complex of L^{9b}



The mixture of Na_2L^{9b} (0.13 mmol) and copper perchlorate (0.26 mmol) in ethanol (25 cm^3) was refluxed and stirred for 1 h in an inert atmosphere and the resulting suspension was then filtered. The crude solids obtained (73.31%) were further purified by recrystallisation using H_2O -EtOH-MeOH as mixed solvent to give crystallized solids: mp=138-142 °C, IR (KBr pellets, cm^{-1}): 3451m, $\nu(\text{O-H})$; 1639s, $\nu(\text{C=N})$; 1559s, $\nu(\text{C=C})$; 1088s, $\nu(\text{O-C})$. A green needle-shaped crystal was selected for X-ray structure determination.

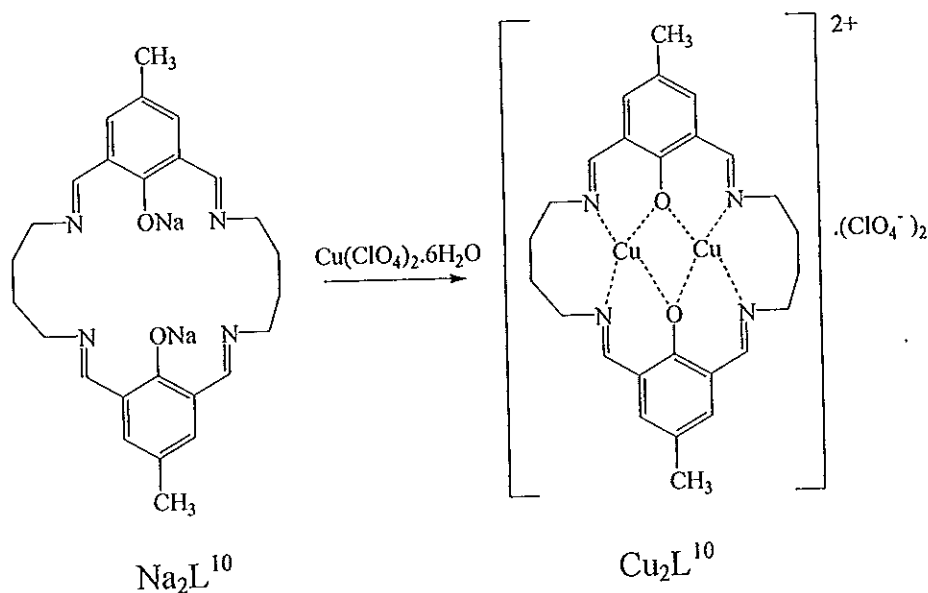
3.3 Disodium complex of macrocyclic ligand L¹⁰



To a suspension of sodium 4-methyl-2,6-diformylphenoxide (1 mmol) in ethanol (30 cm³) under nitrogen atmosphere was added slowly a solution of 1,4-diaminobutane (1 mmol) in ethanol (2 cm³). The mixture was stirred under reflux for 1 h and the solvent was removed under reduced pressure to give the residue, which was dissolved in chloroform. The resulting mixture was washed with saturated NaHCO₃ (30 cm³), water (3×30 cm³), and dried with anhydrous Na₂SO₄. The organic solvent was removed by rotary evaporator to yield viscous oil (73.28%). ¹H NMR (CDCl₃) δ: 8.63 (*s*, 4H, 4×CH=N); 7.37 (*s*, 4H, 4×Ar); 3.60 (*br m*, 8H, 2×N-CH₂-CH₂-CH₂-CH₂-N); 2.30 (*s*, 3H, 2×CH₃-Ar); 1.81 (*br m*, 8H, 2×N-CH₂-CH₂-CH₂-CH₂-N). IR (neat, cm⁻¹): 2923m, ν(C-H); 1640s, ν(C=N); 1600s, 1462w, ν(C=C). UV (CHCl₃) λ_{max} nm (log ε): 248 (5.27); 350 (3.66).

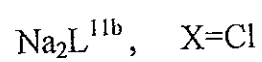
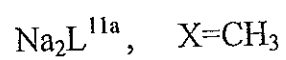
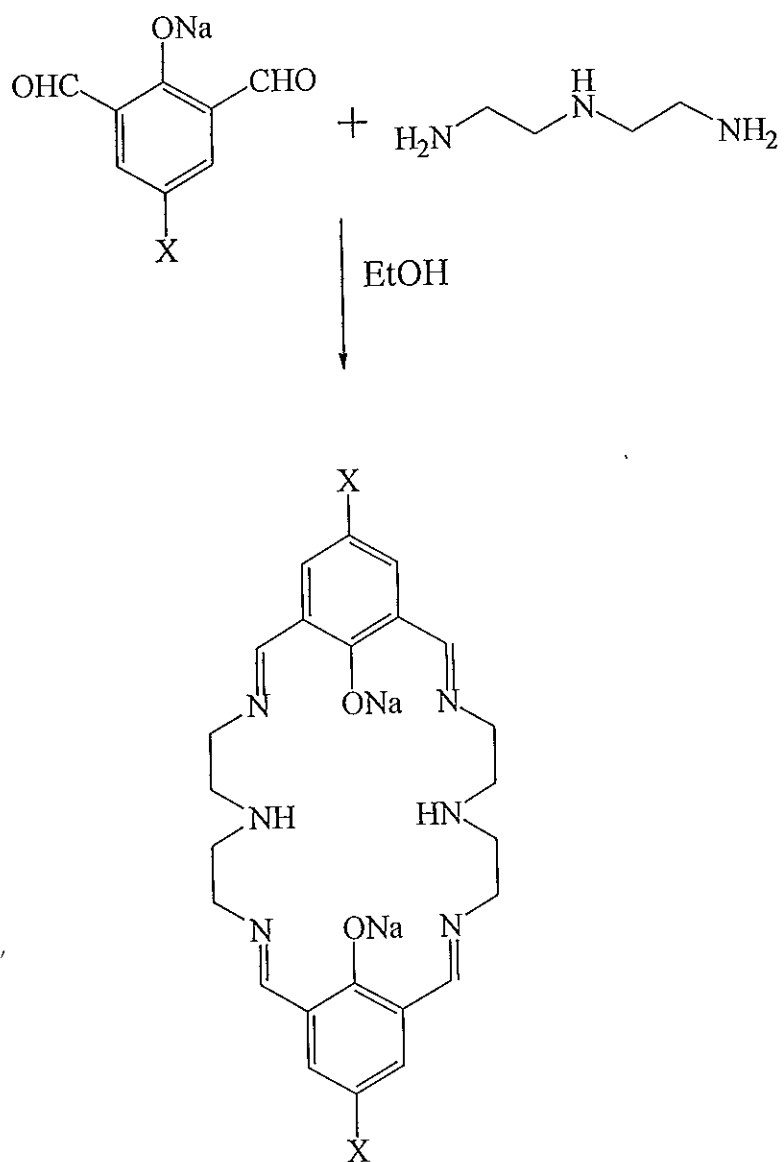
3.3.1 Transmetalation (Na-metal exchange) of Na_2L^{10}

3.3.1.1 Dinuclear copper (II) macrocyclic complex of L^{10}



The mixture of Na_2L^{10} (0.71 mmol) and copper perchlorate (1.51 mmol) in ethanol (25 cm^3) was refluxed under nitrogen. After the reaction was refluxed for 1 h, the resulting suspension was filtered. The crude solid obtained (62.15%) was purified by recrystallisation using EtOH-MeOH as mixed solvent to give crystallized solids: mp > 300 °C, IR (KBr pellets, cm^{-1}): 3444w, $\nu(\text{O-H})$; 1633s, $\nu(\text{C=N})$; 1563s, $\nu(\text{C=C})$. A green crystal was selected for X-ray structure determination.

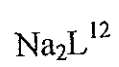
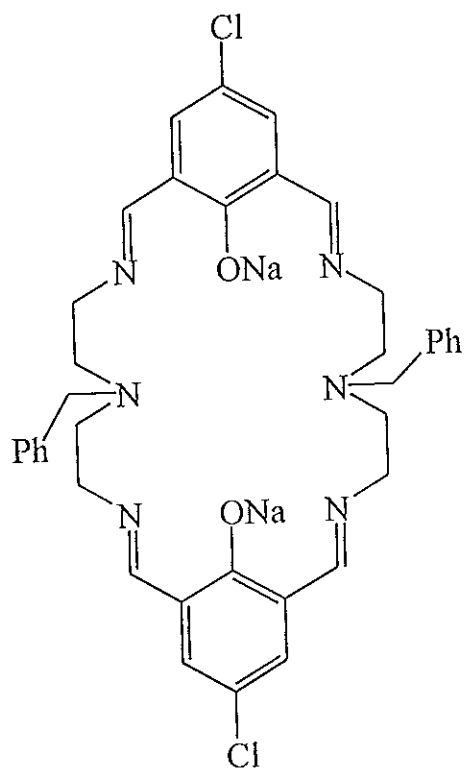
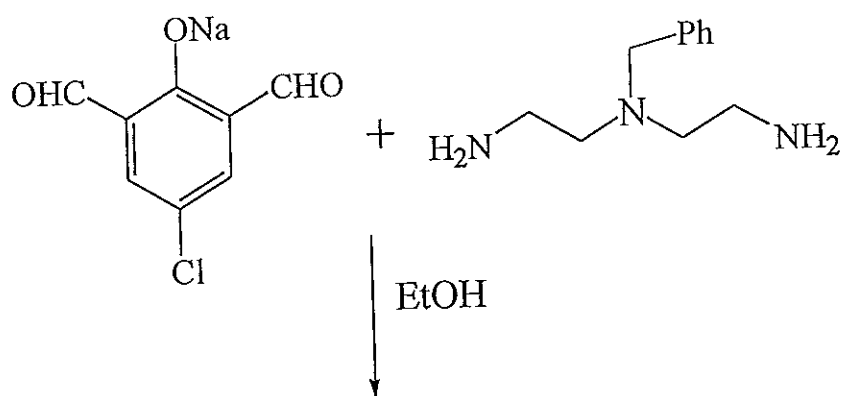
3.4 Disodium complex of macrocyclic ligand L^{11a-11b}



A solution of diethylenetriamine (1.00 mmol) in ethanol (4 cm³) was added slowly to a suspension of sodium 4-substituted-2,6-diformylphenoxide (1 mmol) in ethanol (30 cm³) under nitrogen atmosphere. The mixture was stirred under reflux for 1 h, then the solvent was removed under reduced pressure to give the residue which was dissolved in chloroform. The resulting mixture was washed with saturated NaHCO₃ (30 cm³), water (3 x 30 cm³), and dried with anhydrous Na₂SO₄. The organic solvent was removed by rotary evaporator to yield viscous oil (69% for X=CH₃ (Na₂L^{11a})). ¹H NMR (CDCl₃) δ: 8.10 (*br m*, 4H, 4xCH=N), 7.20 (*s*, 4H, 4xAr), 3.50 (*br m*, 8H, 2xN-CH₂-CH₂-N-CH₂-CH₂-N), 2.80 (*br m*, 8H, 2xN-CH₂-CH₂-N-CH₂-CH₂-N), 2.10 (*s*, 6H, 2xCH₃-Ar). IR (neat, cm⁻¹): 2915m, ν(C-H); 1633s, ν(C=N); 1601s, ν(C=C). UV (CHCl₃) λ_{max} nm (log ε): 241 (4.20), 224 (4.07).

The yield was 70% for X=Cl (Na₂L^{11b}). ¹H NMR (CDCl₃) δ: 8.10 (*br m*, 4H, 4xCH=N), 7.60 (*br m*, 4H, 4xAr), 3.60 (*br m*, 8H, 2xN-CH₂-CH₂-N-CH₂-CH₂-N), 2.90 (*br m*, 8H, 2xN-CH₂-CH₂-N-CH₂-CH₂-N). IR (neat, cm⁻¹): 2934m, ν(C-H); 1636s, ν(C=N); 1442m, ν(C=C). UV (CHCl₃) λ_{max} nm (log ε): 227 (4.10)

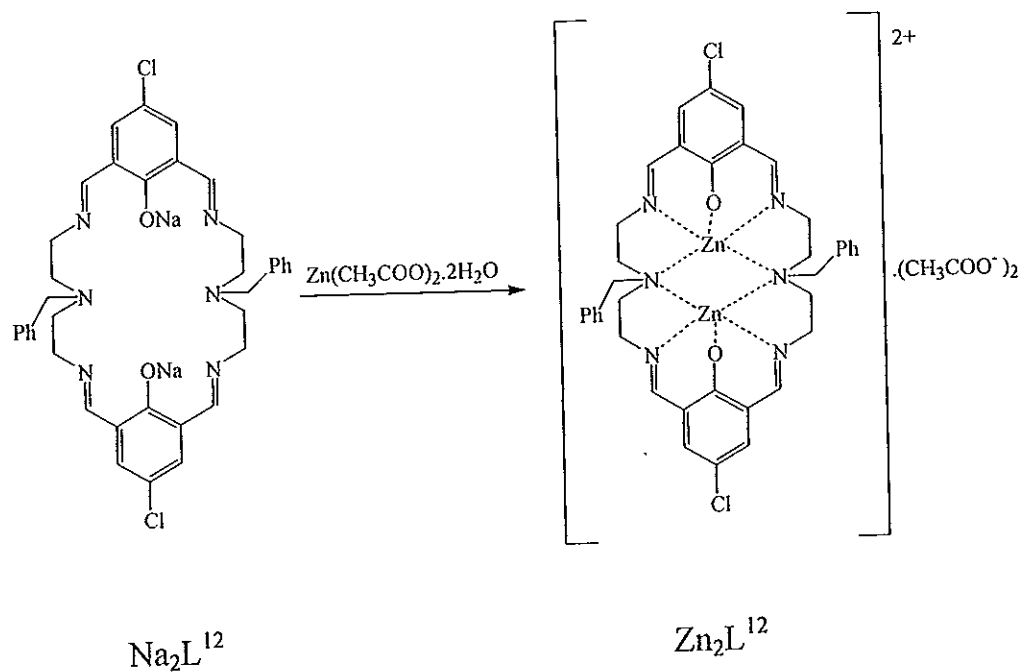
3.5 Disodium complex of macrocyclic ligand L¹²



N^3 -(benzyl)diethylenetriamine-trihydrochloride was dissolved in a small amount of water and the solution was basified with NaOH. Then this basic solution was added slowly to a suspension of sodium 4-chloro-2,6-diformylphenoxide (1 mmol) in ethanol (30 cm³) under nitrogen atmosphere. The mixture was stirred under reflux for 1 h and the solvent was removed under reduced pressure to give the residue which was dissolved in chloroform. The resulting mixture was washed with saturated NaHCO₃ (30 cm³), water (3×30 cm³), and dried with anhydrous Na₂SO₄. The organic solvent was removed by rotary evaporator to yield a viscous liquid residue (93%). ¹H NMR (CDCl₃) δ : 8.0-6.70 (*br m*, aromatic protons), 4.40-2.30 (*br m*, aliphatic proton). IR (neat, cm⁻¹): 2926m, ν (C-H); 1634s, ν (C=N); 1455s, ν (C=C). UV (CHCl₃) λ_{\max} nm (log ϵ): 334 (3.62), 246 (4.09).

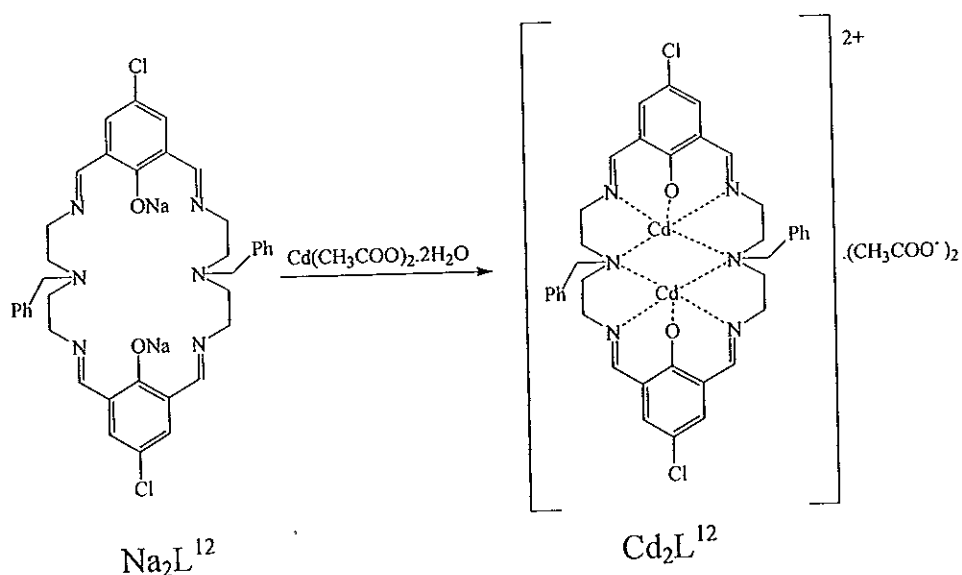
3.5.1 Transmetalation (Na-metal exchange) of Na_2L^{12}

3.5.1.1 Dinuclear zinc (II) macrocyclic complex of L^{12}



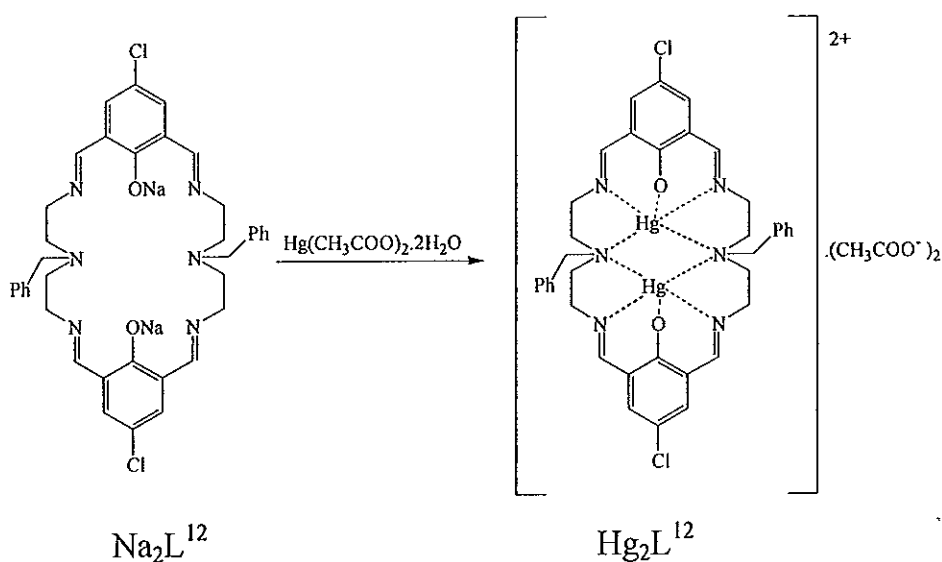
The mixture of Na_2L^{12} (0.40 mmol) and the zinc acetate (0.86 mmol) in ethanol (25 cm^3) was refluxed for 1 h under nitrogen atmosphere. After the reaction was completed, the resulting clear solution was filtered hot and then left to cool at room temperature. After seven days, red-yellow crystals of Zn_2L^{12} were deposited (24.04%): mp=215-226 °C, IR (KBr pellets, cm^{-1}): 3431s, $\nu(\text{O-H})$; 1650s, $\nu(\text{C=N})$; 1553s, $\nu(\text{C=C})$. A reddish-yellow cubic-shaped crystal was selected for X-ray structure determination.

3.5.1.2 Dinuclear cadmium (II) macrocyclic complex of L¹²



The mixture of Na_2L^{12} (0.42 mmol) and the cadmium acetate (0.86 mmol) in ethanol (25 cm^3) was refluxed under nitrogen atmosphere. After the reaction was refluxed for 1 h, the resulting clear solution was filtered hot and then left to cool at room temperature. After seven days, reddish-yellow crystals of Cd_2L^{12} were deposited (more than 3.95%): mp > 158 °C (decompose), IR (KBr pellets, cm^{-1}): 3436m, $\nu(\text{O-H})$; 1647s, $\nu(\text{C=N})$; 1549s, $\nu(\text{C=C})$. A reddish-yellow cubic-shaped crystal was selected for X-ray structure determination.

3.5.1.3 Dinuclear mercuric (II) macrocyclic complex of L¹²



The mixture of Na_2L^{12} (0.5 mmol) and the mercuric acetate (1 mmol) in ethanol (25 cm^3) was refluxed and stirred for 1 h under nitrogen, and the resulting clear solution was filtered hot and then left to cool. After seven days at room temperature, yellow crystals of Hg_2L^{12} were deposited (more than 8.65%): mp=200-206 °C, IR (KBr pellets, cm^{-1}): 3400m, $\nu(\text{O-H})$; 1635s, $\nu(\text{C=N})$; 1577s, 1545s $\nu(\text{C=C})$. A yellow cubic-shaped crystal was selected for X-ray structure determination.

CHAPTER 3

RESULTS AND DISCUSSION

1. Synthesis of sodium 4-substituted-2,6-diformylphenoxide (11a, 11b)

Sodium 4-Chloro-2,6-diformylphenoxide (11a) could be easily prepared in three steps. The reaction of 4-chlorophenol (8a) with 37% formaldehyde solution in the presence of aqueous sodium hydroxide at room temperature for three days gave after acidification a yellow solid, the yield was 37.40% (mp=162-164 °C). IR spectrum (Figure 24) of this solid showed absorption bands at 3413 cm^{-1} and 1476 cm^{-1} corresponding to hydroxy groups and C=C stretching, respectively. ^1H NMR (60 MHz) spectrum (Figure 25) recorded in CDCl_3 showed 3 *singlet* signals at δ 7.10 (2H), 4.80 (4H) and 2.73, which were assigned to aromatic protons, methylene protons and hydroxy protons, respectively. However, the observed integration ratio between aromatic and methylene protons was 1:2 which indicated that the electrophilic aromatic substitution (hydroxymethylation) took place at 2 and 6 positions. From the above spectral data, the possible structure was fitted to 4-chloro-2,6-bis(hydroxymethyl)phenol (9a).

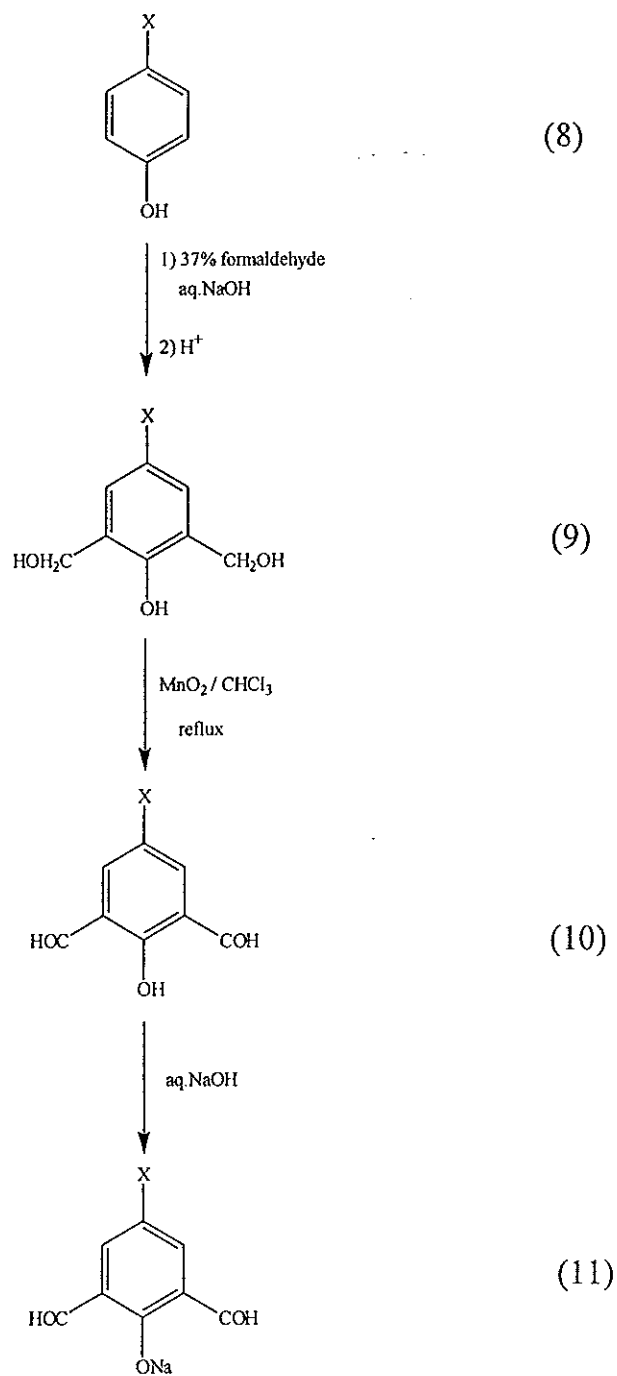
The compound (9a) which having a benzyl alcohol could be oxidized in the second step with mild oxidizing reagents, such as MnO_2 . Treatment of compound (9a) with activated MnO_2 in refluxing chloroform under dried condition for 3-4 days gave yellow solid 55.08% (mp=108-112 °C). IR spectrum (Figure 26) displayed absorption bands at 2840 cm^{-1} , 1686 cm^{-1} and 1439 cm^{-1} , which could be attributed to C-H stretching, C=O stretchings of aldehyde and C=C stretching, respectively. ^1H NMR (60 MHz) spectrum (Figure 27) recorded in CDCl_3 showed 3 *singlet* signals. The signals at δ 11.63 (1H), 10.30 (2H) and 7.83 (2H), could be assigned to chelated OH, aldehydic protons and aromatic protons, respectively. Integration ratio of these signals was 1:2:2 indicating that two hydroxymethyl groups were oxidized to two formyl groups. Thus the above information strongly supported structure (10a).

The final step was the conversion of compound (10a) to the corresponding sodium salt by treatment with aqueous sodium hydroxide. The yellow solid product obtained was 91.80% (mp>300 °C). IR spectrum (Figure 28) exhibited absorption bands at 2840 cm^{-1} , 1686 cm^{-1} and 1439 cm^{-1} corresponding to C-H stretching, C=O stretchings of aldehyde and C=C stretching, respectively. ^1H NMR (60 MHz) spectrum (Figure 29) recorded in $\text{D}_2\text{O} + \text{CD}_3\text{COCD}_3$ showed 2 *singlet* signals at δ 10.00 (2H), 7.60 (2H) which were assigned to formyl and aromatic protons, respectively. By comparison of the ^1H NMR spectrum between (11a) and (10a), it was found that formyl protons and aromatic protons in 11a resonated at slightly higher field than those of the protons in 10a (δ 10.13 and 7.80) as a result of the more powerful shielding effect of electron delocalization of phenoxide ion to the aromatic ring than the corresponding phenol.

By analogous method, 4-methylphenol (8b) was reacted with formaldehyde to give a pale yellow solid, the yield was 55.0% (mp=127-129 °C). IR spectrum (Figure 30) showed absorption bands at 3394 cm^{-1} corresponding to hydroxy groups. ^1H NMR (60 MHz) spectrum (Figure 31) recorded in CDCl_3 showed 4 signals. The signals at δ 6.80 (*t*, 2H), δ 4.67 (*s*, 4H) and δ 2.26 (*s*, 6H) were assigned to aromatic protons, methylene protons and methyl protons, respectively. The signal at δ 4.13 (*br, s*), which was removed by D_2O exchange was assigned to hydroxy protons. Integration ratio of aromatic protons, methylene protons and methyl protons was 2:4:3 indicating that the two hydroxymethyl groups were introduced to the ring at 2 and 6 positions. From the above spectral data, the possible structure should be 4-methyl-2,6-bis(hydroxymethyl)phenol (9b).

Oxidation reaction took place when the compound (9b) was refluxed with MnO_2 in chloroform to give yellow solid, the yield was 34.4% (mp=98-110 °C). IR spectrum (Figure 32) showed absorption bands at 2835 cm^{-1} , 1677 cm^{-1} and 1458 cm^{-1} corresponding to C-H stretching, C=O stretchings of aldehyde and C=C stretching, respectively. ^1H NMR (60 MHz) spectrum (Figure 33) recorded in CDCl_3 presented *singlet* signals at δ 11.39 (1H) and 10.10 (2H) which could be assigned to chelated *OH* and aldehydic protons. The above information supported that two hydroxymethyl groups were converted to two formyl groups and the possible structure of this solid was 4-methyl-2,6-diformylphenol (10b).

Compound (10b) was treated with aqueous sodium hydroxide to afford yellow-green solid, 68.09% (mp>300 °C). IR spectrum (Figure 34) showed absorption bands at 2838 cm^{-1} , 1674 cm^{-1} and 1515 cm^{-1} corresponding to C-H stretching, C=O stretchings of aldehyde groups and C=C stretching, respectively. ^1H NMR (60 MHz) spectrum (Figure 35) recorded in D_2O did not show the chelated OH but exhibited the signals at δ 9.90 (*s*, 2H) and δ 7.43 (*s*, 2H) which were assigned to formyl and aromatic protons, respectively. Thus, the above information indicated the possible structure was sodium 4-methyl-2,6-diformylphenoxide (11b).

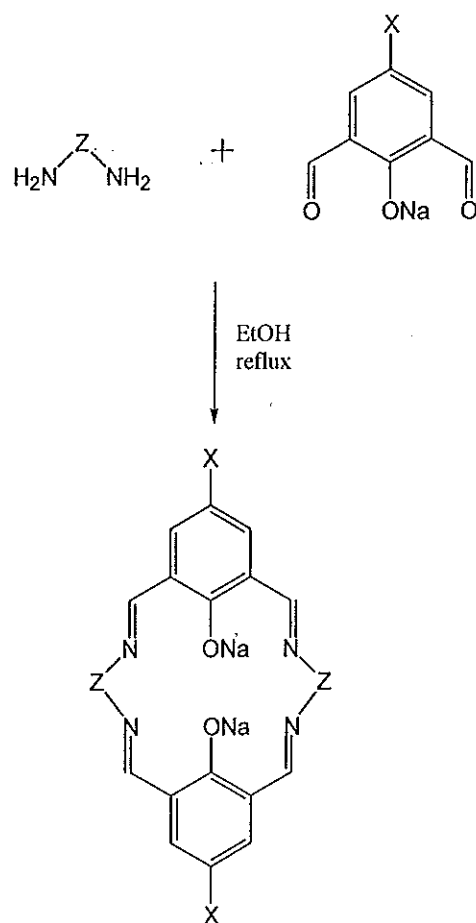


Scheme 11 The synthetic diagram of 4-substituted-2,6-diformylphenoxide (a, X=Cl and b, X=CH₃)

2. Synthesis of disodium macrocyclic ligands

The macrocyclic ligands were prepared by standard sodium template procedure. Sodium 4-substituted-2,6-diformylphenoxide easily formed a [2+2] macrocyclic Schiff base cyclocondensation product with polyamines (see Scheme12) (Gou, *et al.*, 1995). Various products with different number of membered rings were prepared depending on the number of carbons in polyamines. For example, the use of polyamine; ethylenediamine, 1,3-diaminopropane, and 1,4-diaminobutane gave 18-, 20-, and 22-membered ring of the macrocycles, respectively. These prepared macrocycles were less stable and readily hydrolyzed back to amine and aldehyde when treated with acid.

N^3 -(benzyl)diethylenetriamine-trihydrochloride afforded unexpected 18-membered ring instead of expected 24-membered ring. The disodium macrocyclic themselves did not form single crystal, so they were subjected to transmetallation with various metal ions (Cu^{2+} , Fe^{2+} , Co^{2+} , Ni^{2+} , Zn^{2+} , Pb^{2+} , Cd^{2+} and Hg^{2+}) with the aim of getting single crystals. The obtained single crystal enable us to confirm their structures by X-ray diffraction technique.



L^8 X=CH₃ Z=CH₂CH₂ (18-membered ring)

L^{9a} X=CH₃ Z=CH₂CH₂CH₂ (20-membered ring)

L^{9b} X=Cl Z=CH₂CH₂CH₂ (20-membered ring)

L^{10} X=CH₃ Z=CH₂CH₂CH₂CH₂ (22-membered ring)

Scheme 12 Synthetic diagram of sodium macrocyclic complexes

2.1 Disodium complexes of macrocyclic ligand L^8 (18-membered ring)

Cyclocondensation between sodium 4-methyl-2,6-diformylphenoxide and ethylenediamine in ethanol under reflux gave yellow solid, the yield was 59% (mp > 250 °C). The IR spectrum (Figure 36) showed absorption bands at 1639 cm^{-1} and 1527 cm^{-1} corresponding to C=N and C=C stretching. The ^1H NMR (60 MHz) spectrum recorded in $\text{CDCl}_3 + \text{CD}_3\text{OD}$ showed 4 signals (Figure 37). The *singlet* signals at δ 8.36 (4H), 7.33 (4H), 3.96 (8H) and 2.20 (6H) could be assigned to imine protons, aromatic protons, methylene protons and methyl protons, respectively. The NMR spectrum of this compound did not show the signals of formyl protons between 9-10 ppm and the signal of amino protons at 1.3 ppm, these results indicated the formation of cyclic disodium complex of L^8 . Finally, this complex was transmetallated with Cu^{2+} and Ni^{2+} ions and single crystals for X-ray diffraction were grown, as follow:

2.1.1 Dinuclear copper (II) macrocyclic complex of L^8

The complexes of Na_2L^8 underwent cationic exchange (transmetallation) upon treatment with copper perchlorate in ethanol under reflux to give the precipitate. The crude product was crystallized from H_2O and MeOH as reddish brown crystal. The complex was $\text{Cu}_2L^8(\text{ClO}_4)_2$ which was confirmed by the following X-ray diffraction data (Table 1, Figure 15) to be an 18-membered ring macrocycle.

Table 1 Crystal structure data for $\text{Cu}_2\text{L}^8(\text{ClO}_4)_2$

Identification code	091am
Empirical formula	$\text{C}_{22} \text{H}_{22} \text{Cl}_{12} \text{Cu}_2 \text{N}_4 \text{O}_{10}$
Formula weight	700.42
Temperature	293(2) K
Wavelength	0.71073 Å
Crystal system, space group	Triclinic, P-1
Unit cell dimensions	$a = 8.2349(3) \text{ Å}$ $\alpha = 81.263(1) \text{ deg.}$ $b = 8.3574(3) \text{ Å}$ $\beta = 69.035(1) \text{ deg.}$ $c = 9.8522(3) \text{ Å}$ $\gamma = 78.927(1) \text{ deg.}$
Volume	$618.81(4) \text{ Å}^3$
Z	1
Calculated density	1.880 mg/m^3
Absorption coefficient	2.002 mm^{-1}
F(000)	354
Crystal size	0.30 x 0.24 x 0.20 mm
Theta range for data collection	2.22 to 29.61 deg.
Limiting indices	$-10 \leq h \leq 9, -8 \leq k \leq 11,$ $-13 \leq l \leq 10$
Reflections collected / unique	4571 / 3063 [R(int) = 0.2342]
Completeness to theta = 29.61	87.7 %
Absorption correction	Empirical

Table 1 (continued)

Max. and min. transmission	0.6903 and 0.5850
Refinement method	Full-matrix least-squares on F^2
Data / restraints / parameters	3063 / 0 / 164
Goodness-of-fit on F^2	0.933
Final R indices [$I > 2\sigma(I)$]	R1 = 0.1438, wR2 = 0.3202
R indices (all data)	R1 = 0.2162, wR2 = 0.3877
Largest diff. peak and hole	1.916 and -1.987 e.Å ⁻³

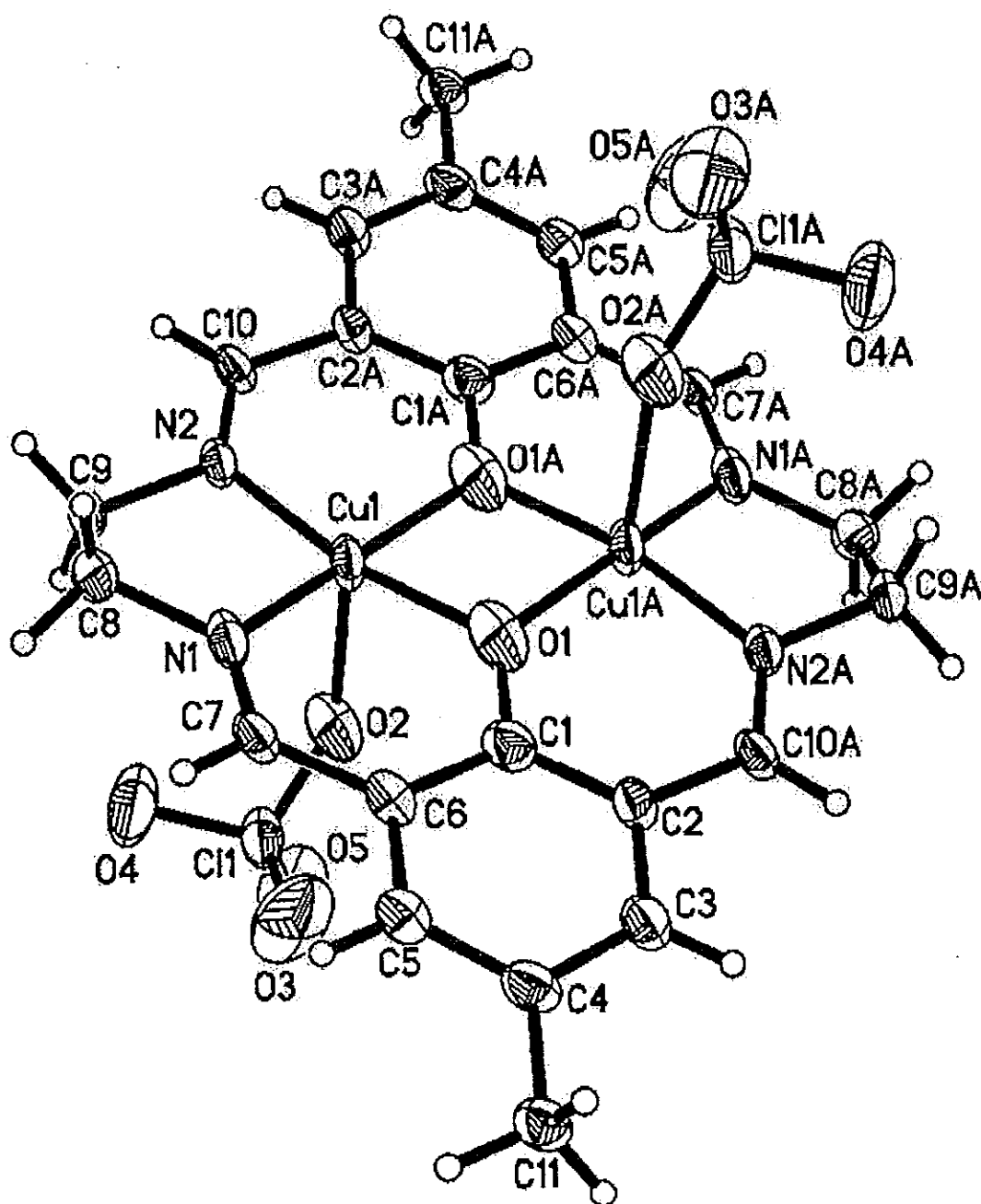


Figure 15 Crystal structure of $\text{Cu}_2\text{L}^8(\text{ClO}_4)_2$

2.1.2 Dinuclear nickle (II) macrocyclic complex of L⁸

The reddish brown cube-shaped crystals, which were obtained from the transmetallation reaction between Na₂L⁸ and nickle perchlorate under reflux showed the 18-membered ring macrocyclic complexes of the [Ni₂L⁸].2ClO₄. The X-ray data of the above complexes was shown below (Table 2, Figure 16).

Table 2 Crystal structure data for [Ni₂L⁸].2ClO₄

Identification code	135am
Empirical formula	C ₂₂ H ₂₂ Cl ₂ N ₄ Ni ₂ O ₁₀
Formula weight	690.76
Temperature	293(2) K
Wavelength	0.71073 Å
Crystal system, space group	Triclinic, P-1
Unit cell dimensions	a = 8.0673(5) Å α = 80.262(1) deg. b = 8.3698(5) Å β = 70.977(1) deg. c = 9.9512(7) Å γ = 81.161(1) deg.
Volume	622.56(7) Å ³
Z	2
Calculated density	1.842 mg/m ³
Absorption coefficient	1.794 mm ⁻¹
F(000)	352

Table 2 (continued)

Crystal size	0.48 x 0.10 x 0.08 mm
Theta range for data collection	2.18 to 29.43 deg.
Limiting indices	-11 ≤ h ≤ 10, -10 ≤ k ≤ 11, -13 ≤ l ≤ 11
Reflections collected / unique	4470 / 2960 [R(int) = 0.0742]
Completeness to theta = 29.43	85.8 %
Absorption correction	Empirical
Max. and min. transmission	0.8698 and 0.4798
Refinement method	Full-matrix least-squares on F ²
Data / restraints / parameters	2960 / 0 / 183
Goodness-of-fit on F ²	1.030
Final R indices [I > 2σ(I)]	R1 = 0.0664, wR2 = 0.1630
R indices (all data)	R1 = 0.0822, wR2 = 0.1701
Extinction coefficient	0.014(3)
Largest diff. peak and hole	1.093 and -1.825 e.Å ⁻³

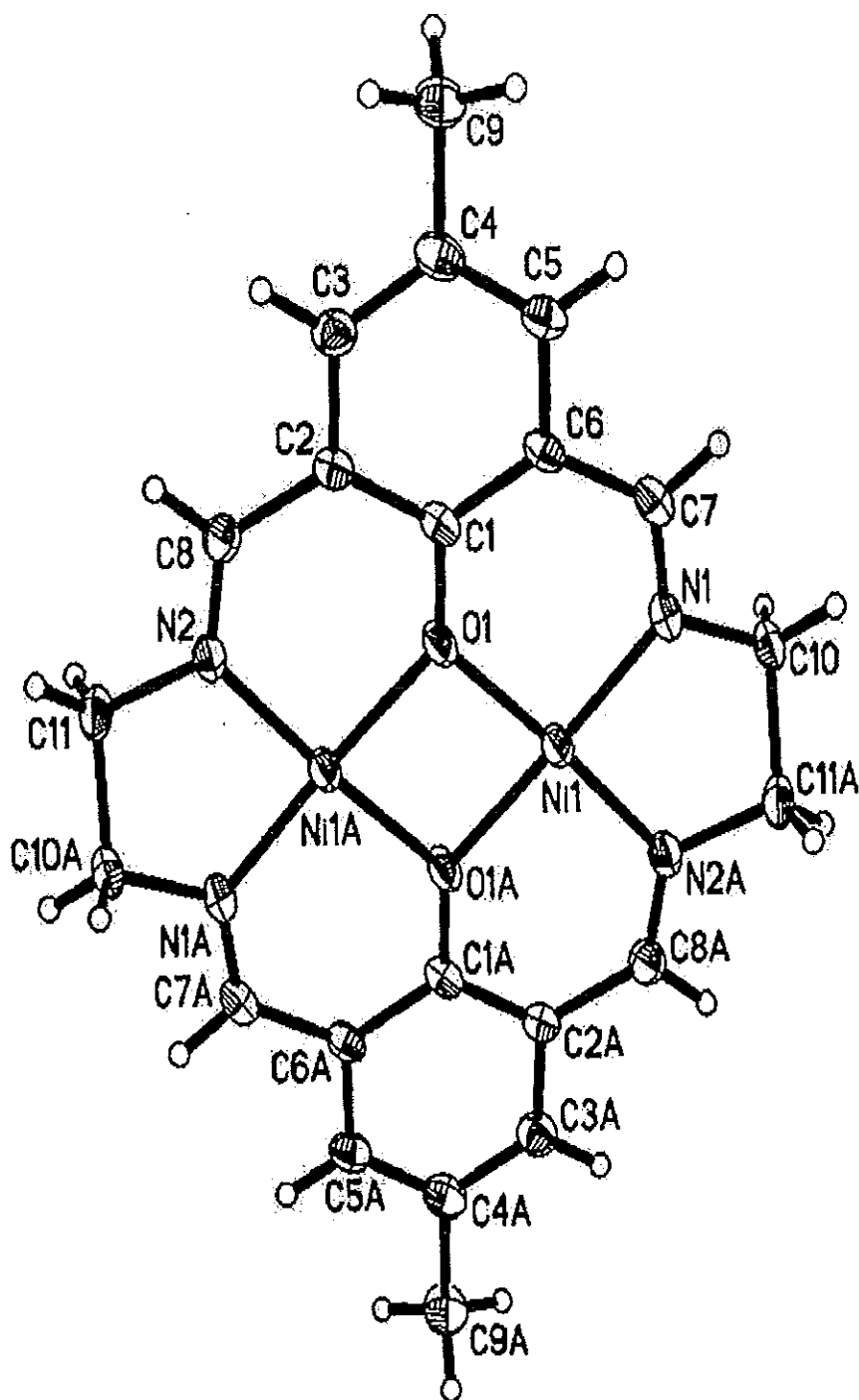


Figure 16 Crystal structure of $[\text{Ni}_2\text{L}^8]\cdot 2\text{ClO}_4$

ClO_4^- counter ions are not shown

2.2 Disodium complexes of macrocyclic ligand L^{9a} (20-membered ring)

By analogous method, the sodium 4-methyl-2,6-diformylphenoxide was reacted with 1,3-diaminopropane to give yellow solid, the yield was 80% (mp > 210 °C, decompose). The IR spectrum (Figure 38) of this compound was similar to the IR spectrum of macrocyclic ligand Na₂L⁸. The ¹H NMR (60 MHz) spectrum recorded in CDCl₃ showed 4 signals (Figure 39). The signals at δ 8.40 (*s*, 4H), 7.30 (*s*, 4H), were assigned to imine protons and aromatic protons, respectively. The signal at δ 3.66 (*t*, *J* = 6 Hz, 8H) could be assigned to methylene protons (2xN-CH₂-CH₂-CH₂-N) and signal range from δ 2.33 to δ 1.80 (*s*, *m*, 10H) were assigned to methyl protons (2xCH₃) superimposing on *multiplet* signal of methylene protons (2xN-CH₂-CH₂-CH₂-N). Integration ratios of each signal were 2:2:4:5, which indicated the formation of [2+2] macrocyclic products. This compound was further transmetallated with Co²⁺ and Cu²⁺ ions, and the structure of both complexes 9L^{9a} were confirmed by the following X-ray diffraction data (Table 3 and Figure 17 for cobalt complex, Table 4 and Figure 18 for copper complex) to be a 20-membered ring macrocycles.

Table 3 Crystal structure data for $[\text{Co}_2\text{L}^{9a}(\text{NO}_3)(\text{CH}_3\text{OH})(\text{H}_2\text{O})]\cdot\text{NO}_3$

Identification code	089am
Empirical formula	$\text{C}_{50} \text{H}_{64} \text{Co}_4 \text{N}_{12} \text{O}_{20}$
Formula weight	1388.85
Temperature	293(2) K
Wavelength	0.71073 Å
Crystal system, space group	Monoclinic, $P2_1$
Unit cell dimensions	$a = 9.2918(2)$ Å $\alpha = 90$ deg. $b = 18.8737(4)$ Å $\beta = 90.699(1)$ deg. $c = 16.4546(4)$ Å $\gamma = 90$ deg.
Volume	$2885.44(11)$ Å ³
Z	2
Calculated density	1.599 mg/m ³
Absorption coefficient	1.216 mm ⁻¹
F(000)	1432
Crystal size	0.38 x 0.18 x 0.16 mm
Theta range for data collection	1.24 to 28.32 deg.
Limiting indices	$-12 \leq h \leq 11$, $-25 \leq k \leq 24$, $-21 \leq l \leq 17$
Reflections collected / unique	19969 / 13155 [R(int) = 0.1269]
Completeness to theta = 28.32	97.6 %
Absorption correction	Empirical

Table 3 (continued)

Max. and min. transmission	0.8292 and 0.6551
Refinement method	Full-matrix least-squares on F^2
Data / restraints / parameters	13155 / 1 / 776
Goodness-of-fit on F^2	0.863
Final R indices [$I > 2\sigma(I)$]	R1 = 0.0742, wR2 = 0.1712
R indices (all data)	R1 = 0.1884, wR2 = 0.2242
Absolute structure parameter	-0.03(3)
Extinction coefficient	0.0024(3)
Largest diff. peak and hole	0.823 and -0.824 e. \AA^{-3}

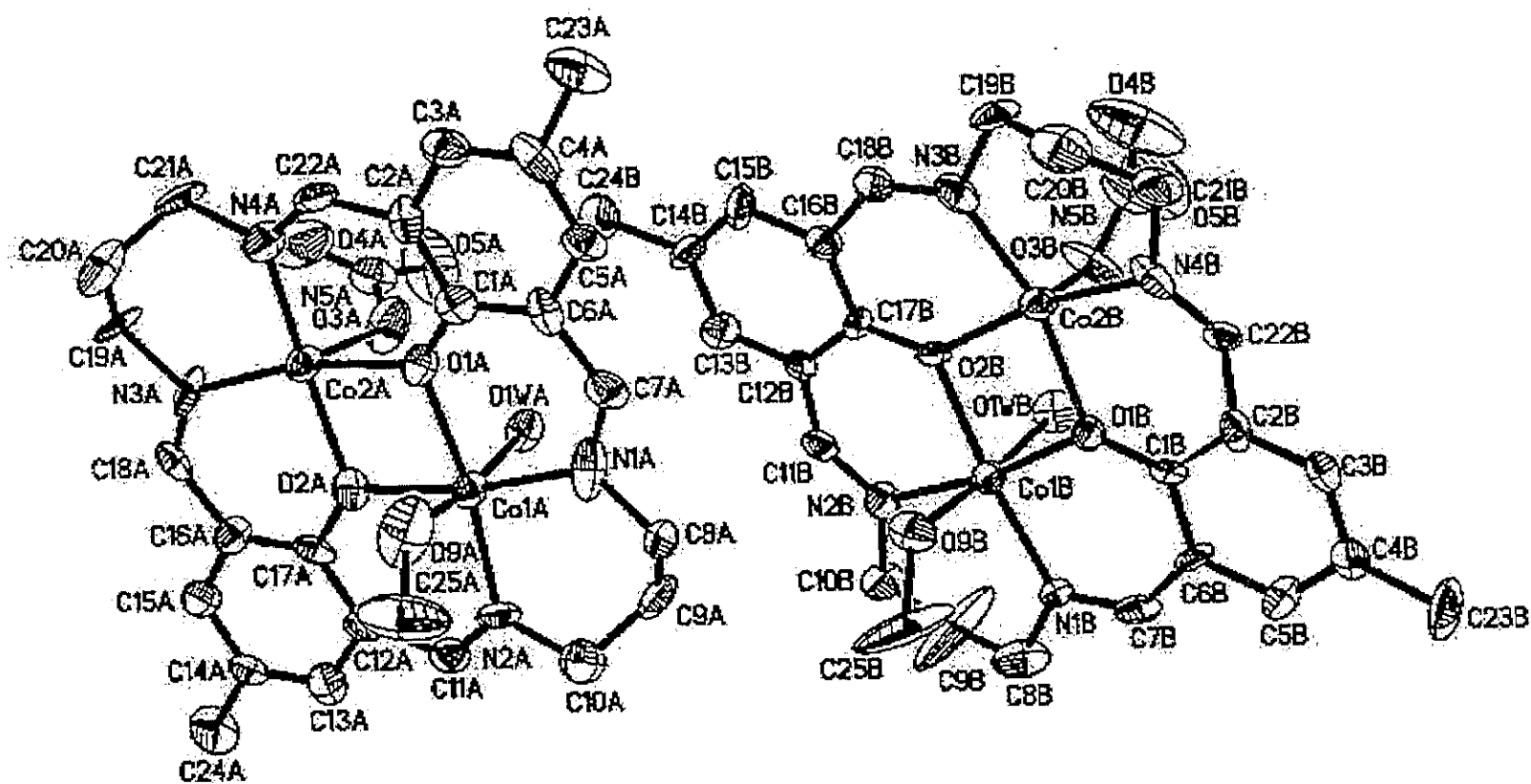


Figure 17 Crystal structure of $[\text{Co}_2\text{L}^{9a}(\text{NO}_3)(\text{CH}_3\text{OH})(\text{H}_2\text{O})]$

NO_3^- counter ion is not shown

Table 4 Crystal structure data for $[\text{Cu}_2\text{L}^{9a}(\text{H}_2\text{O})_2]\cdot 2\text{ClO}_4$

Identification code	083am
Empirical formula	$\text{C}_{24} \text{H}_{29} \text{Cl}_2 \text{Cu}_2 \text{N}_4 \text{O}_{12}$
Formula weight	763.49
Temperature	293(2) K
Wavelength	0.71073 Å
Crystal system, space group	Monoclinic, $P2_1/c$
Unit cell dimensions	$a = 16.5422(3) \text{ Å}$ $\alpha = 90 \text{ deg.}$ $b = 12.4224(1) \text{ Å}$ $\beta = 105.370(1) \text{ deg.}$ $c = 14.8093(2) \text{ Å}$ $\gamma = 90 \text{ deg.}$
Volume	$2934.38(7) \text{ Å}^3$
Z	4
Calculated density	1.728 mg/m^3
Absorption coefficient	1.701 mm^{-1}
F(000)	1556
Crystal size	0.36 x 0.20 x 0.16 mm
Theta range for data collection	1.28 to 28.34 deg.
Limiting indices	$-22 \leq h \leq 20$, $-16 \leq k \leq 16$, $-19 \leq l \leq 18$
Reflections collected / unique	20331 / 7180 [R(int) = 0.1073]
Completeness to theta = 28.34	98.1 %

Table 4 (continued)

Absorption correction	Empirical
Max. and min. transmission	0.7725 and 0.5795
Refinement method	Full-matrix least-squares on F^2
Data / restraints / parameters	7180 / 0 / 398
Goodness-of-fit on F^2	0.950
Final R indices [$I > 2\sigma(I)$]	$R_1 = 0.0590$, $wR_2 = 0.1457$
R indices (all data)	$R_1 = 0.0959$, $wR_2 = 0.1591$
Extinction coefficient	0.0033(4)
Largest diff. peak and hole	1.215 and -1.182 e. \AA^{-3}

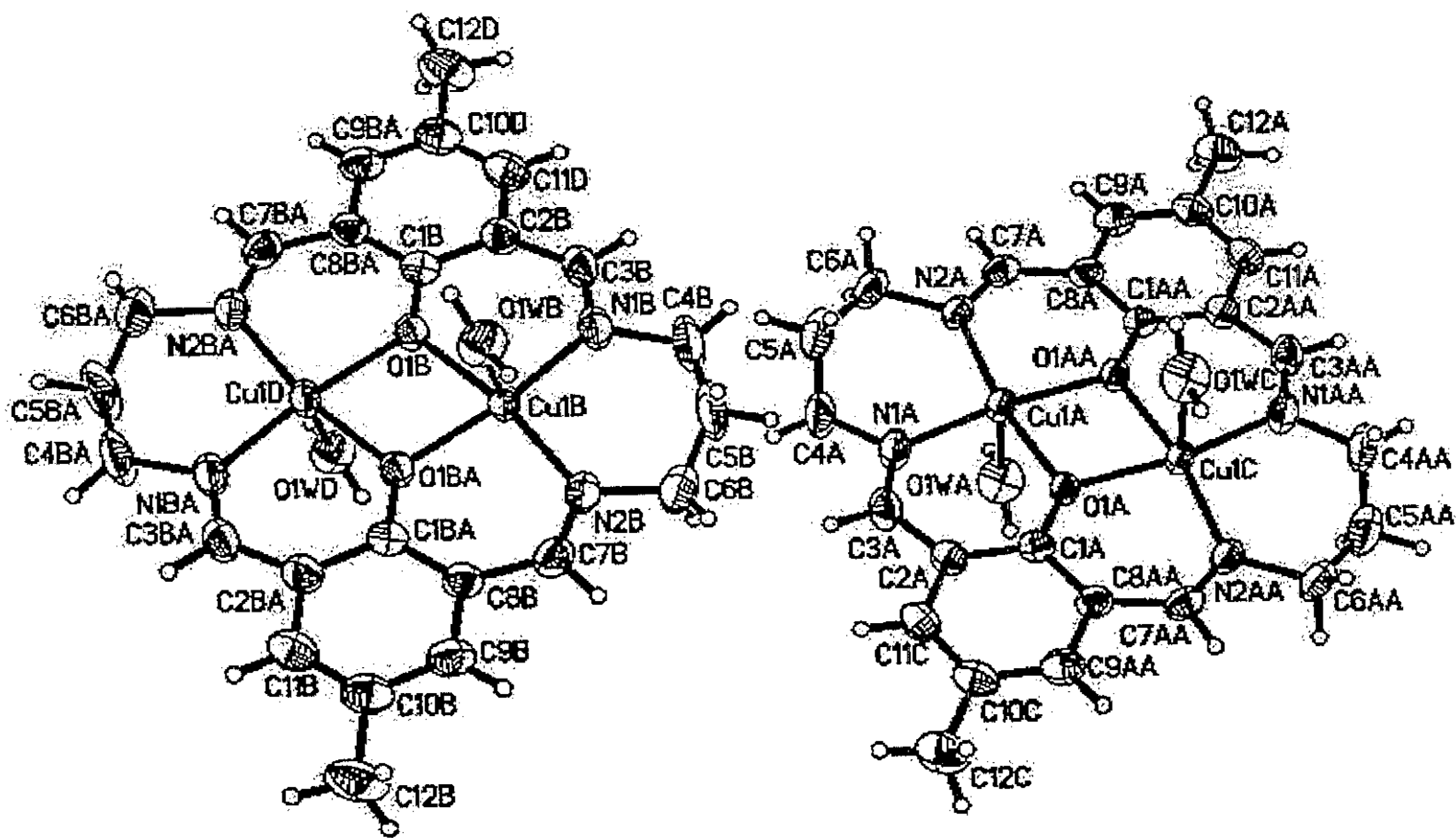


Figure 18 Crystal structure of $[\text{Cu}_2\text{L}^{9a}(\text{H}_2\text{O})_2] \cdot 2\text{ClO}_4$

ClO_4^- counter ions are not shown

2.3 Disodium complexes of macrocyclic ligand L^{9b} (20-membered ring)

By the same method, macrocyclic ligand L^{9b} was prepared from the reaction of sodium 4-chloro-2,6-diformylphenoxide and 1,4-diaminobutane (putesine) to give a yellow solid. The yield was 54% (mp=160-170 °C). The IR spectrum (Figure 40) exhibited absorption bands at 1638 cm⁻¹ and 1435 cm⁻¹ due to C=N and C=C stretching, respectively. The ¹H NMR (60 MHz) spectrum recorded in CDCl₃ displayed 4 signals (Figure 41). The *singlet* signals at δ 8.36 (4H), and δ 7.46 (4H) were assigned to imine and aromatic protons, respectively. The *triplet* signal at δ 3.74 ($J = 6$ Hz, 8H) was assigned to methylene protons (2xN-CH₂-CH₂-CH₂-N) and *multiplet* signals at δ 2.23 (4H) could be assigned to methylene protons (2xN-CH₂-CH₂-CH₂-N). Integration ratios of each signal were 1:1:2:1 indicating that the starting materials was converted to the [2+2] macrocyclic ligand, which was further transmetallated to the copper complex and the single crystals were formed. The structure of the copper complex showed a 20-membered ring of macrocycle L^{9b} as confirmed by X-ray diffraction measurement. The X-ray data of this complex was shown below (Table 5, Figure 19).

Table 5 Crystal structure data for $[\text{Cu}_2\text{L}^{9b}(\text{H}_2\text{O})_2]\cdot 2\text{ClO}_4$

Identification code	084am
Empirical formula	$\text{C}_{22} \text{H}_{24} \text{Cl}_4 \text{Cu}_2 \text{N}_4 \text{O}_{12}$
Formula weight	805.33
Temperature	293(2) K
Wavelength	0.71073 Å
Crystal system, space group	Pbcn
Unit cell dimensions	$a = 14.34200(10) \text{ Å}$ $\alpha = 90 \text{ deg.}$ $b = 12.05300(10) \text{ Å}$ $\beta = 90 \text{ deg.}$ $c = 17.1535(2)$ $\gamma = 90 \text{ deg.}$
Volume	$2965.22(5) \text{ Å}^3$
Z	4
Calculated density	1.804 mg/m^3
Absorption coefficient	1.863 mm^{-1}
F(000)	1624
Crystal size	0.46 x 0.14 x 0.12 mm
Theta range for data collection	2.21 to 28.25 deg.
Limiting indices	$-13 \leq h \leq 18, -14 \leq k \leq 15,$ $-22 \leq l \leq 22$
Reflections collected / unique	19710 / 3637 [R(int) = 0.1263]
Completeness to theta = 28.25	99.2 %

Table 5 (continued)

Max. and min. transmission	0.8074 and 0.4812
Refinement method	Full-matrix least-squares on F^2
Data / restraints / parameters	3637 / 0 / 200
Goodness-of-fit on F^2	0.984
Final R indices [$I > 2\sigma(I)$]	$R_1 = 0.0644$, $wR_2 = 0.1773$
R indices (all data)	$R_1 = 0.0921$, $wR_2 = 0.1909$
Extinction coefficient	0.0035(7)
Largest diff. peak and hole	0.956 and -0.790 e. \AA^{-3}

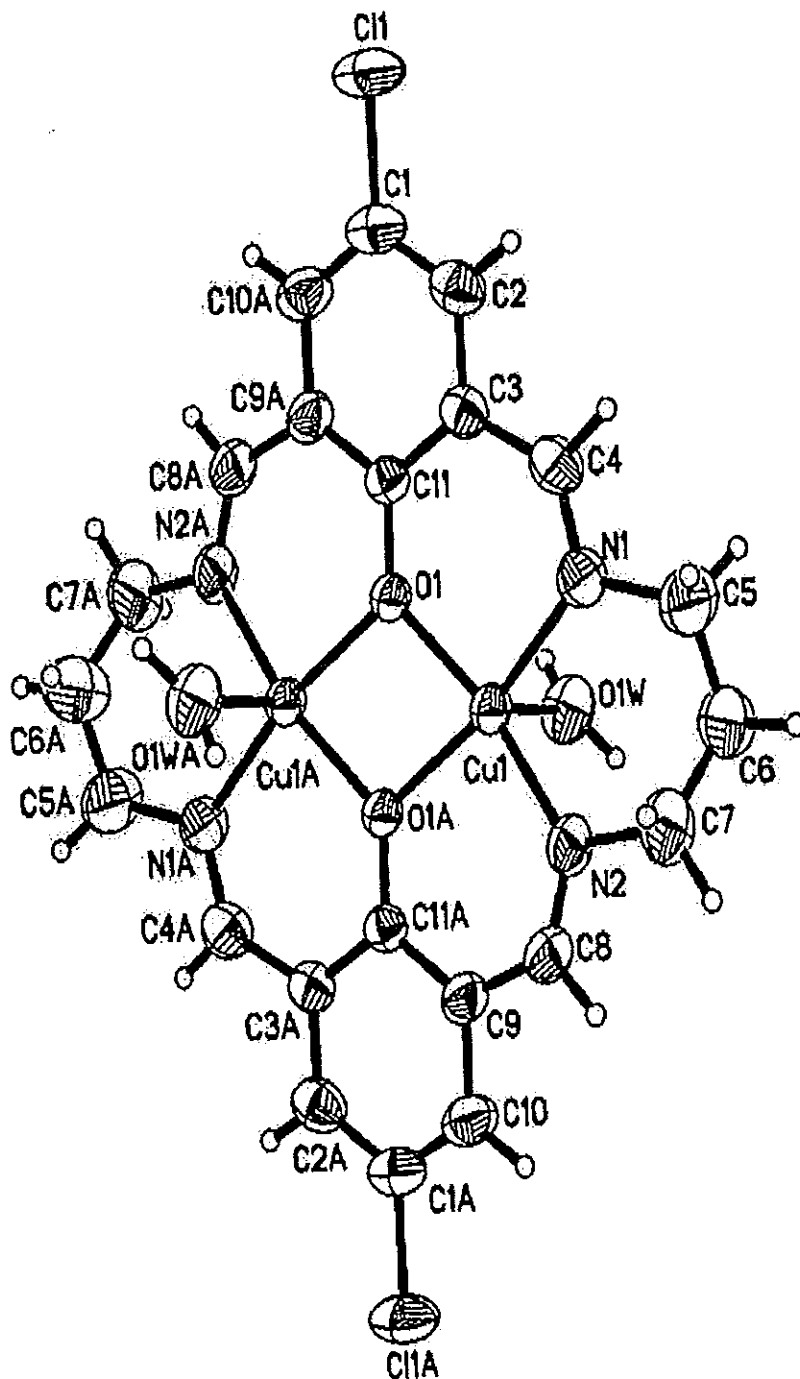


Figure 19 Crystal structure of $[\text{Cu}_2\text{L}^{9b}(\text{H}_2\text{O})_2]\cdot 2\text{ClO}_4$

ClO_4^- counter ions are not shown

2.4 Disodium complexes of macrocyclic ligand L¹⁰ (22-membered ring)

By analogous method, cyclocondensation reaction of sodium 4-methyl-2,6-diformylphenoxide with 1,4-diaminobutane gave a yellow viscous oil product, the yield was 73.28%. The UV spectrum (CHCl₃, see Figure 42) exhibited absorption bands at 248 nm and 350 nm corresponding to conjugated double bonds. The IR spectrum (Figure 43) showed absorption bands at 2923 cm⁻¹, 1640 cm⁻¹ and 1600 cm⁻¹ which were assigned to C-H, C=N and C=C stretching, respectively. ¹H NMR (60 MHz) spectrum recorded in CDCl₃ showed 5 signals (Figure 44). The signals at δ 8.63 (*s*, 4H), 7.37 (*s*, 4H), 3.60 (*br m*, 8H), 2.30 (*s*, 6H) and 1.81 (*br m*, 8H) were assigned to imine protons, aromatic protons, methylene protons (2xN-CH₂-CH₂-CH₂-CH₂-N) methyl protons and methylene protons (2xN-CH₂-CH₂-CH₂-CH₂-N), respectively. Integration ratios of each signal were 2:2:4:3:4, indicating the reaction product to be a [2+2] macrocycle. Finally, this product was transmetallated into the form of copper complex, the structure of which has been proven by X-ray diffraction. The X-ray data (Table 6, Figure 20) showed the 22-membered ring macrocyclic complex of the [Cu₂L¹⁰].2ClO₄.

Table 6 Crystal structure data for $[\text{Cu}_2\text{L}^{10}]\cdot 2\text{ClO}_4$

Identification code	09am
Empirical formula	$\text{C}_{26}\text{H}_{30}\text{Cl}_2\text{Cu}_2\text{N}_4\text{O}_{10}$
Formula weight	756.52
Temperature	293(2) K
Wavelength	0.71073 Å
Crystal system, space group	Monoclinic, $P2_1/c$
Unit cell dimensions	$a = 8.5686(4)$ Å $\alpha = 90$ deg. $b = 16.6268(9)$ Å $\beta = 98.072(1)$ deg. $c = 9.9339(5)$ Å $\gamma = 90$ deg.
Volume	$1401.24(12)$ Å ³
Z	2
Calculated density	1.793 mg/m ³
Absorption coefficient	1.775 mm ⁻¹
F(000)	772
Crystal size	0.30 x 0.12 x 0.06 mm
Theta range for data collection	2.40 to 29.51 deg.
Limiting indices	$-11 \leq h \leq 11$, $-22 \leq k \leq 18$, $-13 \leq l \leq 13$
Reflections collected / unique	9698 / 3544 [R(int) = 0.1014]
Completeness to theta = 29.51	90.8 %

Table 6 (continued)

Absorption correction	Empirical
Max. and min. transmission	0.9010 and 0.6180
Refinement method	Full-matrix least-squares on F^2
Data / restraints / parameters	3544 / 0 / 200
Goodness-of-fit on F^2	0.945
Final R indices [$I > 2\sigma(I)$]	$R_1 = 0.0465$, $wR_2 = 0.1070$
R indices (all data)	$R_1 = 0.0800$, $wR_2 = 0.1336$
Extinction coefficient	0.0089(12)
Largest diff. peak and hole	0.850 and -0.973 e. \AA^{-3}

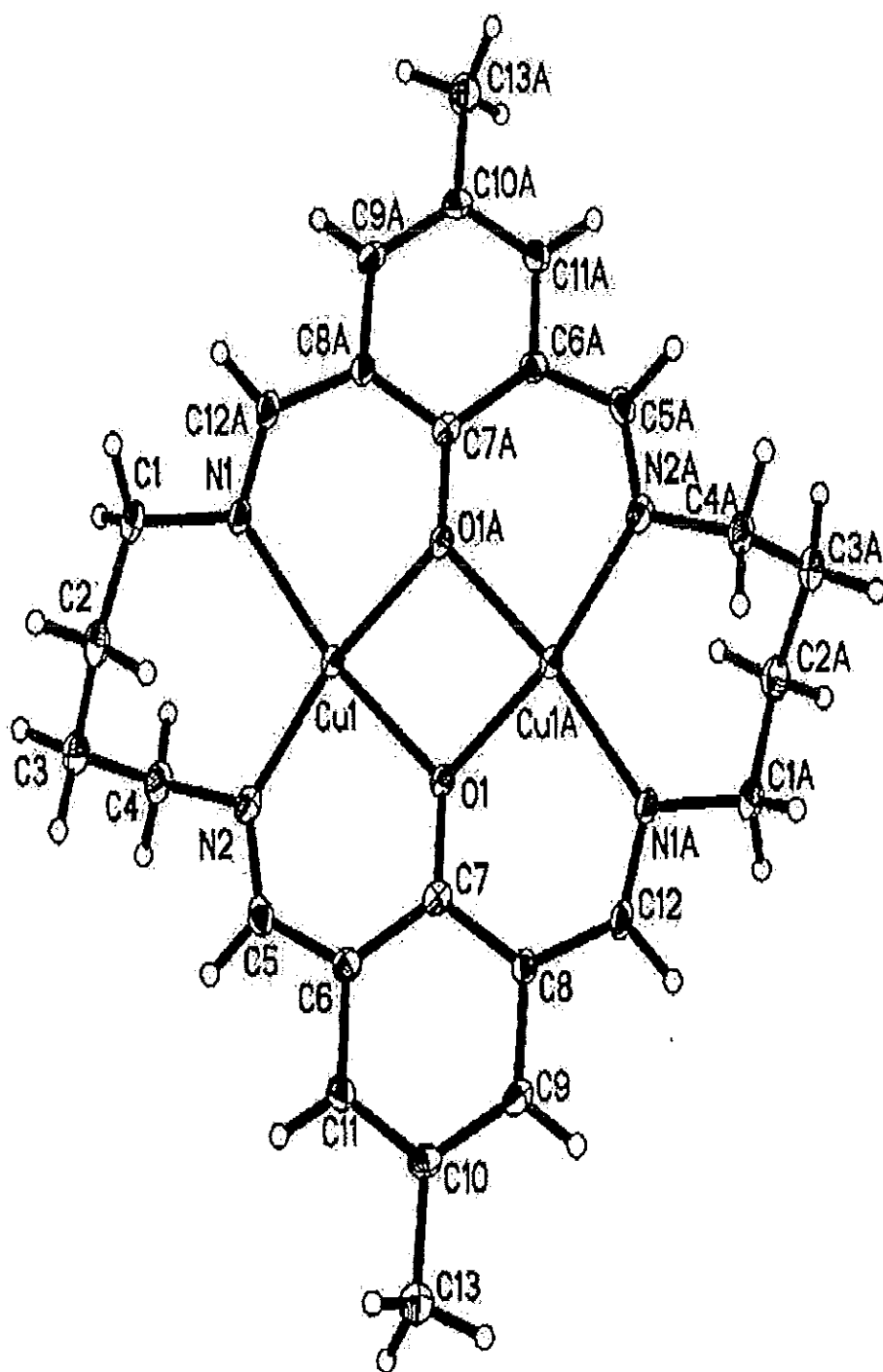


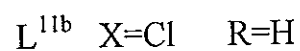
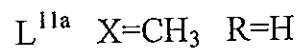
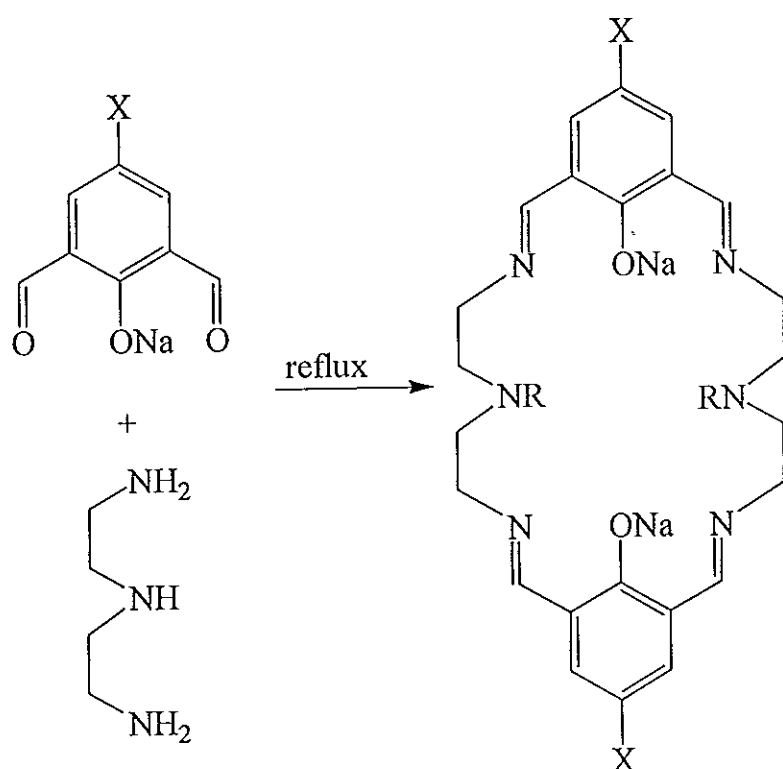
Figure 20 Crystal structure of $[\text{Cu}_2\text{L}^{10}]\cdot 2\text{ClO}_4$

ClO_4^- counter ions are not shown

2.5 Disodium complex of macrocyclic ligand L^{11a-11b}

(expected 24-membered ring)

By analogous method, for the 24-membered ring we used diethylenetriamine to react with sodium 4-substituted-2,6-diformylphenoxide to give a yellow viscous oil product (Scheme 13).



Scheme 13 Synthetic diagram of disodium macrocyclic complexes of L^{11a-12}

The yield was 96% for X=CH₃ and R=H (L^{11a}). The UV spectrum (CHCl₃, see Figure 45) exhibited absorption at 241 nm indicating the presence of an aromatic chromophore in the molecule. The IR (Figure 46) showed absorption bands at 2915, 1633 and 1601cm⁻¹ corresponding to C-H, C=N and C=C stretching, respectively. The ¹H NMR (60 MHz) spectrum recorded in CDCl₃ showed 5 signals (Figure 47). The signals at δ 8.10 (*br m*, 4H) and δ 7.20 (*s*, 4H) could be assigned to imine and aromatic protons, respectively. The signals at δ 3.50 (*br m*, 8H) and δ 2.80 (*br m*, 8H) were assigned to methylene protons (2xN-CH₂-CH₂-N-CH₂-CH₂-N and 2xN-CH₂-CH₂-N-CH₂-CH₂-N) and the signal at δ 2.10 (*s*, 6H) represented methyl protons.

The yield was 70% for X=Cl and R=H (L^{11b}). The UV spectrum (CHCl₃, see Figure 48) exhibited absorption at 227 nm indicating the presence of an aromatic chromophore in the molecule. The IR (Figure 49) showed absorption bands at 2934, 1636 and 1442 cm⁻¹ corresponding to C-H, C=N and C=C stretching, respectively. The ¹H NMR (60 MHz) spectrum recorded in CDCl₃ showed 4 signals (Figure 50). The *broad multiplet* signals at δ 8.10 (4H) and δ 7.60 (4H) could be assigned to imine and aromatic protons, respectively. The *broad multiplet* signals at δ 3.60 (8H) and δ 2.90 (8H) were assigned to methylene protons (2xN-CH₂-CH₂-N-CH₂-CH₂-N and 2xN-CH₂-CH₂-N-CH₂-CH₂-N).

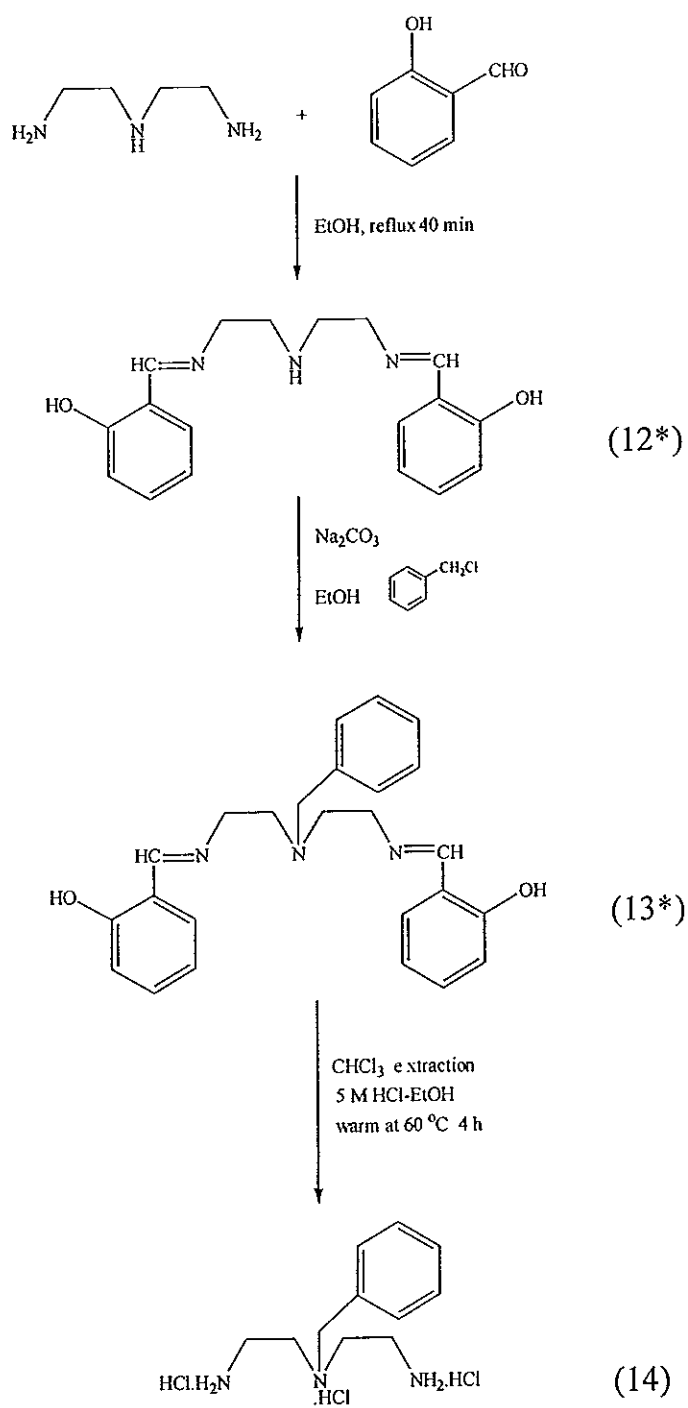
From the above spectroscopic information of both compounds, the possible structure should be 24-membered ring macrocycles. In order to prove them to be the 24-membered ring macrocyclic structures we have to convert these disodium compounds into the corresponding dinuclear complexes of other metals. Various metal ions have been tried (Cu^{2+} , Fe^{2+} , Co^{2+} , Zn^{2+} , Pb^{2+} , Cd^{2+} and Hg^{2+} ions) but we still could not obtain any crystals for X-ray measurement. This might be due to a large cavity of the above macrocyclic ligand, which was not suitable for complexation with the above selected metal cations. We rationalized that increasing the steric hindrance of the middle nitrogen of the diethylenetriamine by introducing the benzyl group and let it form the [2+2] macrocyclic Schiff base cyclocondensation product might enable us to obtain crystal for X-ray diffraction. The incorporation of benzyl group in the macrocycle would create the transannular steric interaction, so that this molecule would rearrange itself in order to minimize the steric interaction and the shape of the cavity might be distorted and might fit for some selected metals in complexation. It would thus be possible to obtain the crystals for X-ray diffraction.

Synthesis of N³-(benzyl)diethylenetriamine-trihydrochloride (14)

N³-(benzyl)diethylenetriamine-trihydrochloride (14) could be synthesized from a reaction of the diethylenetriamine and benzyl chloride in three following steps. The first step was the N-protection of two terminal amine groups into the form of diimine compound (12) by treatment of diethylenetriamine with salicylaldehyde under reflux. The second step was the alkylation at the middle nitrogen atom of diimine to give benzylated diimine intermediate (13). The last step was the hydrolysis of diimine bonds to obtain triamine, which was converted spontaneously to the corresponding triamine-trihydrochloride (14) under an acidic medium. The yield was 11.17% (mp = 264-270 °C). The synthetic diagram was shown in Scheme 14.

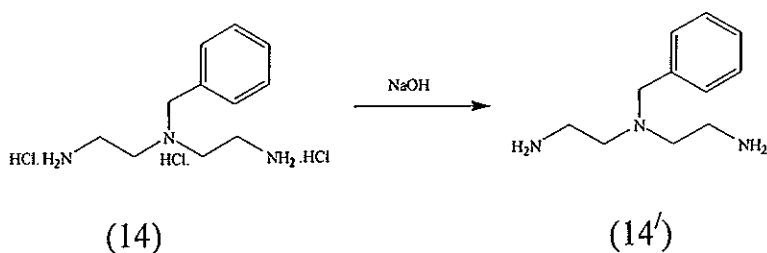
UV spectrum (with CH₃OH as solvent, Figure 51) of the above trichloride salt exhibited absorption at 208 nm indicating the presence of an aromatic chromophore in the molecule. IR spectrum (Figure 52) showed absorption bands at 2939-2896 cm⁻¹ (broad band), 2754-2674 cm⁻¹ (broad band) and 1586 cm⁻¹ corresponding to ammonium salt of -⁺NH₃, -⁺NH stretching and C=C stretching, respectively. The ¹H NMR (60 MHz) spectrum (Figure 53) recorded in D₂O without TMS signal exhibited 4 signals relative to the HOD peak at δ 4.70 as reference. The approximate signals at δ 7.70 (*s*, 5H) and δ 4.30 (*s*, 2H) were assigned to aromatic protons and methylene protons of benzyl group, respectively. The *singlet* signal at δ 3.60 (4H) and *multiplet* signal at δ 3.53 (4H) could be assigned to methylene protons of backbone.

Whereas the ^1H NMR (60 MHz) spectrum (Figure 54) of the corresponding free N^3 -(benzyl)diethylenetriamine ($14'$) (Scheme 15) recorded in CDCl_3 showed similar pattern of signals at δ 7.20, 3.70, 2.60 corresponding to compound (14) signals at δ 7.70, 4.30, and δ 3.60-3.53 respectively. The δ 1.80 of ($14'$) was assigned to amine protons. Each signal of trihydrochloride salt resonated at the lower field due to the deshielding effect of positive charges on N-atom.



Scheme 14 Synthetic diagram of N³-(benzyl)diethylenetriamine-trihydrochloride

(12*) and (13*) were unisolated intermediates



Scheme 15 Reaction of (14) with aqueous sodium hydroxide

We then tried to synthesize the 24-membered ring again using compound (14) as a starting material. A 24-membered ring (L^{12} , scheme 14) was an expected product. The disodium complexes of macrocyclic L^{12} was obtained as yellow viscous oil, the yield was 93.21%. The UV spectrum (in CHCl_3 , see Figure 55) showed absorption bands at 334 nm and 246 nm which could be assigned to conjugated double bonds. The IR spectrum (Figure 56) exhibited absorption bands at 1634 cm^{-1} and 1455 cm^{-1} corresponding to $\text{C}=\text{N}$ and $\text{C}=\text{C}$ stretching. The ^1H NMR (60 MHz) spectrum recorded in CDCl_3 (Figure 57) showed two groups of signals. The first group exhibited at δ 8.00-6.70 was assigned to aromatic protons and the second group exhibited at δ 4.40-2.30 was assigned to aliphatic protons. Finally, this product was transmetallated with Zn^{2+} (Wongratchasee, *et al.*, 2002), Cd^{2+} and Hg^{2+} (Chantrapomma, *et al.*, 2002) ions and single crystals for X-ray diffraction were grown.

Table 7 Crystal structure data for $[\text{Zn}_2\text{L}^{13}(\text{CH}_3\text{COO})_2] \cdot 1.75\text{C}_2\text{H}_6\text{O} \cdot 0.25\text{H}_2\text{O}$

Identification code	wb181m
Empirical formula	$\text{C}_{46} \text{H}_{56} \text{Cl}_2 \text{N}_6 \text{O}_8 \text{Zn}_2$
Formula weight	1022.61
Temperature	293(2) K
Wavelength	0.71073 Å
Crystal system, space group	$P2_1/c$
Unit cell dimensions	$a = 26.0725(4)$ Å $\alpha = 90$ deg. $b = 9.58360(10)$ Å $\beta = 103.6580(10)$ deg. $c = 19.74830(10)$ Å $\gamma = 90$ deg.
Volume	$4794.94(9)$ Å ³
Z	4
Calculated density	1.417 mg/m ³
Absorption coefficient	1.169 mm ⁻¹
F(000)	2128
Crystal size	0.54 x 0.44 x 0.26 mm
Theta range for data collection	2.44 to 28.17 deg.
Limiting indices	$-30 \leq h \leq 34$, $-12 \leq k \leq 12$, $-23 \leq l \leq 26$
Reflections collected / unique	27834 / 11348 [R(int) = 0.0799]
Completeness to theta = 28.17	96.4 %

Table 7 (continued)

Max. and min. transmission	0.7508 and 0.5708
Refinement method	Full-matrix least-squares on F^2
Data / restraints / parameters	11348 / 2 / 584
Goodness-of-fit on F^2	0.968
Final R indices [$I > 2\sigma(I)$]	R1=0.0559, wR2 = 0.1425
R indices (all data)	R1=0.0847, wR2 = 0.1566
Extinction coefficient	0.0036(4)
Largest diff. peak and hole	1.167 and -0.794 e. \AA^{-3}

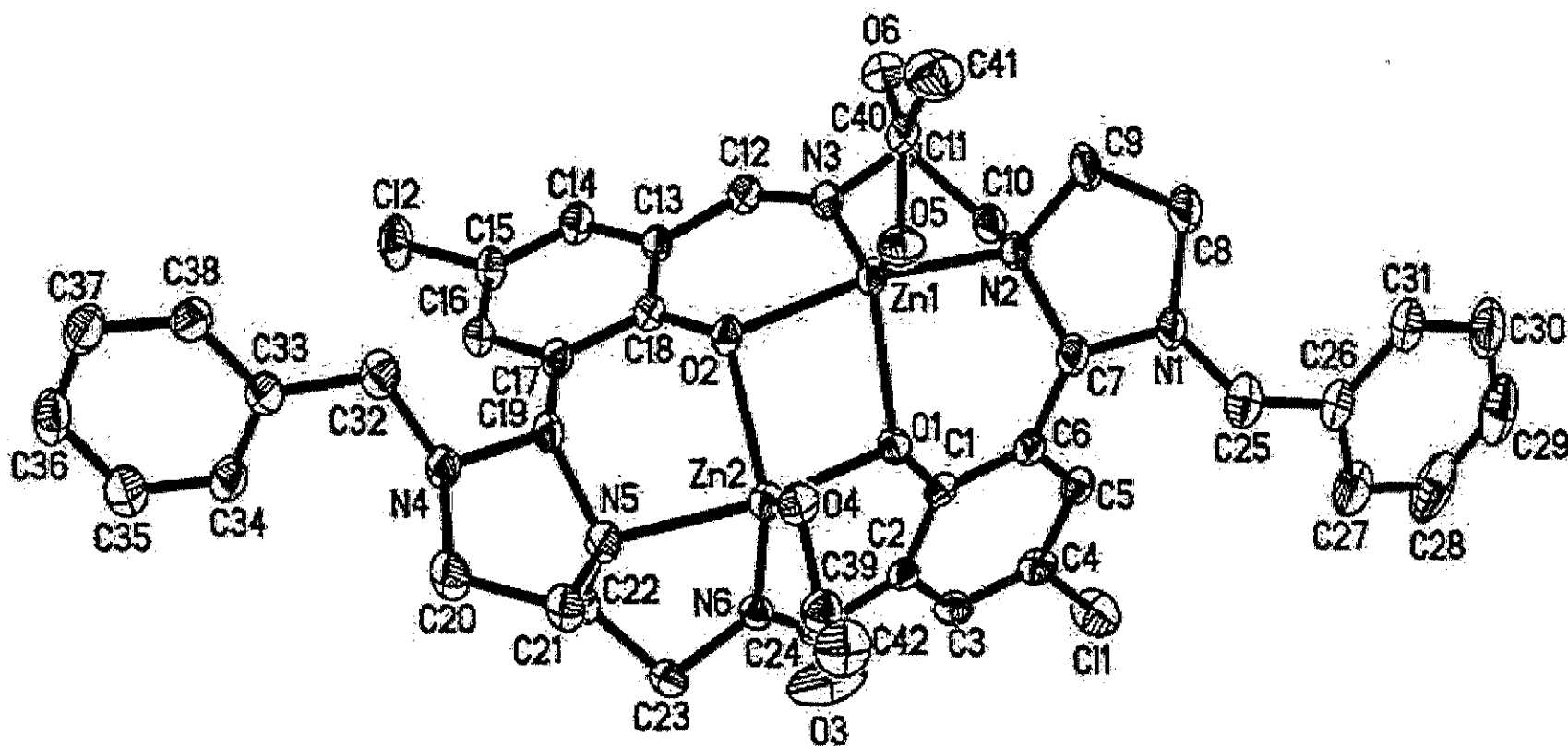


Figure 21 Crystal structure of $[Zn_2L^{13}(CH_3COO)_2] \cdot 1.75(C_2H_6O) \cdot 0.25H_2O$

Water and ethanol molecules are not shown

Table 8 Crystal structure data for $\text{Cd}_2\text{L}^{13}(\text{CH}_3\text{COO})_2$

Identification code	w176bm
Empirical formula	$\text{C}_{126} \text{H}_{142} \text{Cd}_6 \text{Cl}_6 \text{N}_{18} \text{O}_{24}$
Formula weight	3179.68
Temperature	183(2) K
Wavelength	0.71073 Å
Crystal system, space group	Triclinic, P-1
Unit cell dimensions	$a = 18.0930(10) \text{ Å}$ $\alpha = 107.035(1) \text{ deg.}$ $b = 19.8090(10) \text{ Å}$ $\beta = 89.930(1) \text{ deg.}$ $c = 23.6910(10) \text{ Å}$ $\gamma = 113.686(1) \text{ deg.}$
Volume	$7368.5(6) \text{ Å}^3$
Z	2
Calculated density	1.433 mg/m^3
Absorption coefficient	1.026 mm^{-1}
F(000)	3212
Crystal size	0.40 x 0.40 x 0.30 mm
Theta range for data collection	2.46 to 28.55 deg.
Limiting indices	$-15 \leq h \leq 23$, $-26 \leq k \leq 26$, $-31 \leq l \leq 30$
Reflections collected / unique	42272 / 31966 [R(int) = 0.1155]
Completeness to theta = 28.55	85.2 %
Absorption correction	Empirical

Table 8 (continued)

Max. and min. transmission	0.7482 and 0.6842
Refinement method	Full-matrix least-squares on F^2
Data / restraints / parameters	31966 / 0 / 1589
Goodness-of-fit on F^2	1.001
Final R indices [$I > 2\sigma(I)$]	R1=0.1168, wR2=0.2960
R indices (all data)	R1=0.1947, wR2=0.3369
Largest diff. peak and hole	2.712 and -2.349 e.Å ⁻³

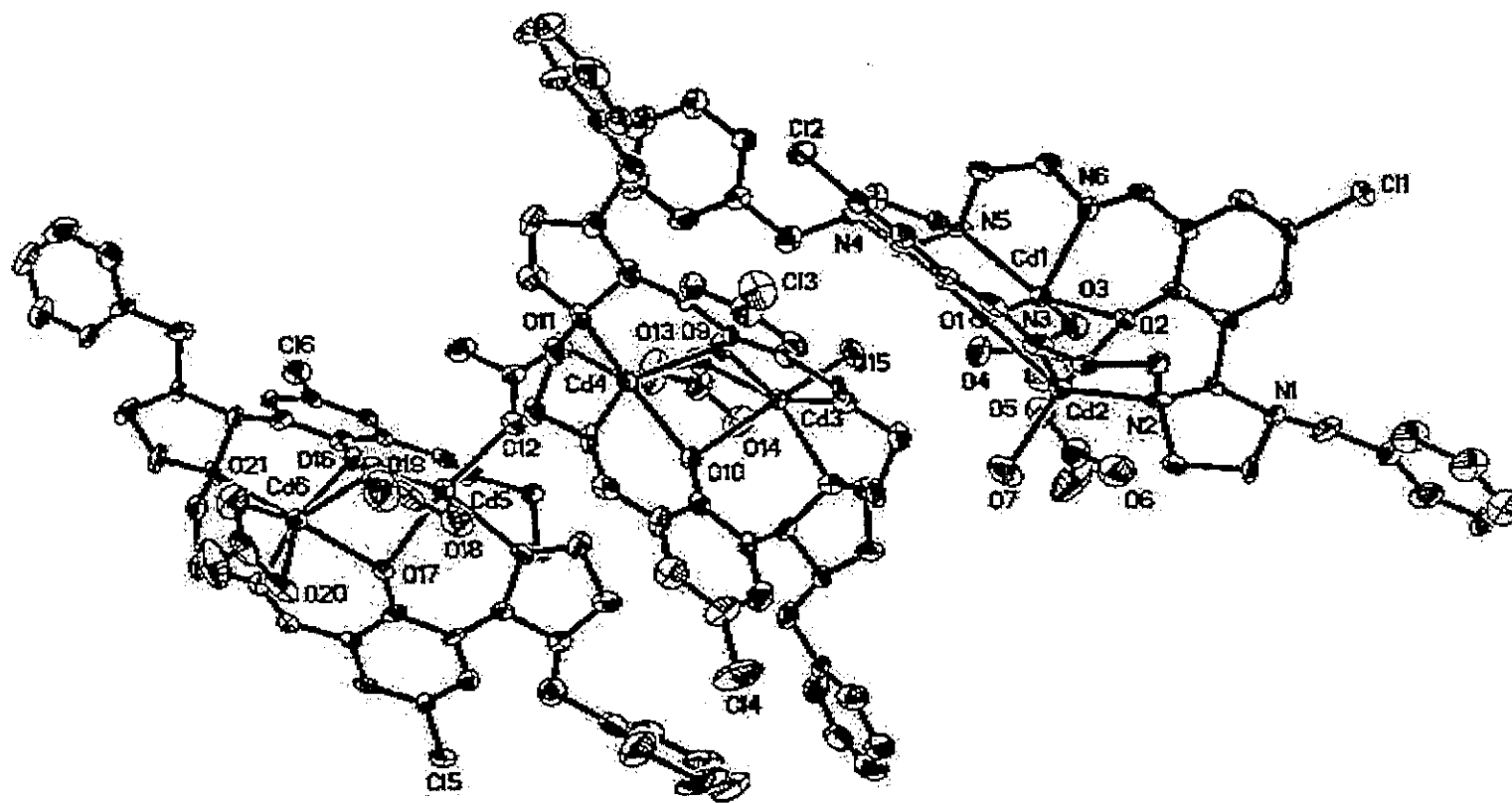
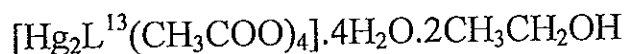


Figure 22 Crystal structure of $\text{Cd}_2\text{L}^{13}(\text{CH}_3\text{COO})_2$

Table 9 Crystal structure data for

Identification code	w172m
Empirical formula	$\text{C}_{46}\text{H}_{58}\text{Cl}_2\text{Hg}_2\text{N}_6\text{O}_{14}$
Formula weight	1391.06
Temperature	293(2) K
Wavelength	0.71073 Å
Crystal system, space group	P-1
Unit cell dimensions	$a=10.13760(10)$ Å $\alpha=87.5990(10)$ deg. $b=11.0131(2)$ Å $\beta=71.3880(10)$ deg. $c=13.4833(2)$ Å $\gamma=79.1350(10)$ deg.
Volume	$1400.79(4)$ Å ³
Z	1
Calculated density	1.649 mg/m ³
Absorption coefficient	5.632 mm ⁻¹
F(000)	682
Crystal size	0.12 x 0.10 x 0.08 mm
Theta range for data collection	2.68 to 25.00 deg.
Limiting indices	$-11 \leq h \leq 12$, $-13 \leq k \leq 12$, $-16 \leq l \leq 13$
Reflections collected / unique	6437 / 4581 [R(int) = 0.1010]
Completeness to theta =25.0	63.1

Table 9 (continued)

Max. and min. transmission	0.6614 and 0.5514
Refinement method	Full-matrix least-squares on F^2
Data / restraints / parameters	4581 / 0 / 310
Goodness-of-fit on F^2	0.943
Final R indices [$I > 2\sigma(I)$]	R1=0.0953, wR2=0.2076
R indices (all data)	R1=0.1186, wR2=0.2195
Largest diff. peak and hole	2.716 and -2.927 e. \AA^{-3}

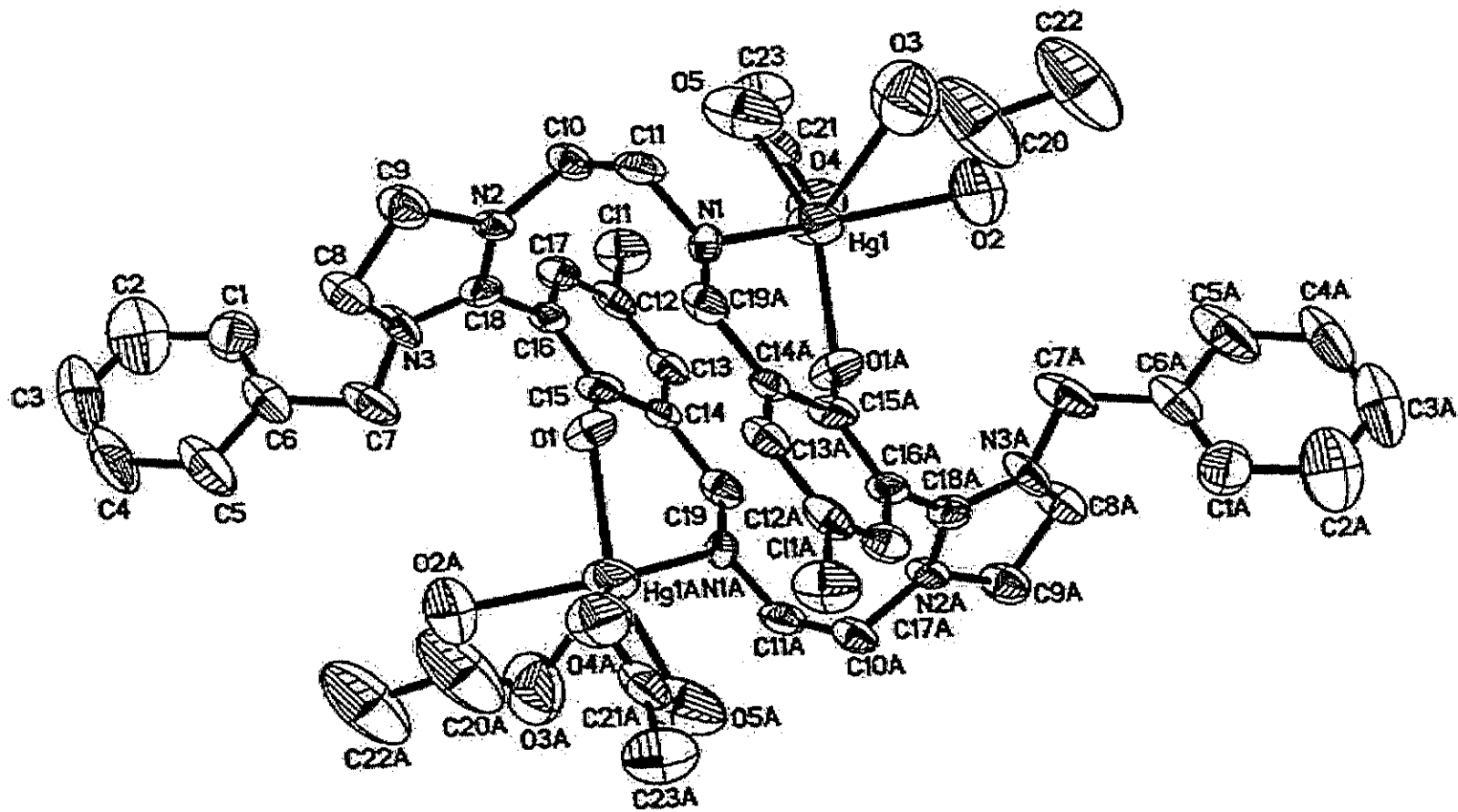
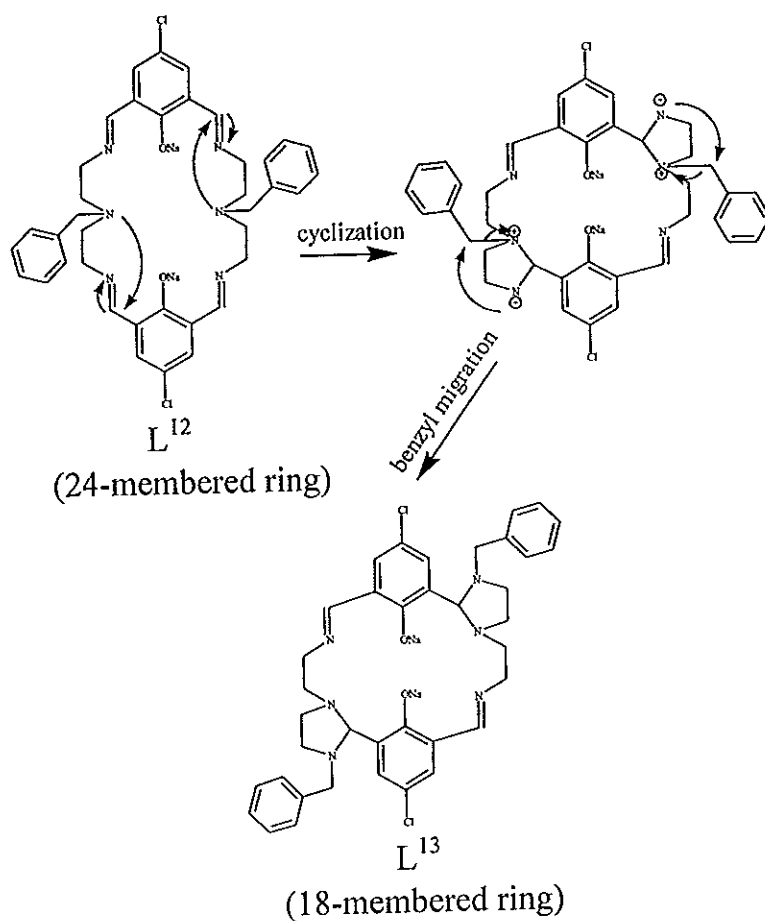


Figure 23 Crystal structure of $[\text{Hg}_2\text{L}^{13}(\text{CH}_3\text{COO})_4] \cdot 4\text{H}_2\text{O} \cdot 2\text{CH}_3\text{CH}_2\text{OH}$

Water and ethanol molecules are not shown

The X-ray data showed that these complexes possess 18-membered rings L^{13} instead of the expected 24-membered rings L^{12} . We proposed that the formation of 18-membered rings L^{13} was a result of ring contraction of the initially-formed 24-membered rings L^{12} by two possible pathways.

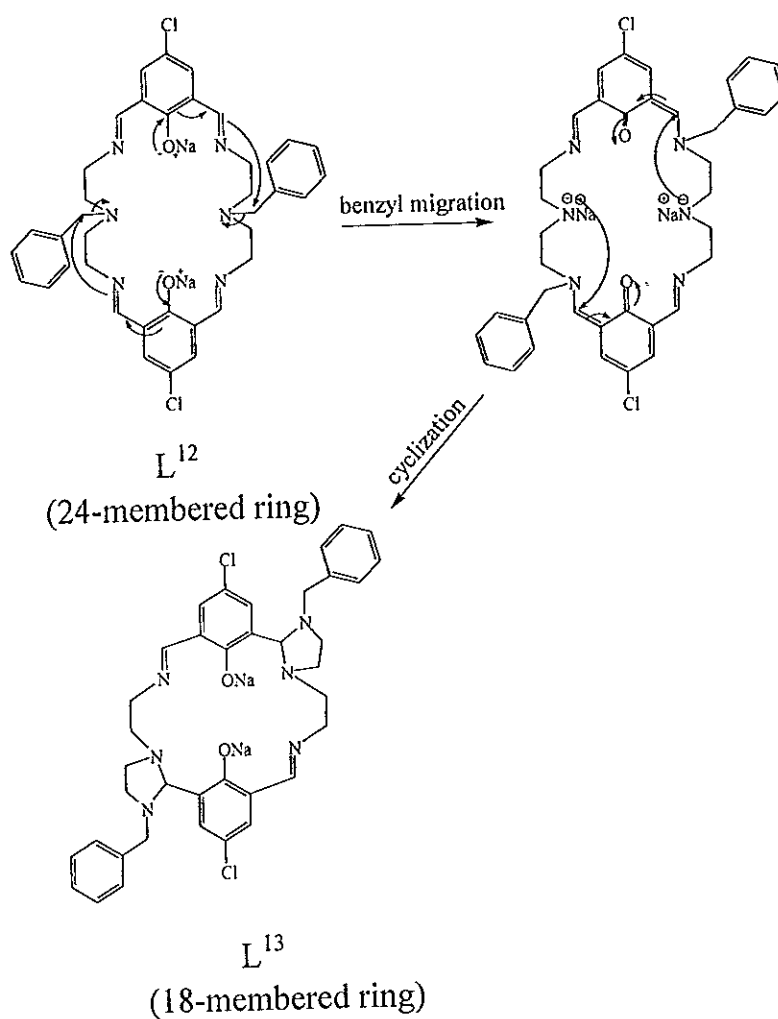
Pathway I



Scheme 16 The formation of 18-membered ring (L^{13}) (pathway I)

Cyclization occurred by the nucleophilic addition of tertiary amine groups across the C=N bond to form two imidazolidine rings followed by the benzyl migration between the two nitrogen atoms (see Scheme 16).

Pathway II



Scheme 17 The formation of 18-membered ring (L¹³) (pathway I)

Benzyl migration occurred first followed by a cyclization (see Scheme 17).

Conclusion

1. Reaction between sodium 4-substituted-2,6-diformylphenoxide and polyamines resulted in a [2+2] cyclocondensation product.
2. We successfully synthesized 18-, 20- and 22-membered ring macrocyclic complexes by varying the number of carbons in polyamine.
3. [2+2] Cyclocondensation between 4-chloro-2,6-diformylphenoxide and N³-(benzyl)diethylenetriamine-trihydrochloride gave an unexpected 18-membered ring macrocyclic complexes which we proposed to occur by ring contraction of the initially formed 24-membered ring by two possible pathways.

BIBLIOGRAPHY

- Adams, H. ; Bailey, N.A. ; Bertrand, P. ; Collinson, S.R. ; Fenton, D.E. ; Kitchen, S. 1996. "Unexpected Ring Contraction in the Barium-Assisted Cyclocondensation of 2,6-diformylpyridine and N,N-bis(2-aminoethyl)-2-phenylethylamine", *J. Chem. Soc. Dalton Trans.* 1181-1183.
- Adams, H. ; Bailey, N.A. ; Fenton, D.E. ; Good, R.J. ; Moody, R. ; Rodriguez de Barbarin, C.O. 1987. "Complexes of Ligands Providing Endogenous Bridges. The Syntheses and Crystal Structures of Barium and Lead (II) Complexes of Macrocyclic Schiff Bases derived from Heterocyclic Dicarboxyls and 1,N-Diamino-N'-hydroxyalkanes (N,N' = 3,2; 4,2; or 5,3) †", *J. Chem. Soc. Dalton Trans.* 207-218.
- Bright, D. ; Truter, M. R. 1970. "Crystal Structures of Complexes between Alkali-metal Salts Cyclic Polyethers. Part I. Complex between Rubidium Sodium Isothiocyanate and 2,3,11,12-Dibenzo-1,4,7,10,13,16-hexaoxocyclo-octadeca-2,11-diene ('Dibenzo-18-crown-6')", *J. Chem. Soc. (B)*. 1544-1550.
- Bush, M. A. ; Truter, M. R. 1972. "Crystal Structures of Complexes between Alkali-metal Salts and Cyclic Polyethers. Part IV.¹ The Crystal Structures of Dibenzo-30-crown-10(2,3:17,18-dibenzo-1,4,7,10,13,16,19,22,25,28-decaoxacyclotriaconta-2,17-diene) and of its Complex with Potassium Iodide", *J. Chem. Soc. Perkin*. 345-350.

- Cabiness, D.K. ; Margerum, D.W. 1996. "Macrocyclic Effect on the Stability of Copper(II) Tetramine Complexes", *J. Am. Chem. Soc.* 91(23), 6540-6541.
- Chantrapromma, S. ; Fun, H.K. ; Usman, A. ; Karalai, C. ; Wongratchasee, W. ; Ponglimanont, C. ; Gou, S. 2002. "Unexpected Ring Contraction in a Dinuclear mercury (II) Complex of a Pendant-arm Macrocyclic Complex", *Acta Cryst.* E58, m206-m208.
- Dietrich, B. ; Viout, P. ; Lehn, J.-M. 1993. Macrocyclic Chemistry. pp. 9, New York: VCH Verlagsgesellschaft mbH, Weinheim (Federal Republic of Germany) VCH Publishers, Inc.
- Dietrich, B. ; Viout, P. ; Lehn, J.-M. 1993. Macrocyclic Chemistry. pp. 71, New York: VCH Verlagsgesellschaft mbH, Weinheim (Federal Republic of Germany) VCH Publishers, Inc.
- Dietrich, par B. ; Lehn, J.M. ; Sauvage, J.P. 1969. "Diaza-polyoxa-Macrobicycles", *Tetrahedron Lett.* 30, 2885-2888.
- Drew, M. G. B. ; Nelson, J. ; Nelson, S. M. 1981. "Metal-ion-controlled Transamination in the Synthesis of Macrocyclic Schiff-base Ligands. Part 2¹. Stepwise Synthesis, Ring Expansion/Contraction, and the Crystal and Molecular Structure of a Ten-coordinate Barium (II) Complex", *J. Chem. Soc. Dalton Trans.* 1678-1684.

- Gou, S. ; Fenton, D.E. 1994. "A novel Sodium Template Approach for Preparing Tetraimine Macrocycles of 2,6-diformyl-4-methylphenol and Diamino Derivative", *Inorg. Chim. Acta.* 223, 169-172.
- Gou, S. ; Adams, H. ; Bailey, N. A. ; Bertrand, P. ; Feton, D. V. ; Rodriguez de Barbaring, C. O. 1995. "Dinuclear Zinc (II) Complexes of Robson Macrocycle †", *J. Chem. Soc. Dalton Trans.* 275-279.
- Hill, W. ; Carothers, W.H. 1933. "Studies of Polymerization. XIX.¹ Many-Membered Cyclic Anhydrides", *J. Am. Chem. Soc.* 55, 5023-5042.
- Illuminati, G. ; Mandolini, L. ; Masci, B. 1974. "Ring-Closure Reaction. II.¹ Kinetics of Six- to Ten-membered Ring Formation from *o-ω*-Bromoalkoxyphenoxides", *J. Chem. Soc.* 6, 1422-1427.
- Liebman, J.F. ; Greenberg, A. 1976. "A Survey of Strained Organic Molecules", *Chem. Rev.* 76(3), 311-365.
- Menif, R. ; Martell, A. E. ; Squattrito, P. J. ; Clearfield, A. 1990. "New Hexaaza Macrocyclic Binucleating Rings. Oxygen Insertion with a Dicopper (I) Schiff-base Macrocyclic Complex", *Inorg. Chem.* 29, 4723-4729.

- Nelson, S.M. ; Knox, C.V. ; McCann, M. 1981. "Metal-ion-controlled Transamination in the Synthesis of Macrocyclic Schiff-base Ligands. Part 1. Reactions of 2,6-Diacetylpyridine and Dicarboxyl Compounds with 3,6-Dioxaoctane-1,8-diamine", *J. Chem. Soc. Dalton Trans.* 1669-1677.
- Simmons, H.D. ; Park, C.H. 1968. "Macrocyclic amines. I. *out-in* Isomerism of 1,($k + 2$)-Diazabicyclo[$k.l.m$]alkanes", *J. Am. Chem. Soc.* 90(9), 2428-2429.
- Truter, M. R. ; Mallinson, P. R. 1972. "Crystal Structures of Complexes between Alkali-metal Salts and Cyclic Polyethers. Part V.¹ The 1:2 Complex formed between Potassium Iodide and 2,3,5,6,8,9,11,12-Octahydro-1,4,7,10,13-benzopenta Pentadecin (Benzo-15-crown-5)", *J. Chem. Soc.* 1818-1823.
- Winnik, M.A. 1981. "Cyclization and the Conformation of Hydrocarbon Chains", *Chem. Rev.* 81, 491-524.
- Wongratchasee, W. ; Chantrapromma, S. ; Fun, H.K. ; Usman, A. ; Karalai, C. ; Ponglimanont, C. ; Chantrapromma, K. 2002. "Ring Contraction in a Dinuclear zinc (II) Complex of a Robson Macrocycle", *Acta Cryst.* E58, m344-m346.

APPENDIX

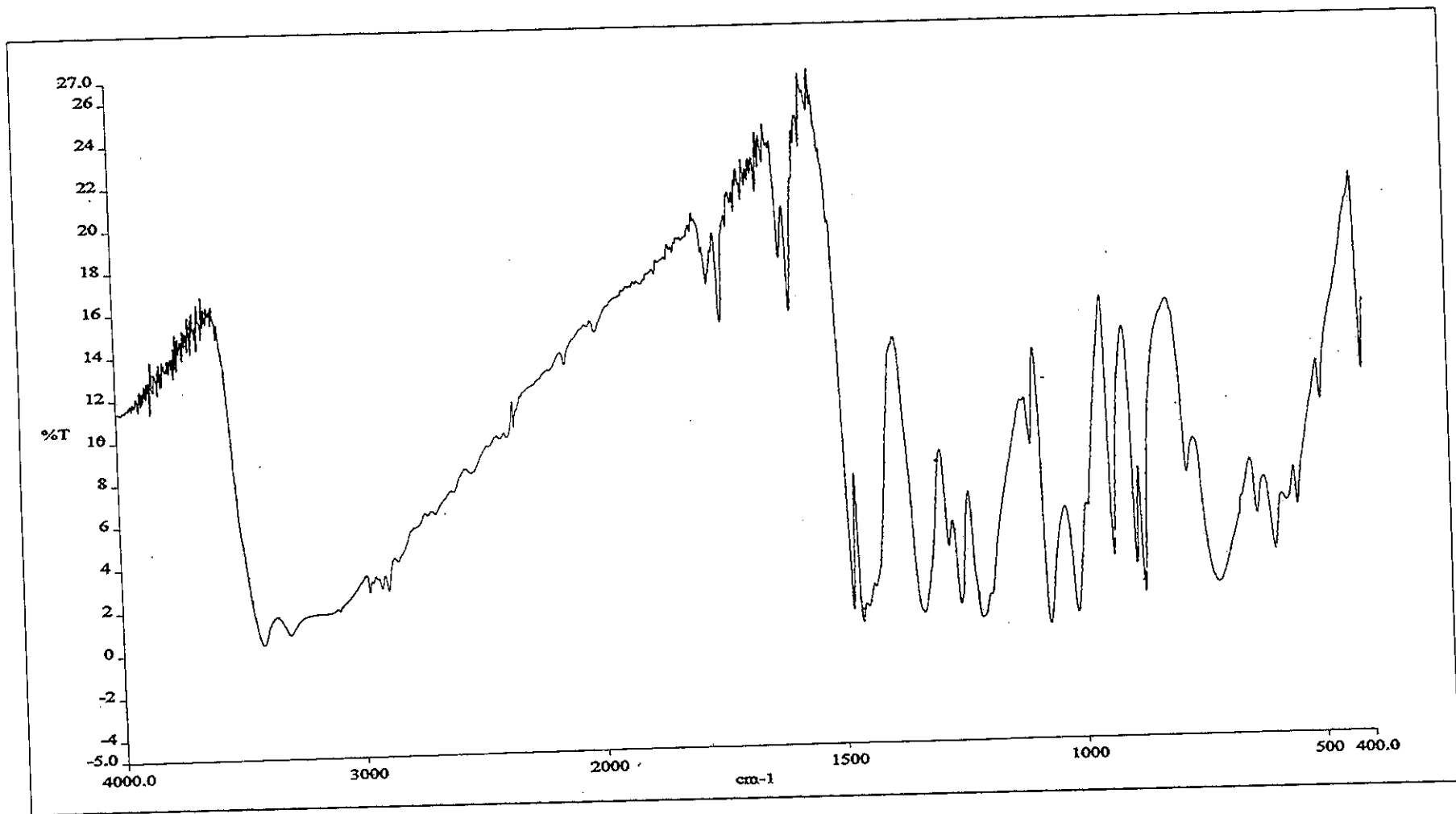


Figure 24 FTIR spectrum (KBr pellets) of 4-chloro-2,6-bis(hydroxymethyl)phenol (9a)

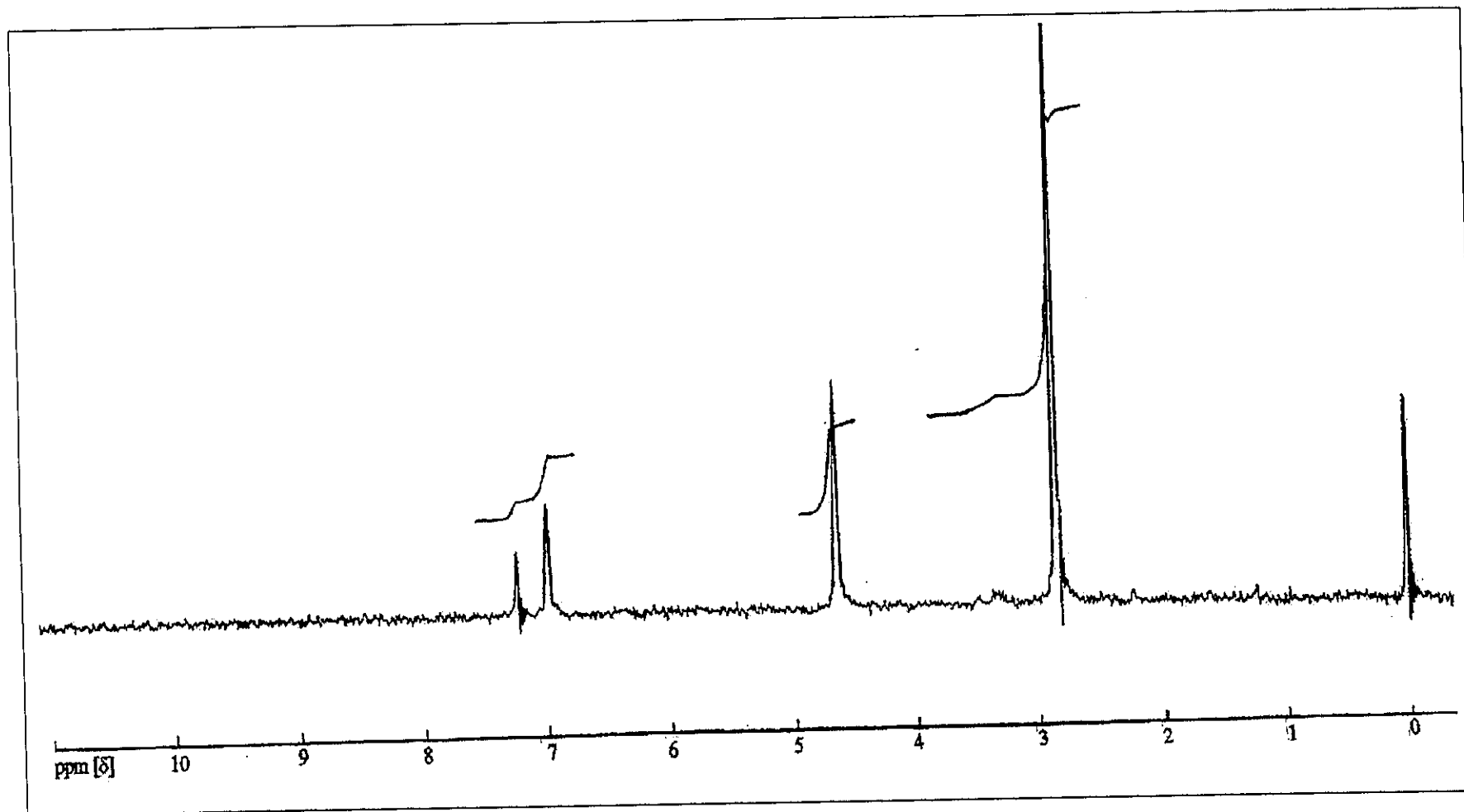


Figure 25 ^1H NMR spectrum (CDCl_3) of 4-chloro-2,6-bis(hydroxymethyl)phenol (9a)

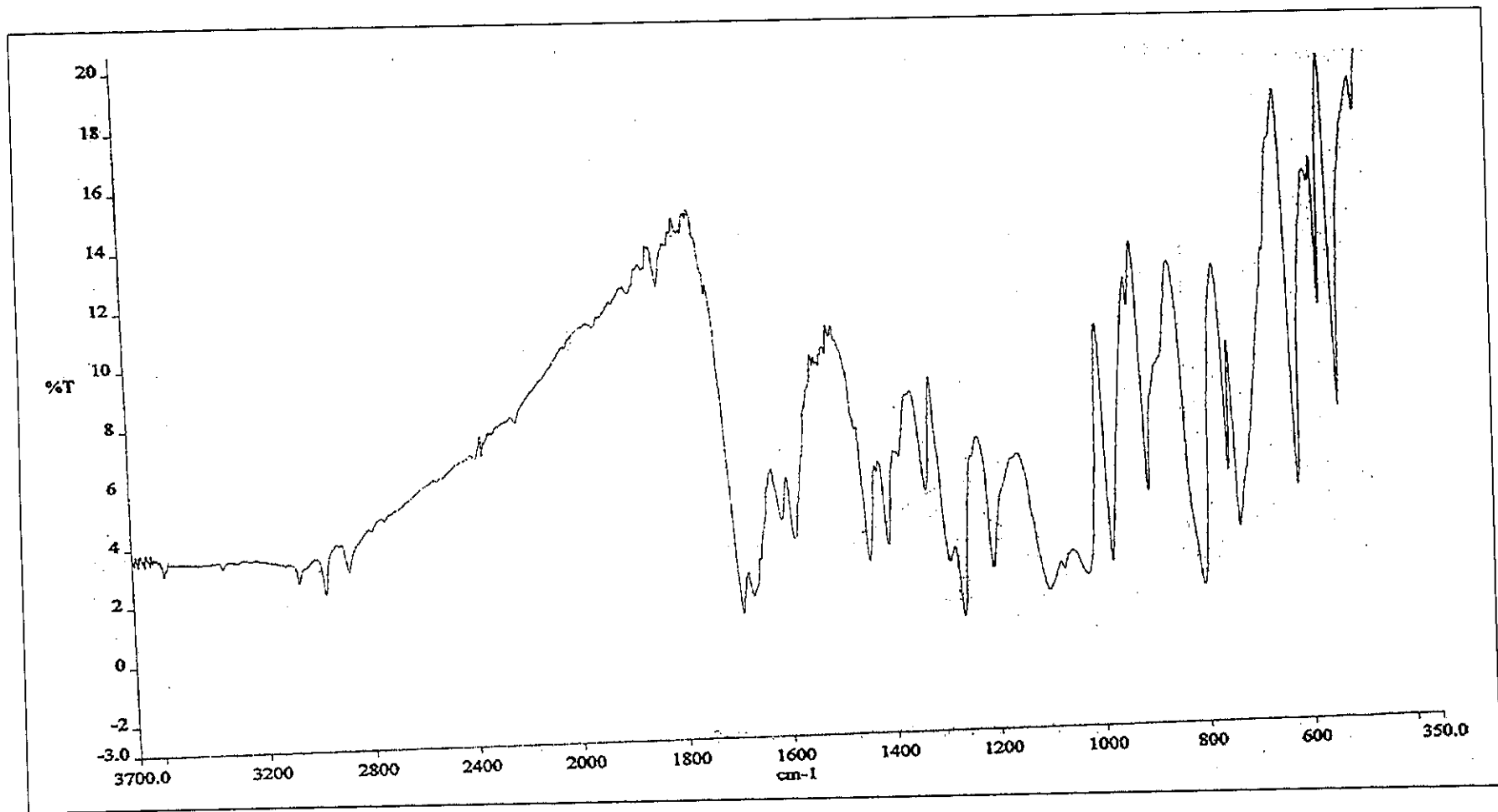


Figure 26 FTIR spectrum (KBr pellets) of 4-methyl-2,6-diformylphenol (10a)

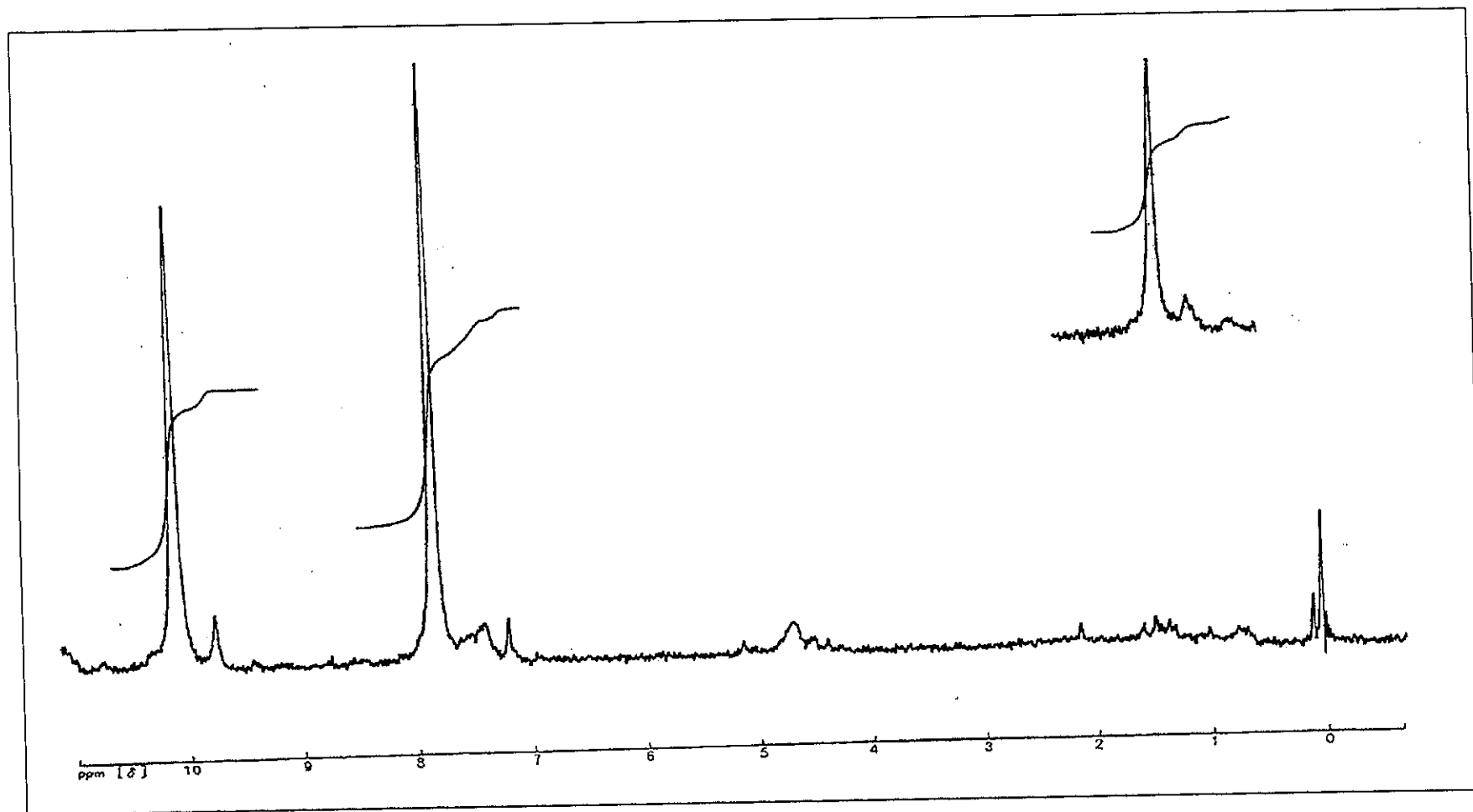


Figure 27 ^1H NMR spectrum (CDCl_3) of 4-chloro-2,6-diformylphenol (10a)

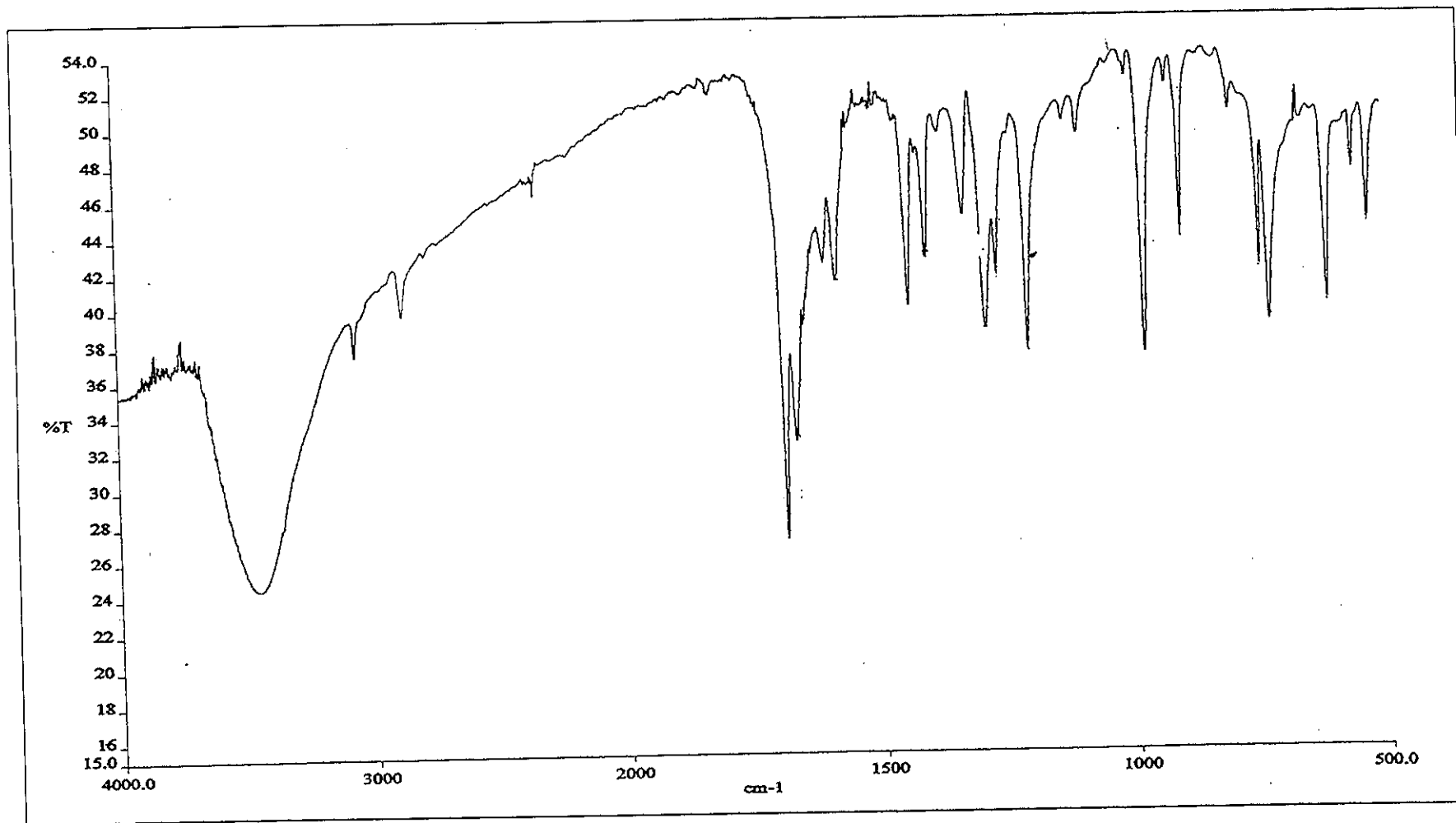


Figure 28 FTIR spectrum (KBr pellets) of 4-chloro-2,6-diformylphenoxide (11a)

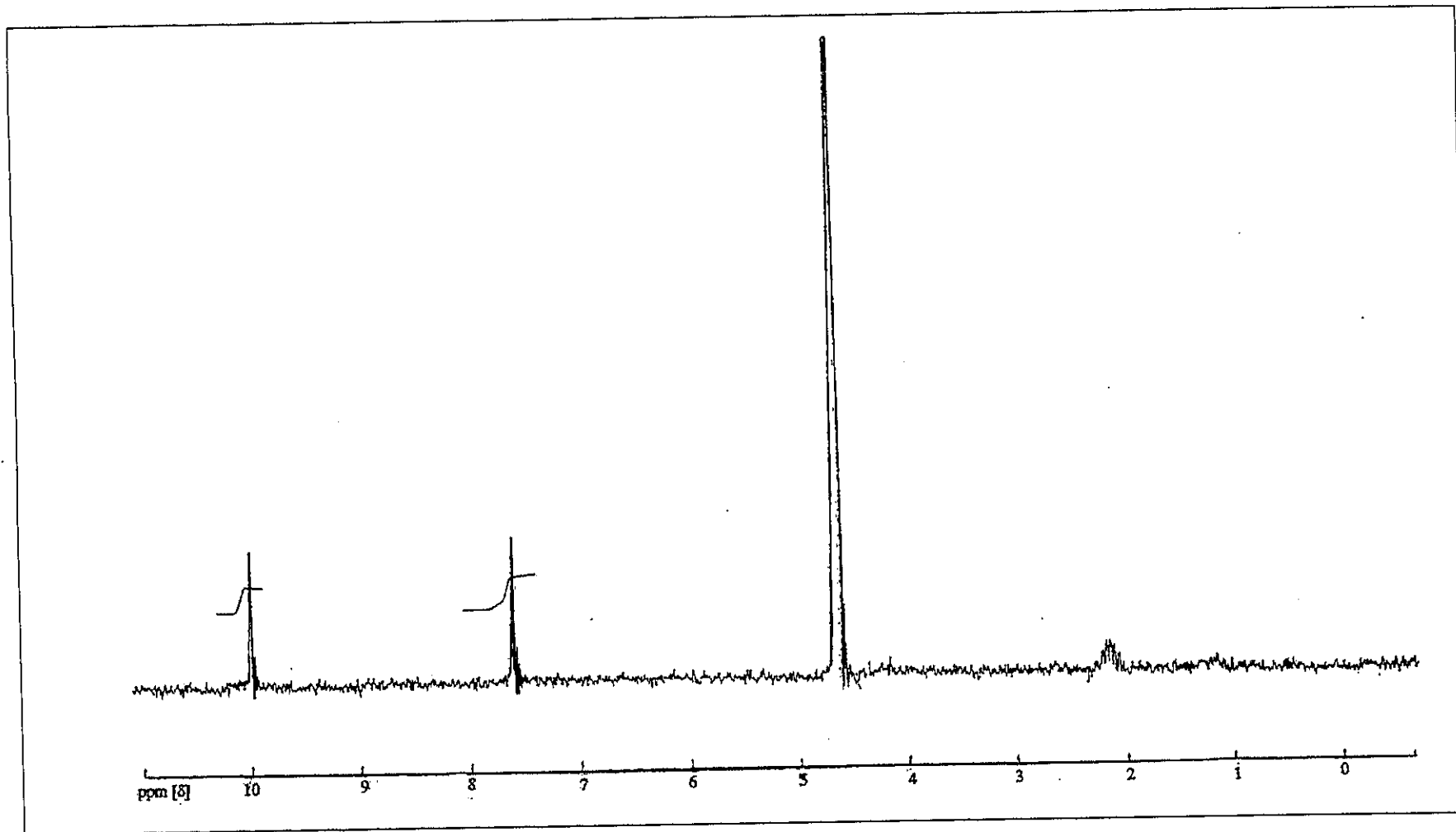


Figure 29 ^1H NMR spectrum ($\text{D}_2\text{O} + \text{CD}_3\text{COCD}_3$) of 4-chloro-2,6-diformylphenoxide (11a)

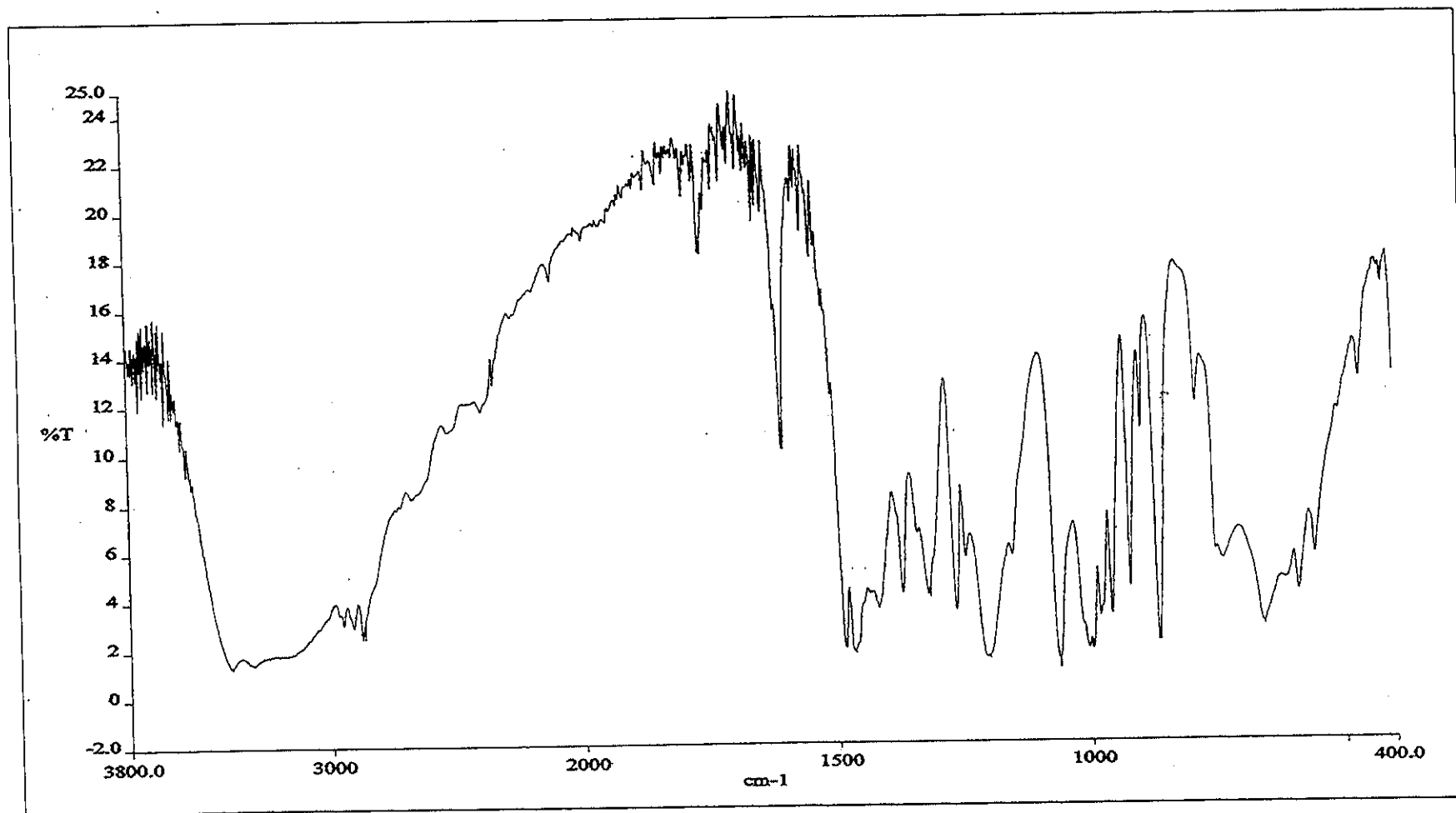


Figure 30 FTIR spectrum (KBr pellets) of 4-methyl-2,6-bis(hydroxymethyl)phenol (9b)

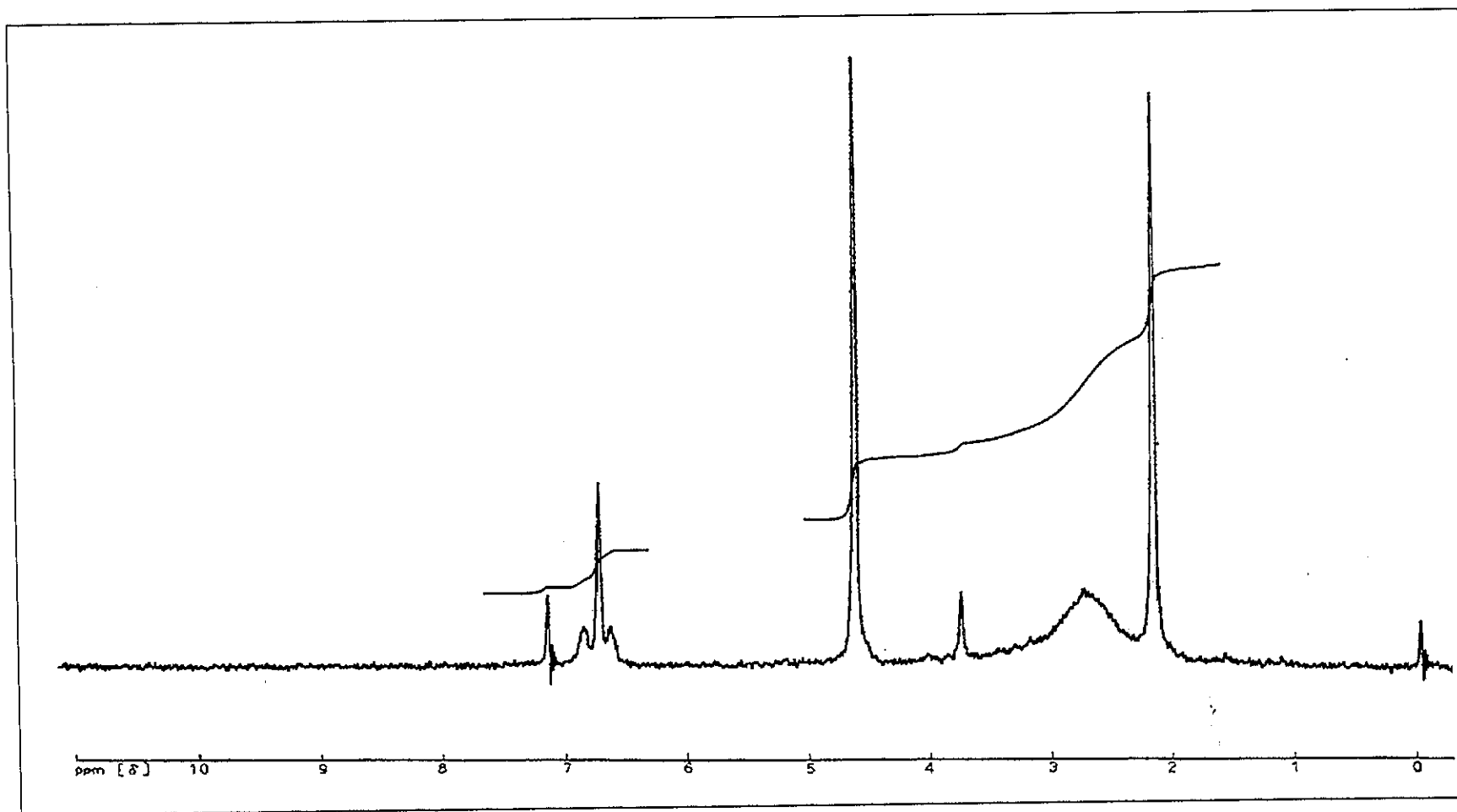


Figure 31 ^1H NMR spectrum (CDCl_3) of 4-methyl-2,6-bis(hydroxymethyl)phenol (9b)

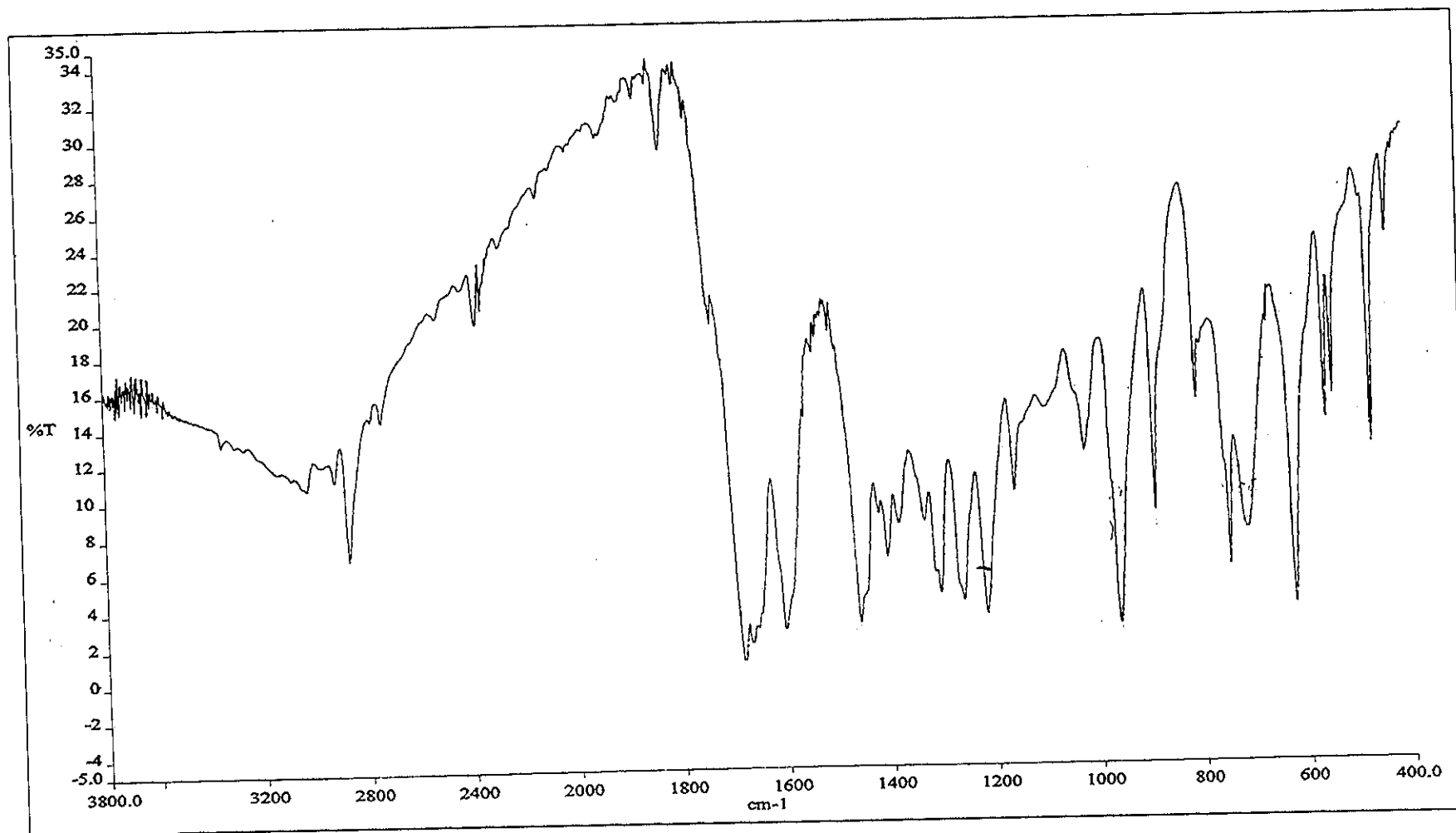


Figure 32 FTIR spectrum (KBr pellets) of 4-methyl-2,6-diformylphenol (10b)

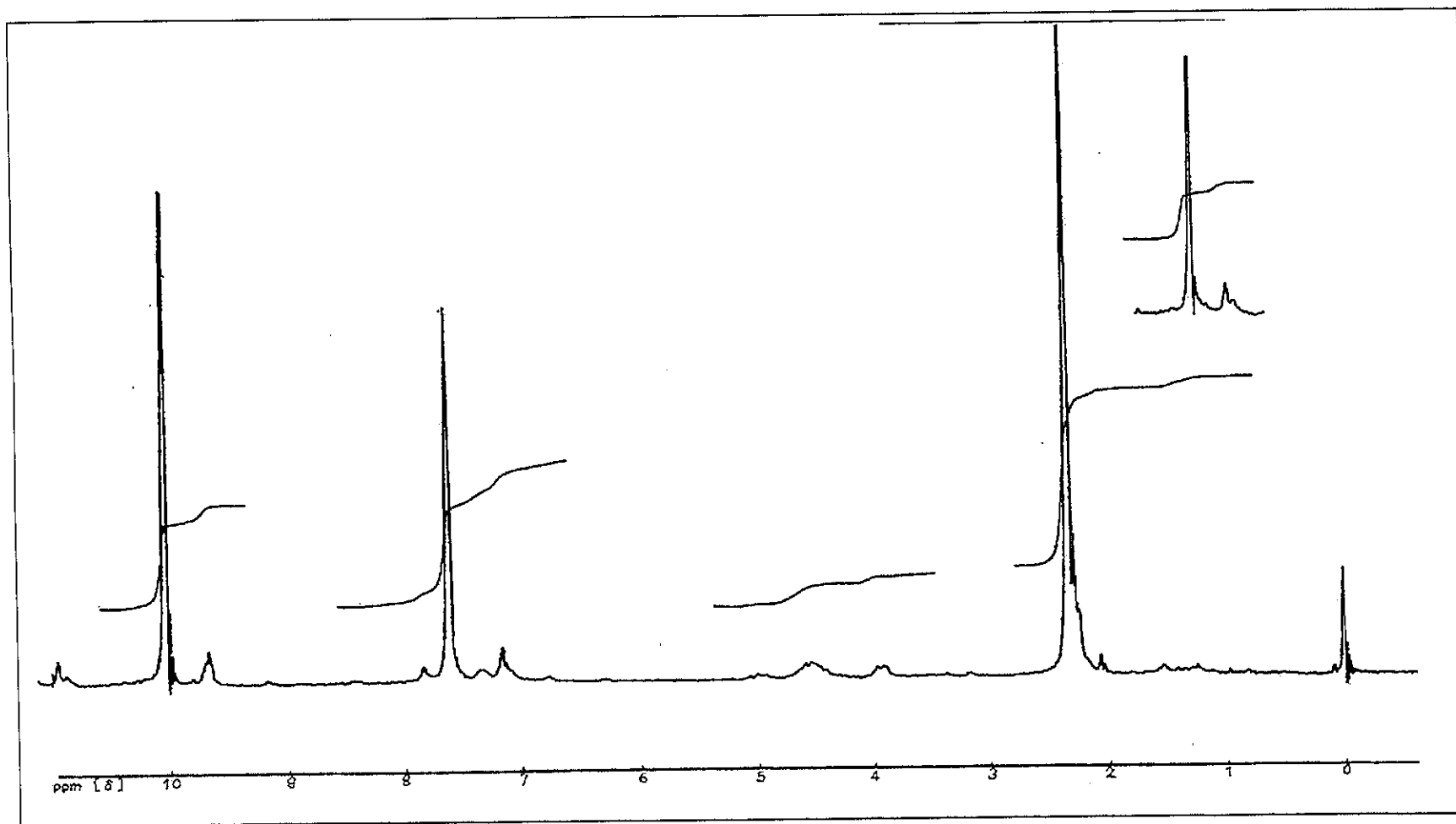


Figure 33 ^1H NMR spectrum (CDCl_3) of 4-methyl-2,6-diformylphenol (10b)

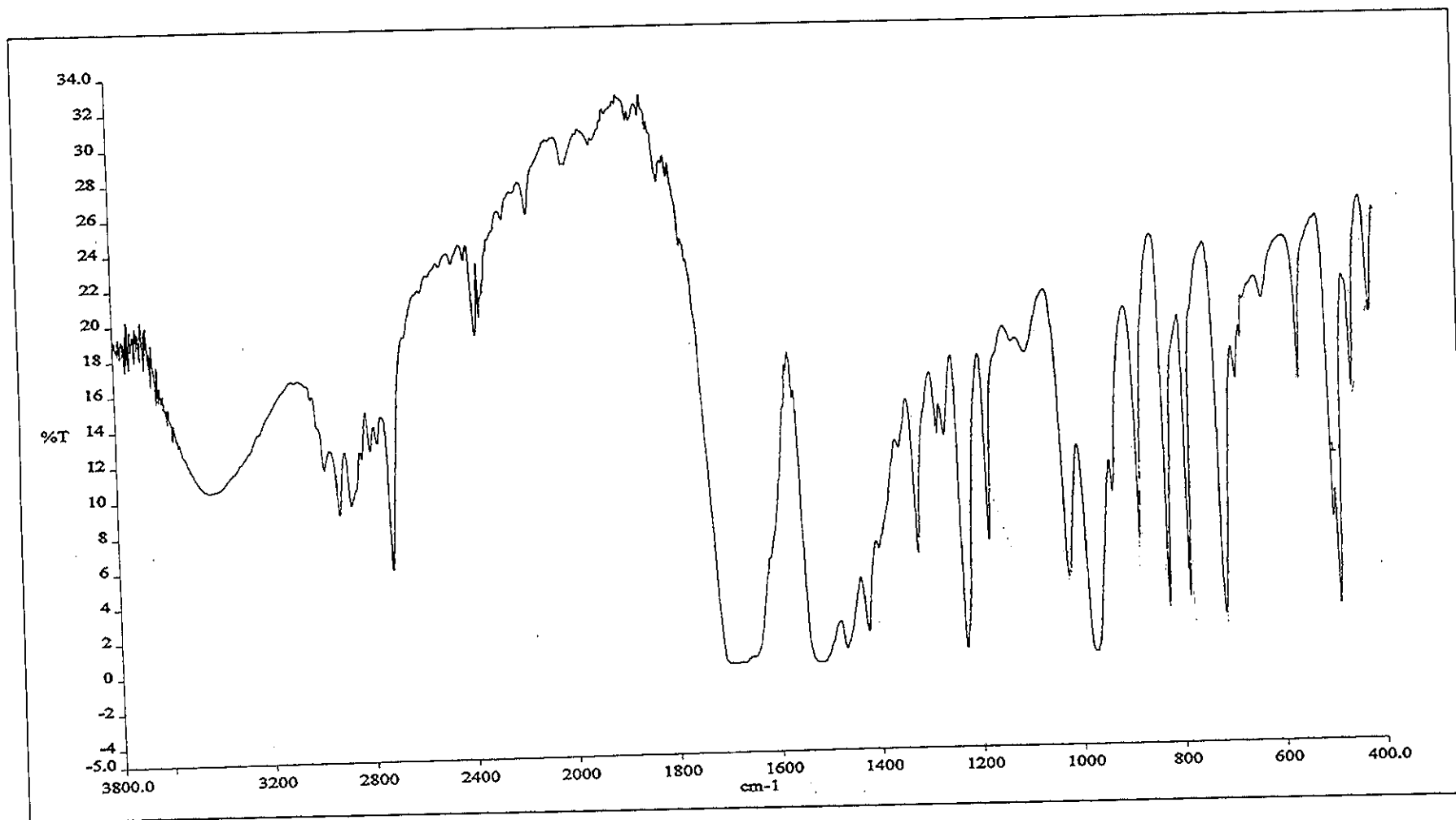


Figure 34 FTIR spectrum (KBr pellets) of 4-methyl-2,6-diformylphenoxide (11b)

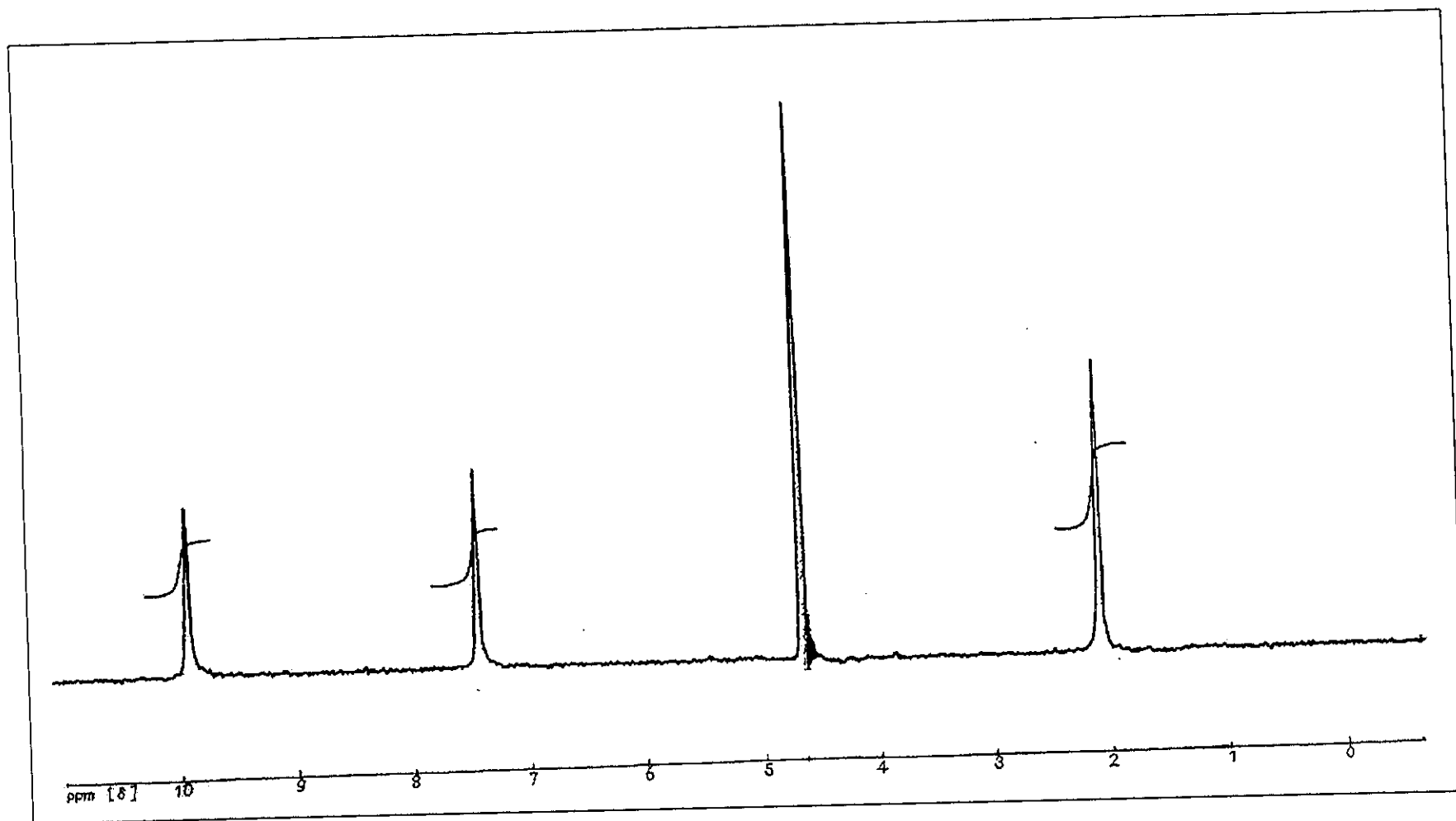


Figure 35 ^1H NMR spectrum (D_2O) of 4-methyl-2,6-diformylphenoxide (11b)

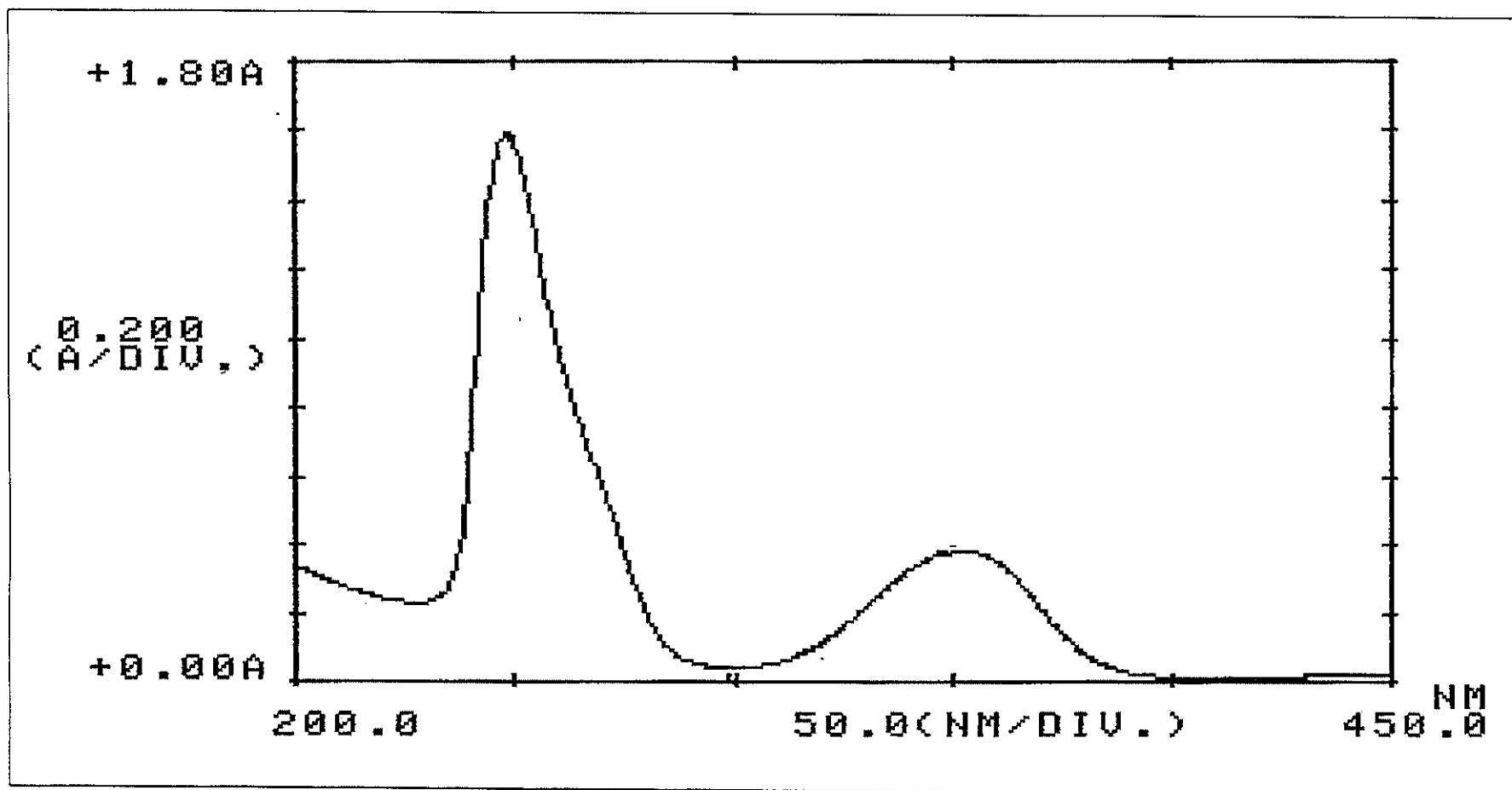


Figure 42 UV spectrum (CHCl₃) of disodium complex of macrocyclic ligand L¹⁰

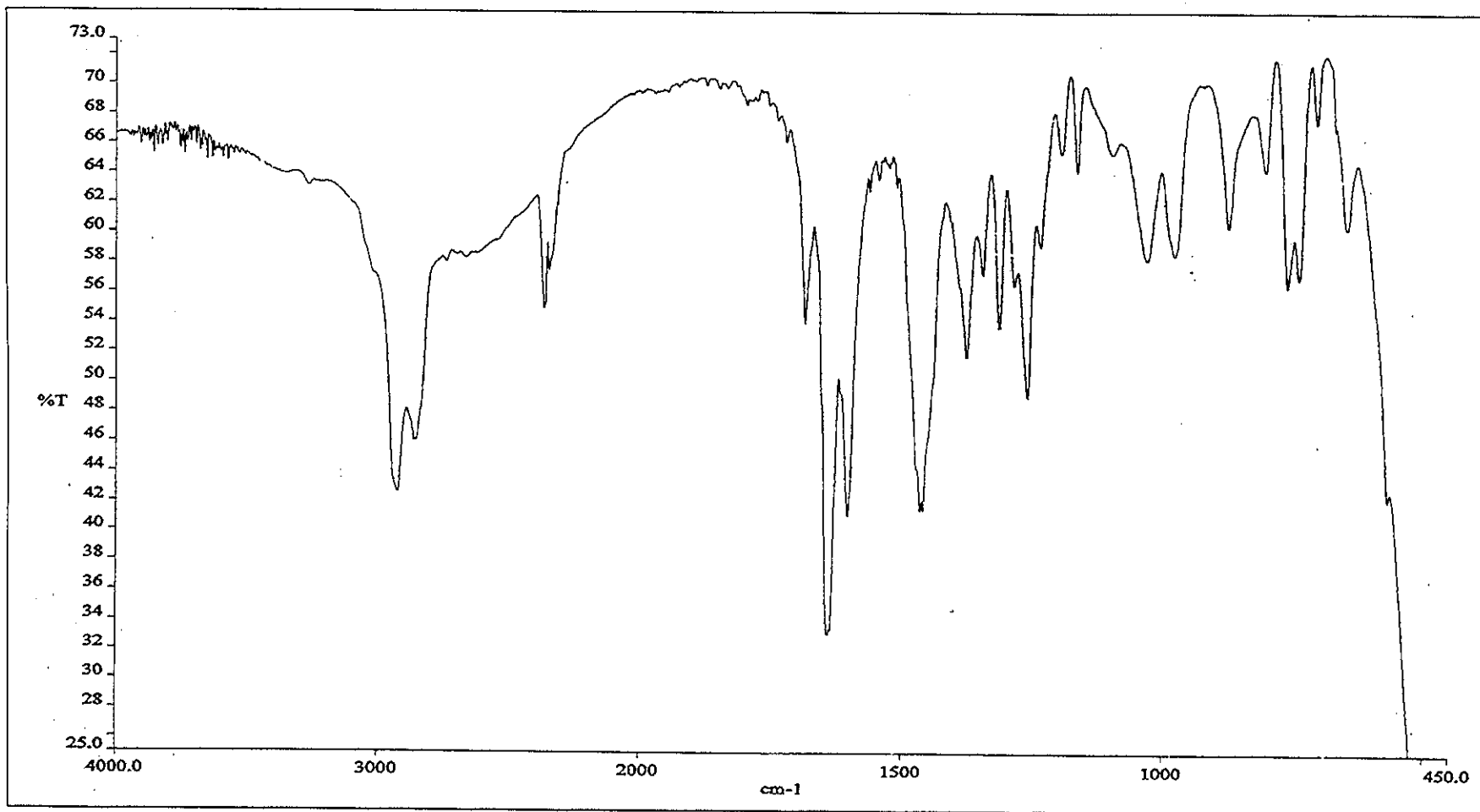


Figure 43 FTIR spectrum (neat) of disodium complex of macrocyclic ligand L¹⁰

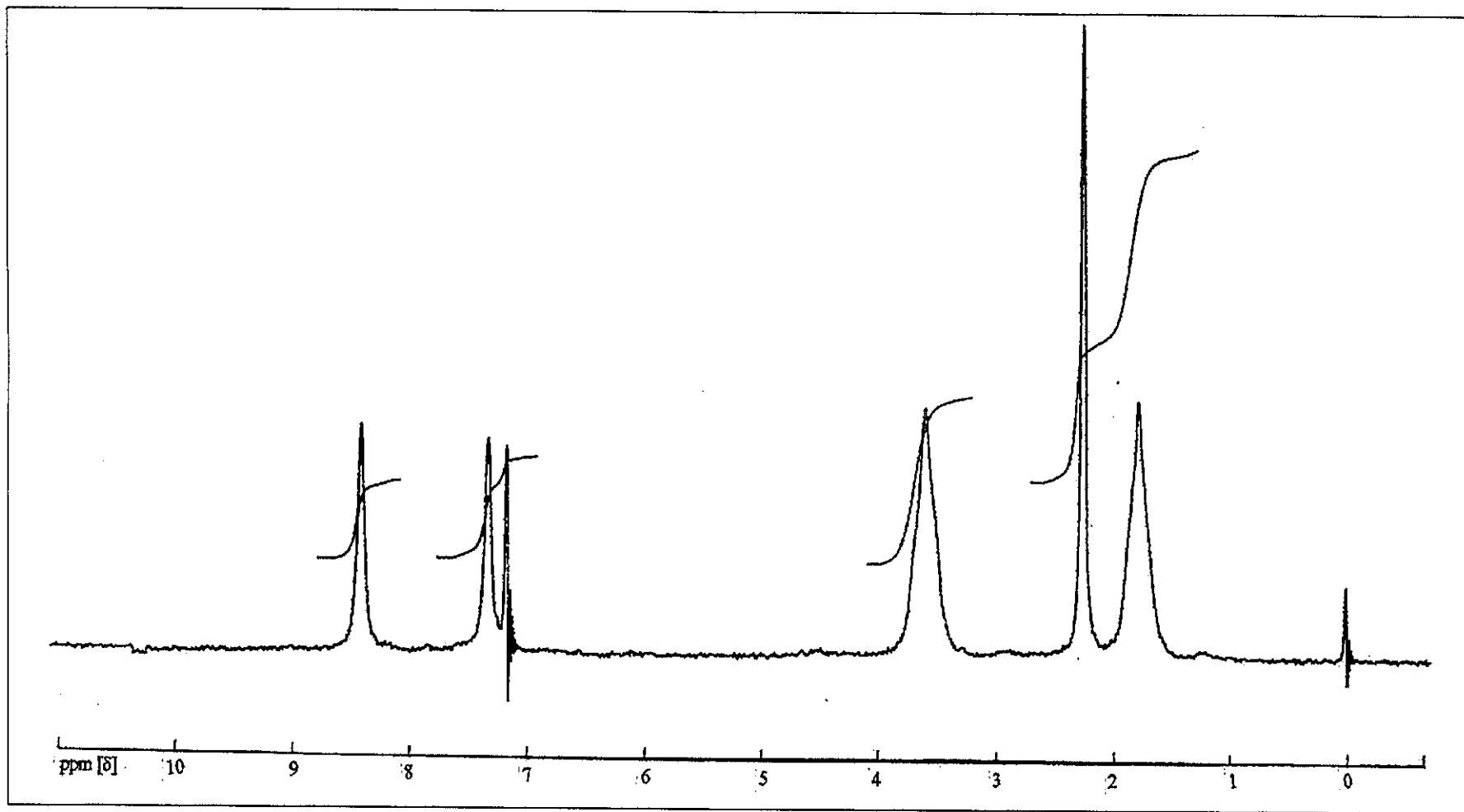


Figure 44 ^1H NMR spectrum (CDCl_3) of disodium complexes of macrocyclic ligand L^{10}

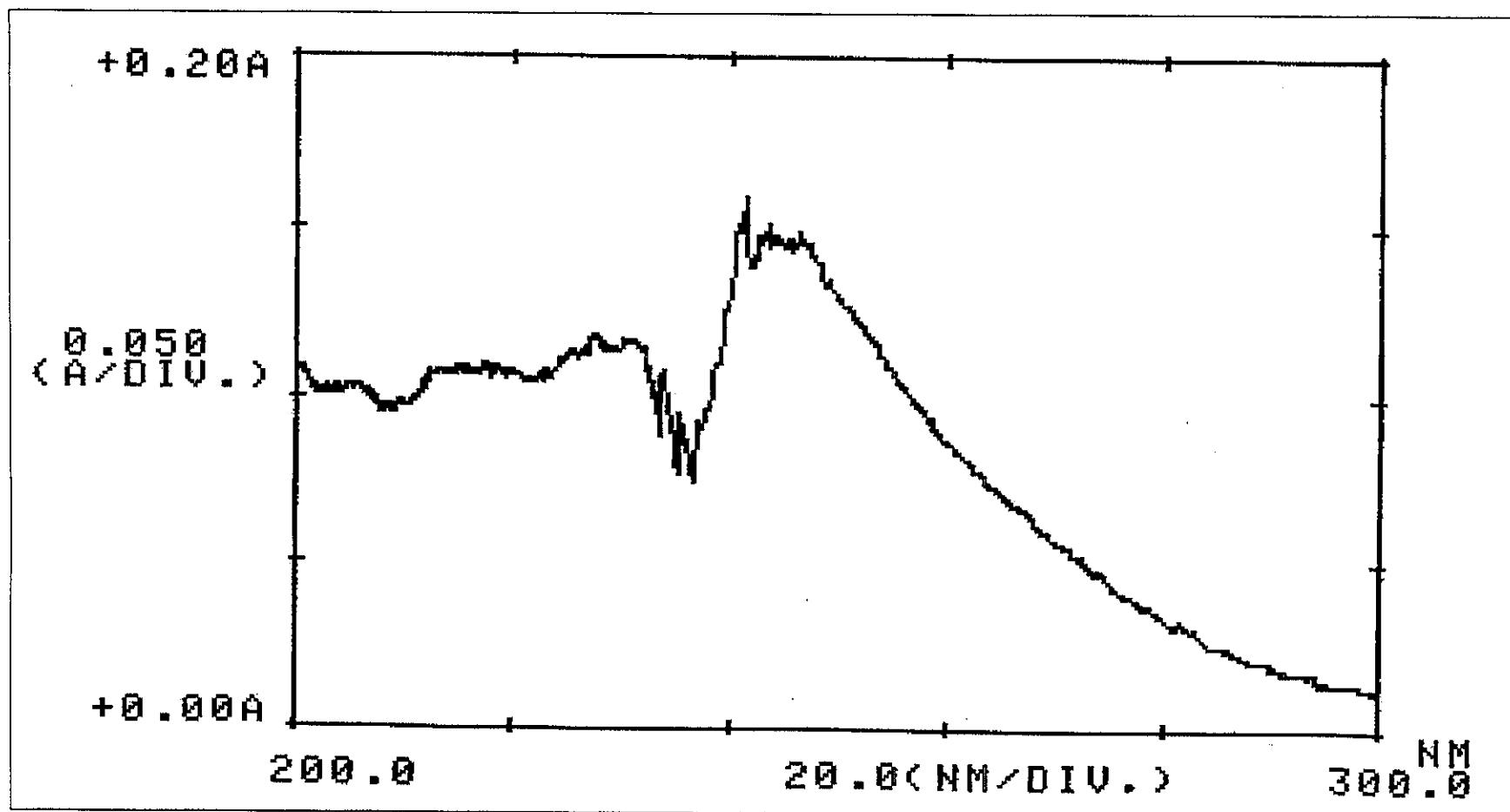


Figure 45 UV spectrum (CHCl_3) of disodium complex of macrocyclic ligand L^{11a}

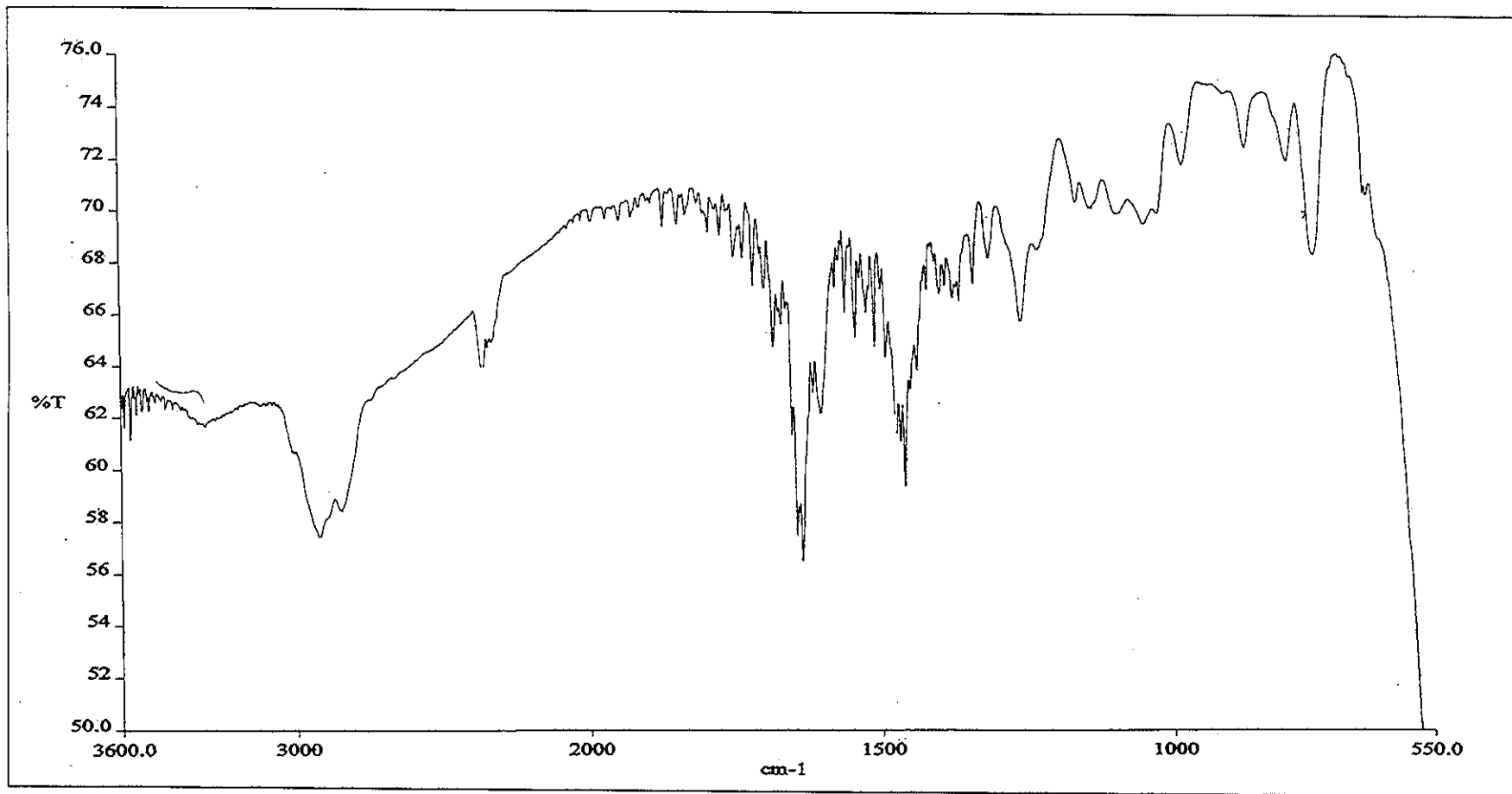


Figure 46 FTIR spectrum (neat) of disodium complex of macrocyclic ligand L^{11a}

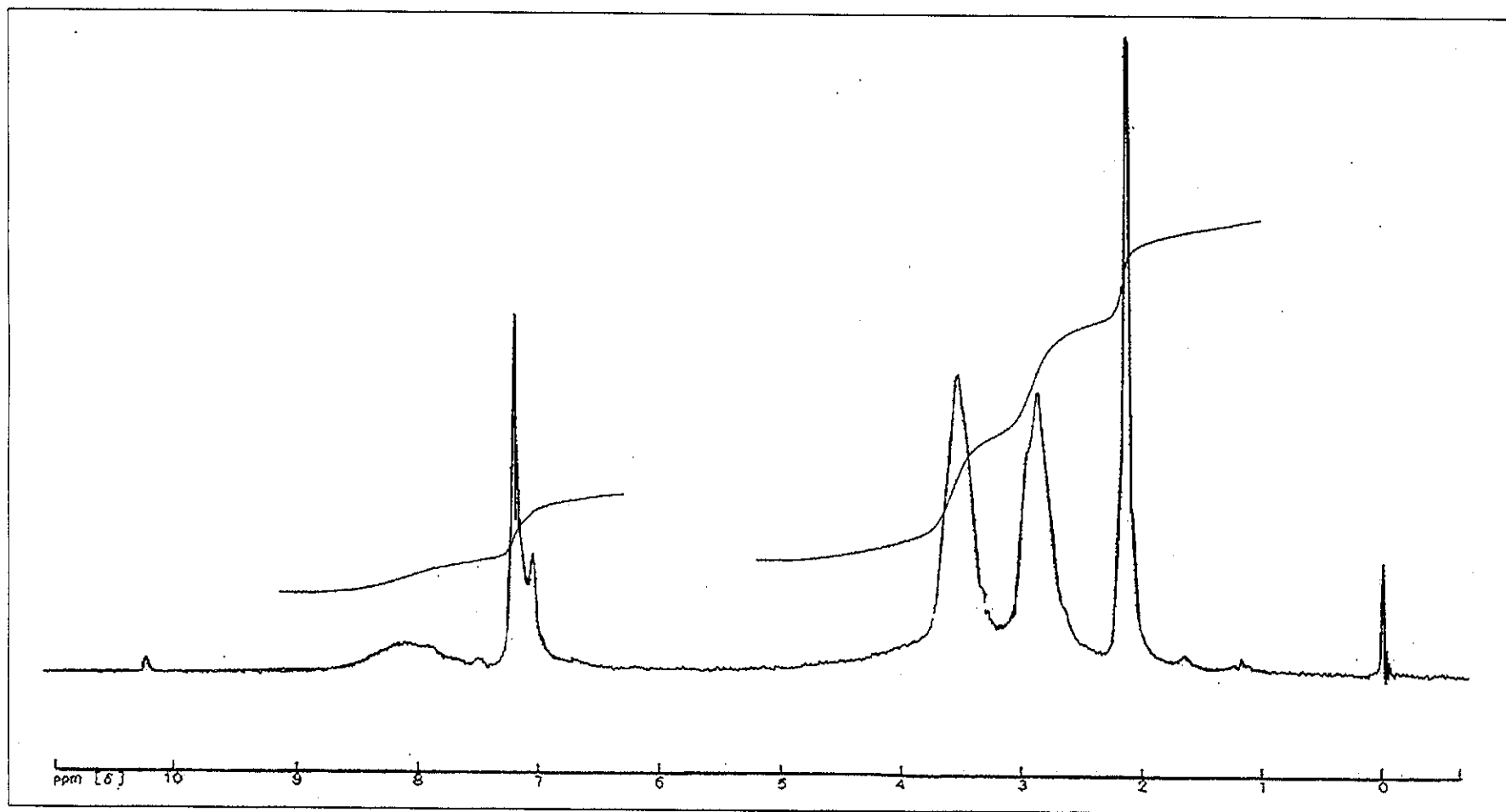


Figure 47 ^1H NMR spectrum (CDCl_3) of disodium complexes of macrocyclic ligand $\text{L}^{11\text{a}}$

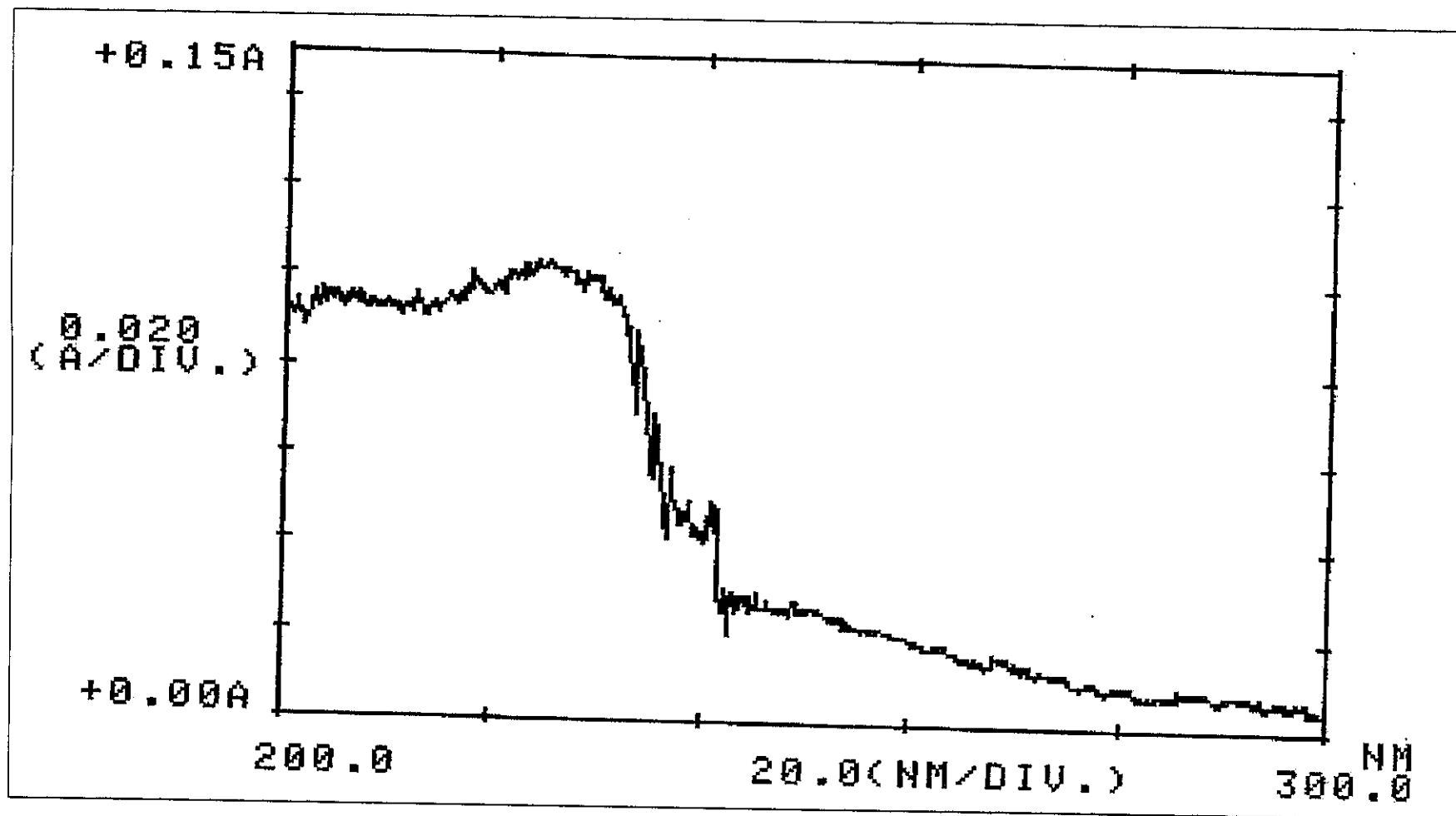


Figure 48 UV spectrum (CHCl_3) of disodium complex of macrocyclic ligand $\text{L}^{11\text{b}}$

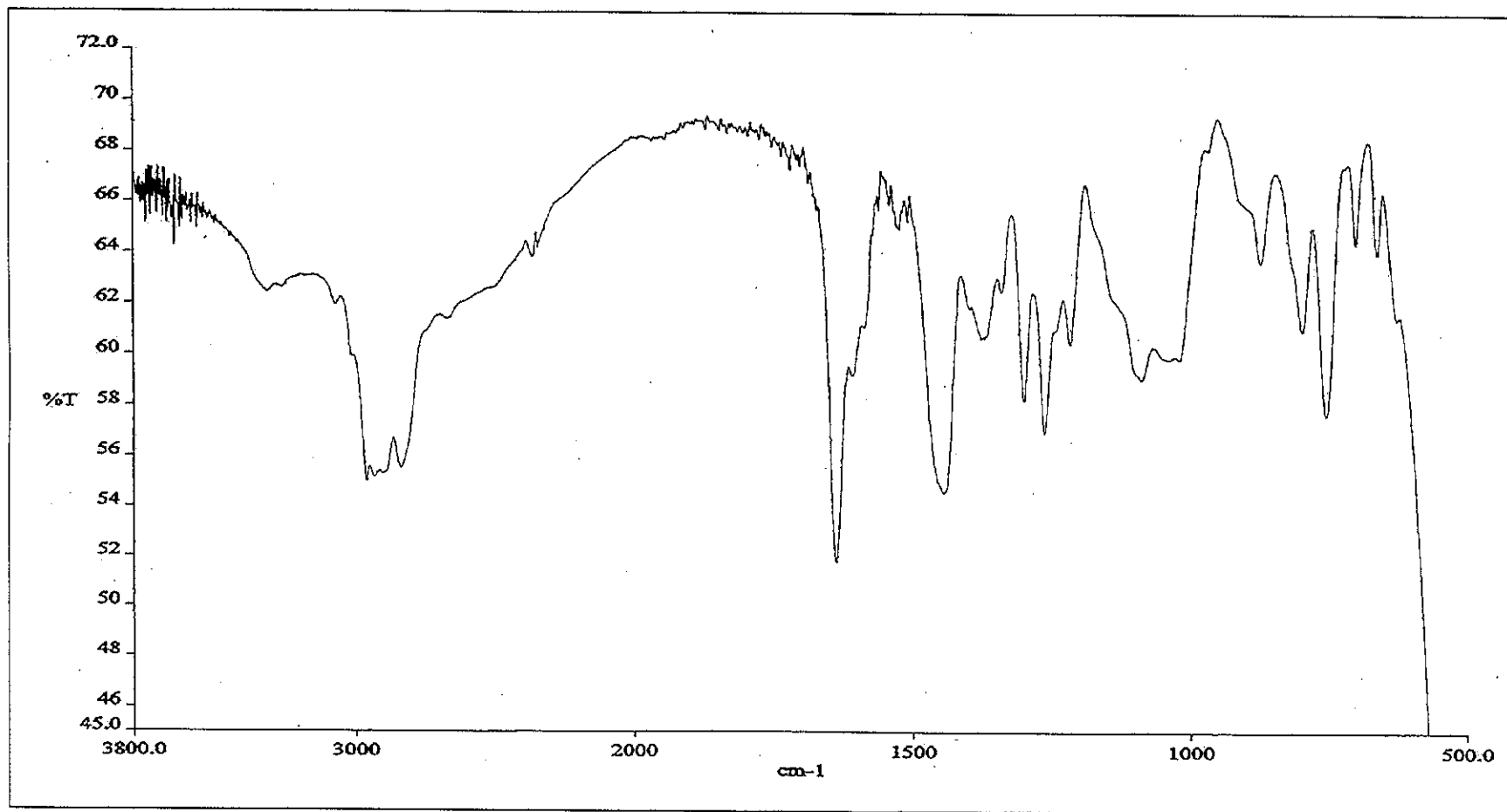


Figure 49 FTIR spectrum (neat) of disodium complex of macrocyclic ligand L^{11b}

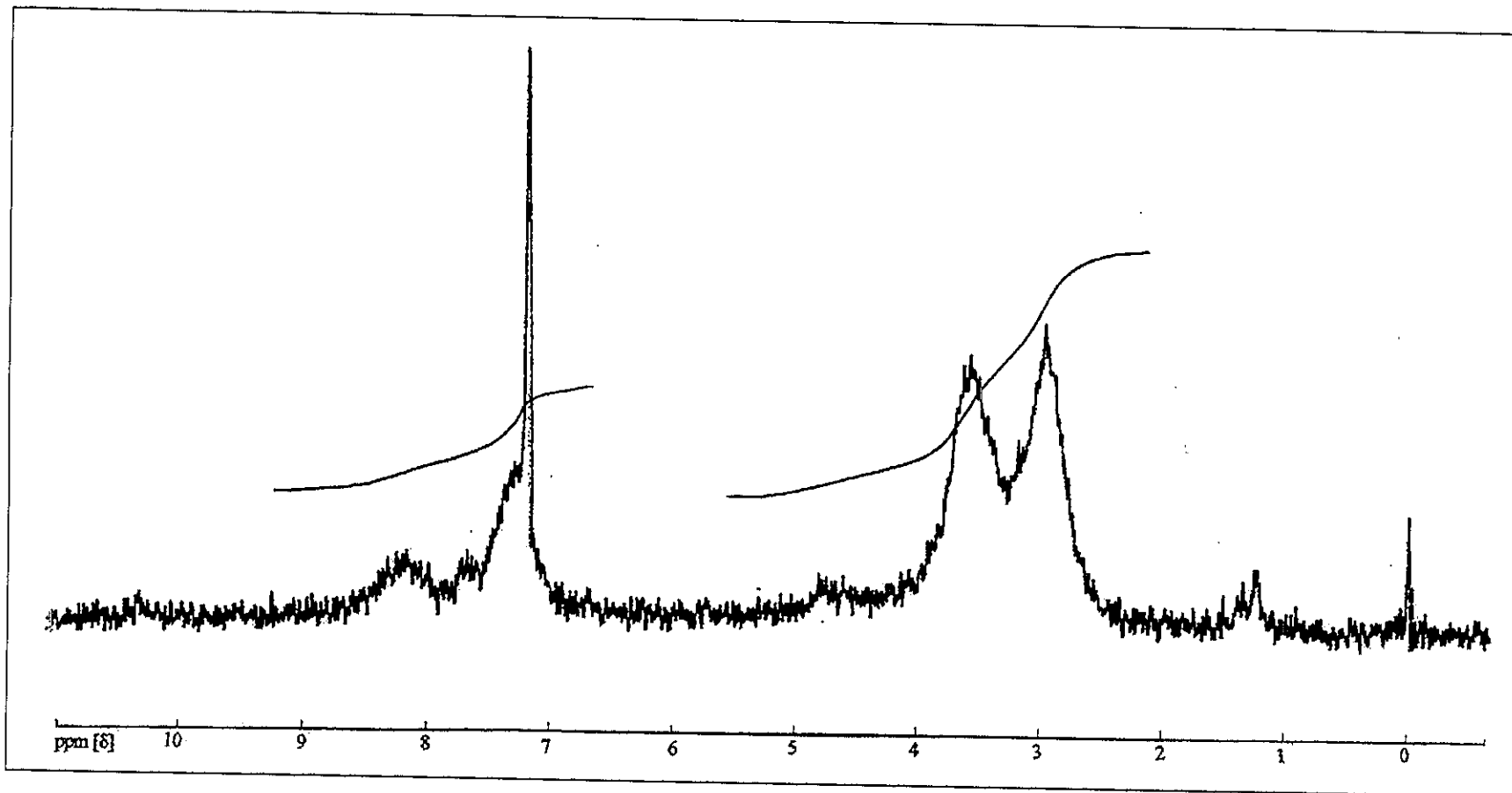


Figure 50 ^1H NMR spectrum (CDCl_3) of disodium complexes of macrocyclic ligand $\text{L}^{11\text{b}}$

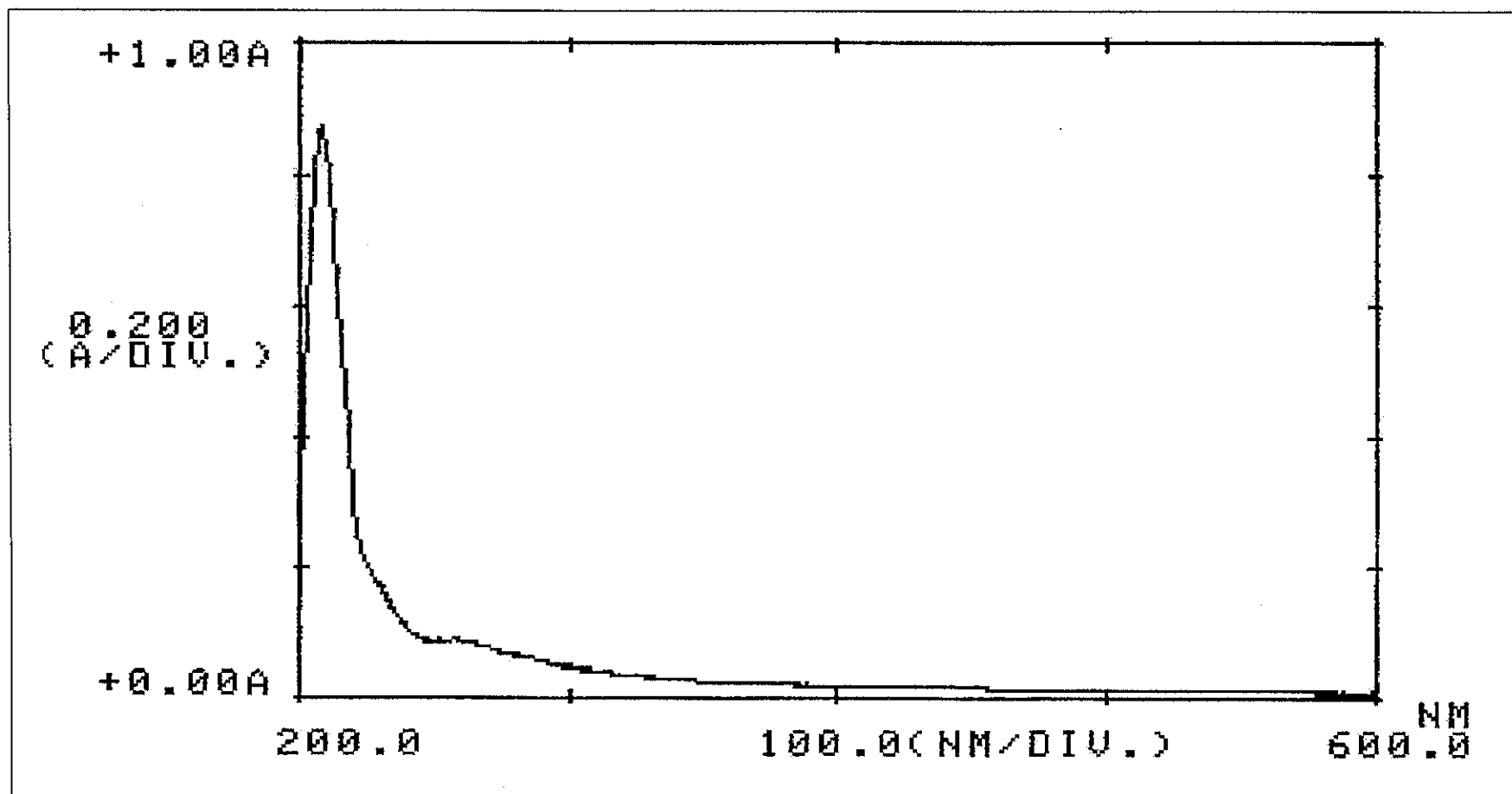


Figure 51 UV spectrum (CH₃OH) of N³-(benzyl)diethylenetriamine-trihydrochloride (14)

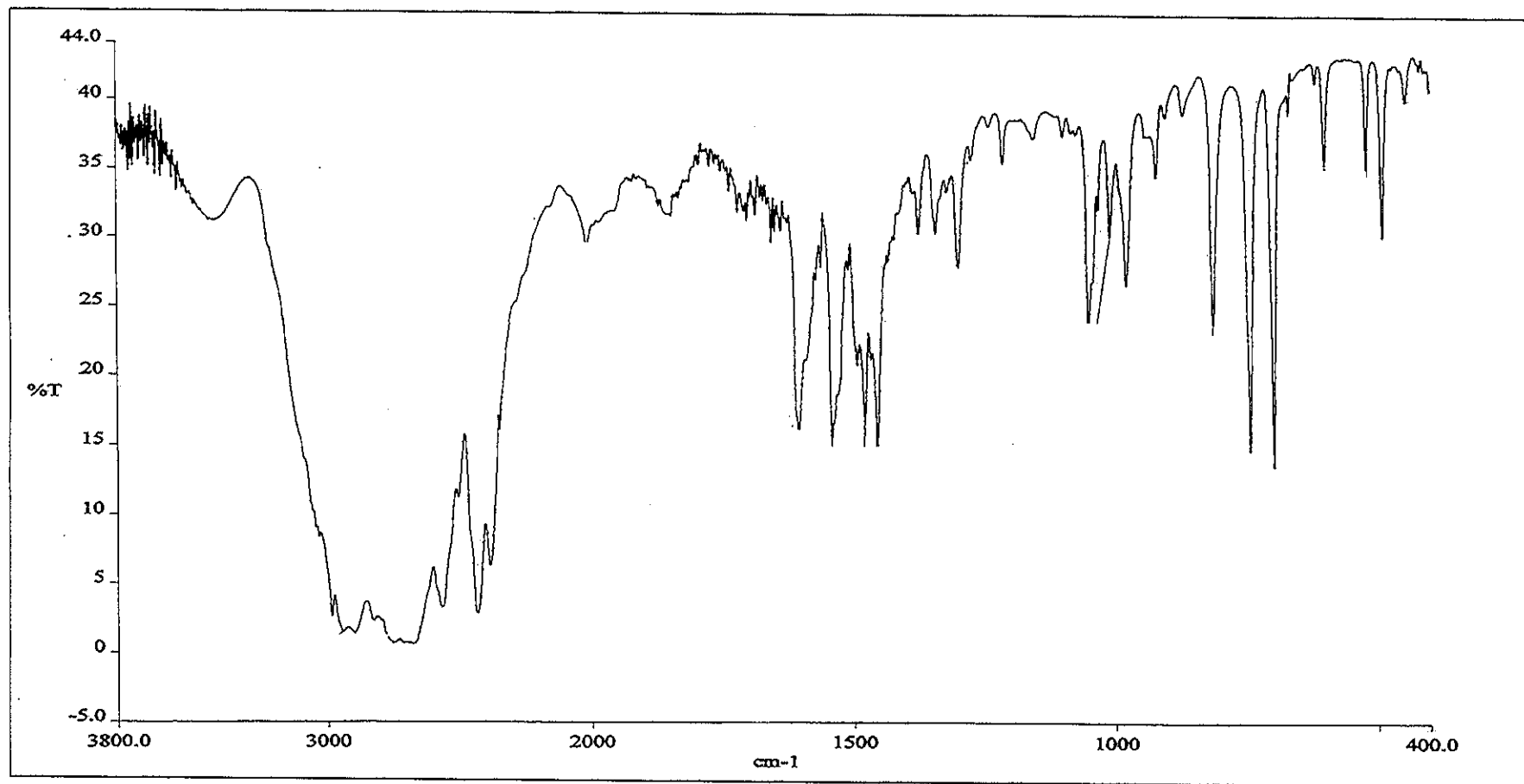


Figure 52 FTIR spectrum (KBr pellets) of N³-(benzyl)diethylenetriamine-trihydrochloride (14)

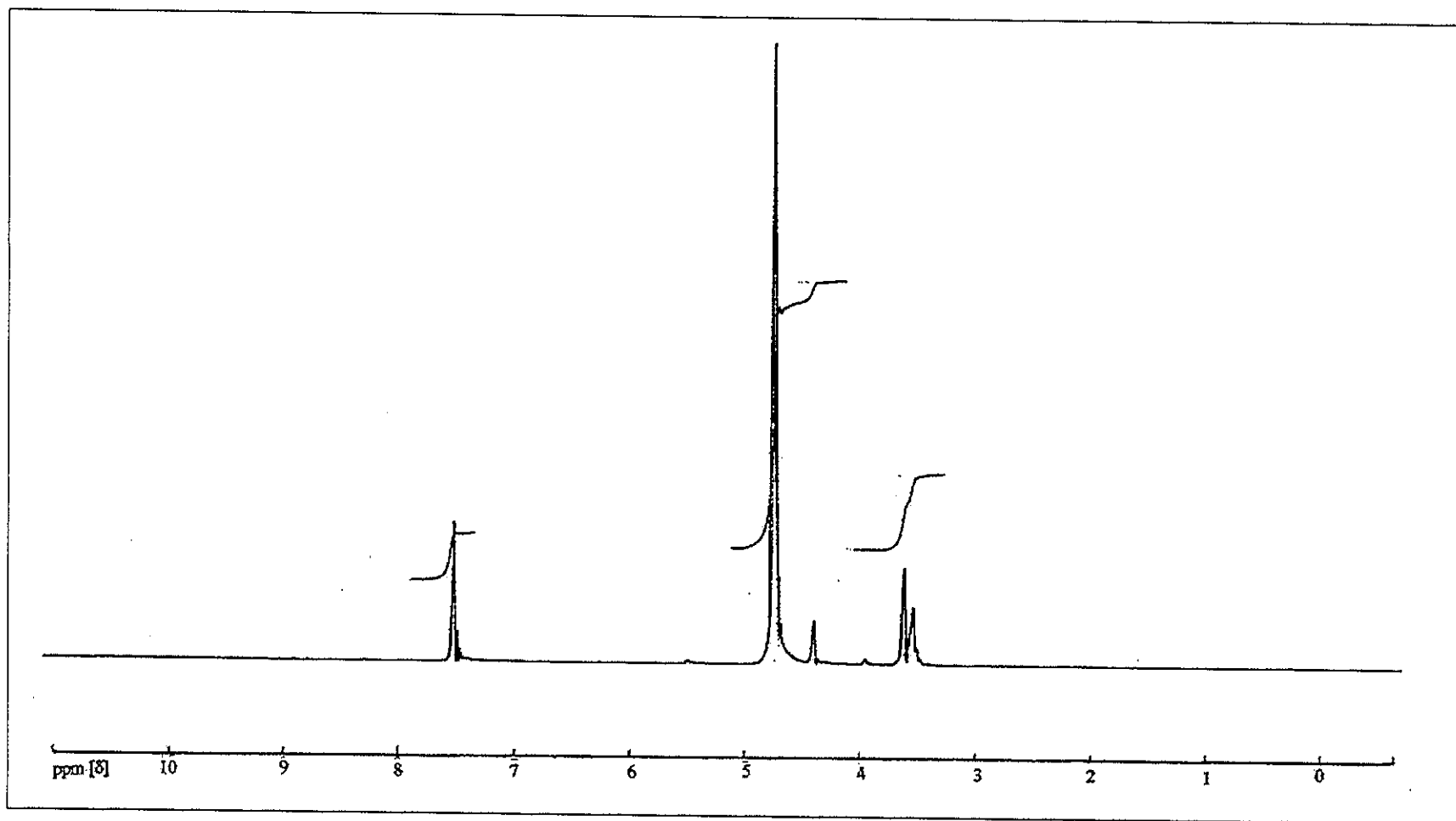


Figure 53 ^1H NMR spectrum (D_2O) of N^3 -(benzyl)diethylenetriamine-trihydrochloride (14)

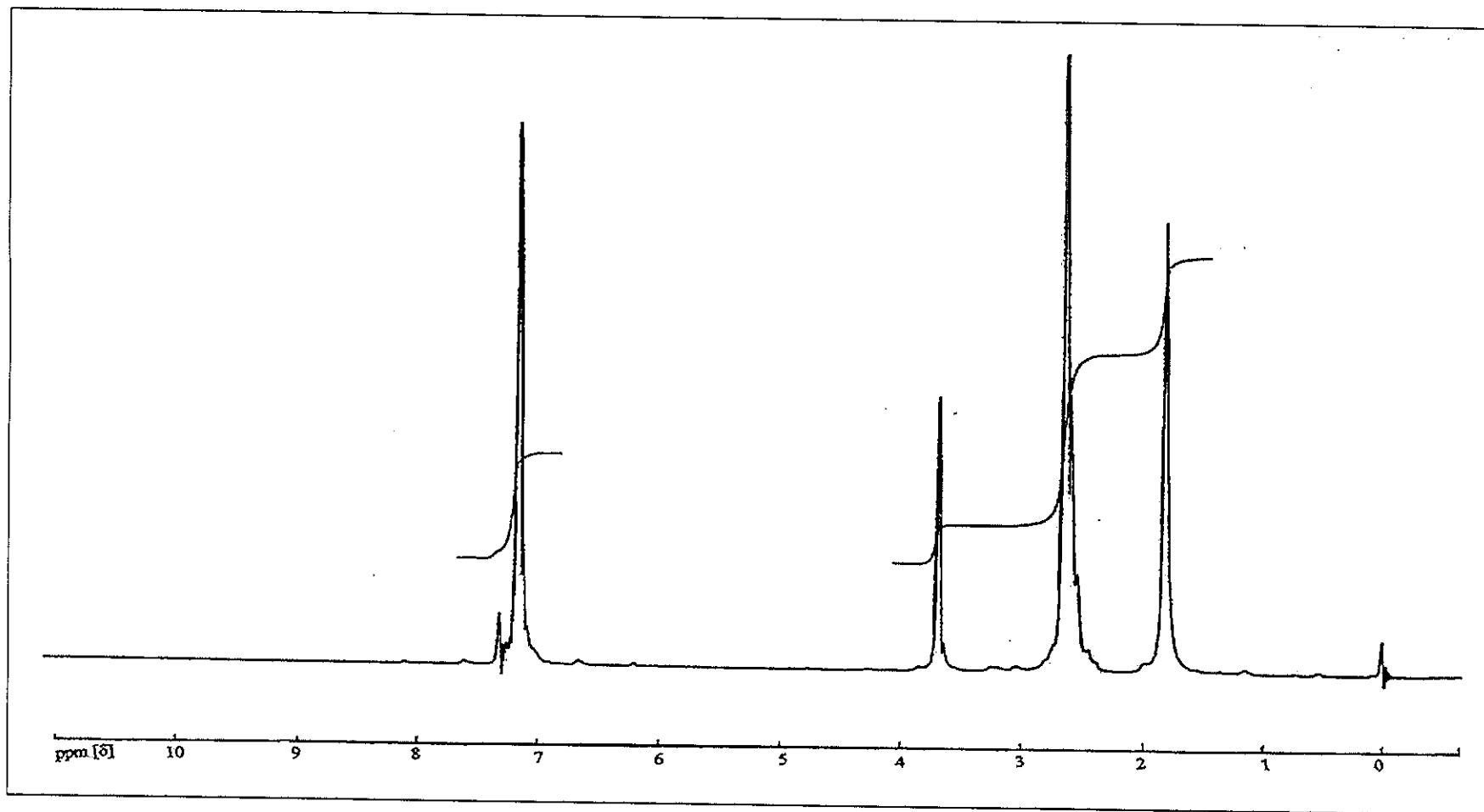


Figure 54 ¹H NMR spectrum (CDCl₃) of N³-(benzyl)diethylenetriamine (14')

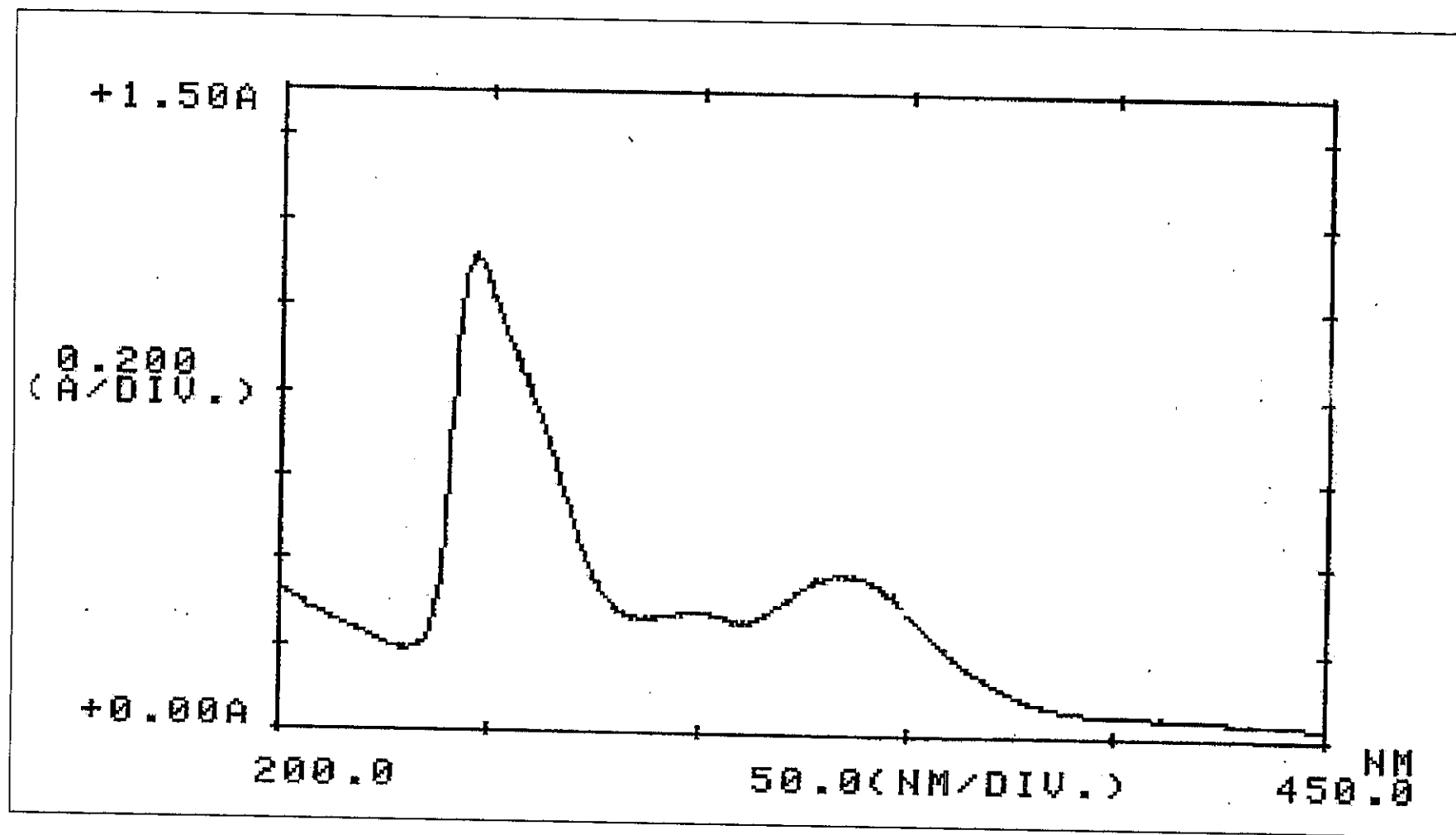


Figure 55 UV spectrum (CHCl₃) of disodium complex of macrocyclic ligand L¹²

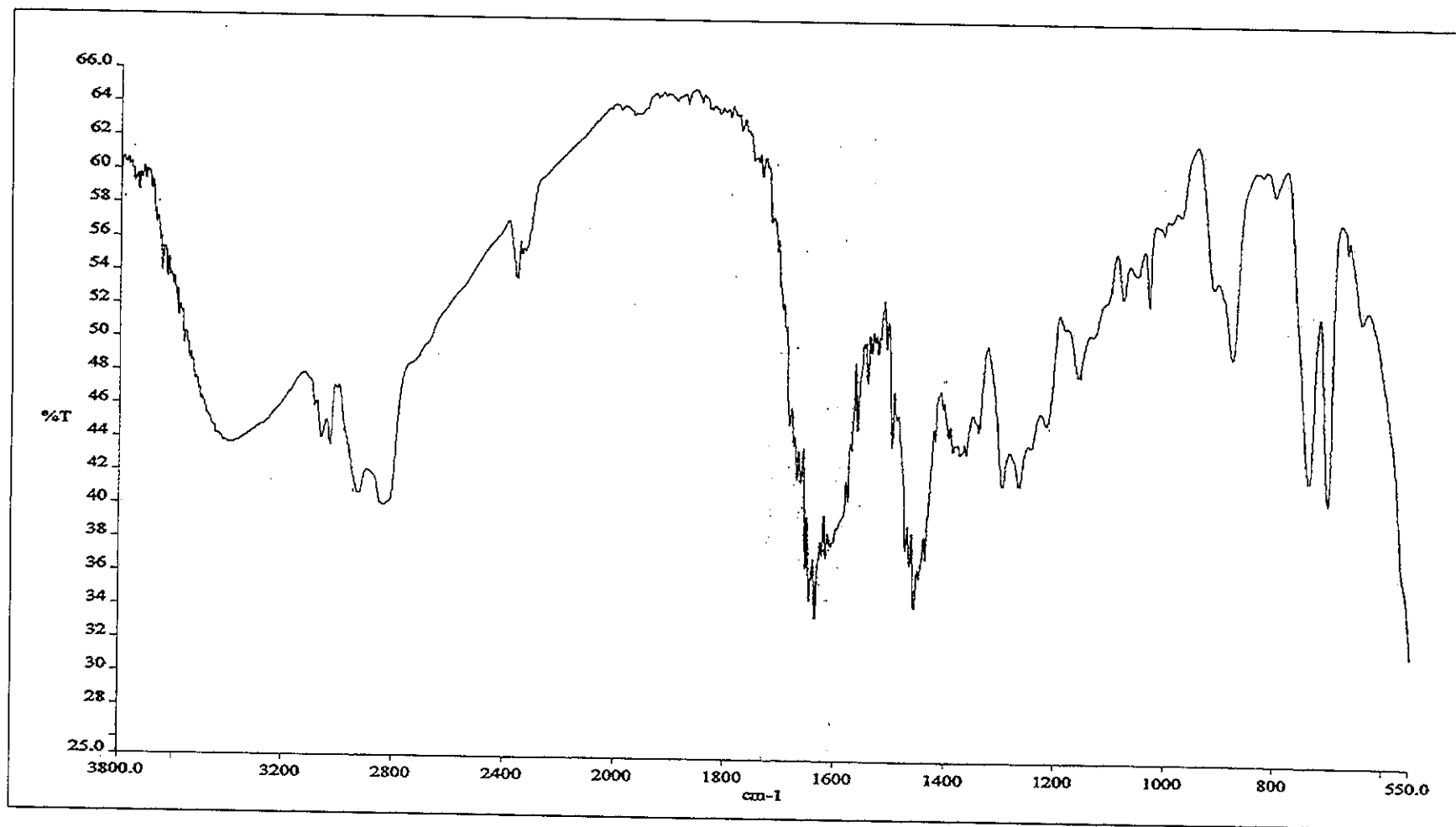


Figure 56 FTIR spectrum (neat) of disodium complex of macrocyclic ligand L¹²

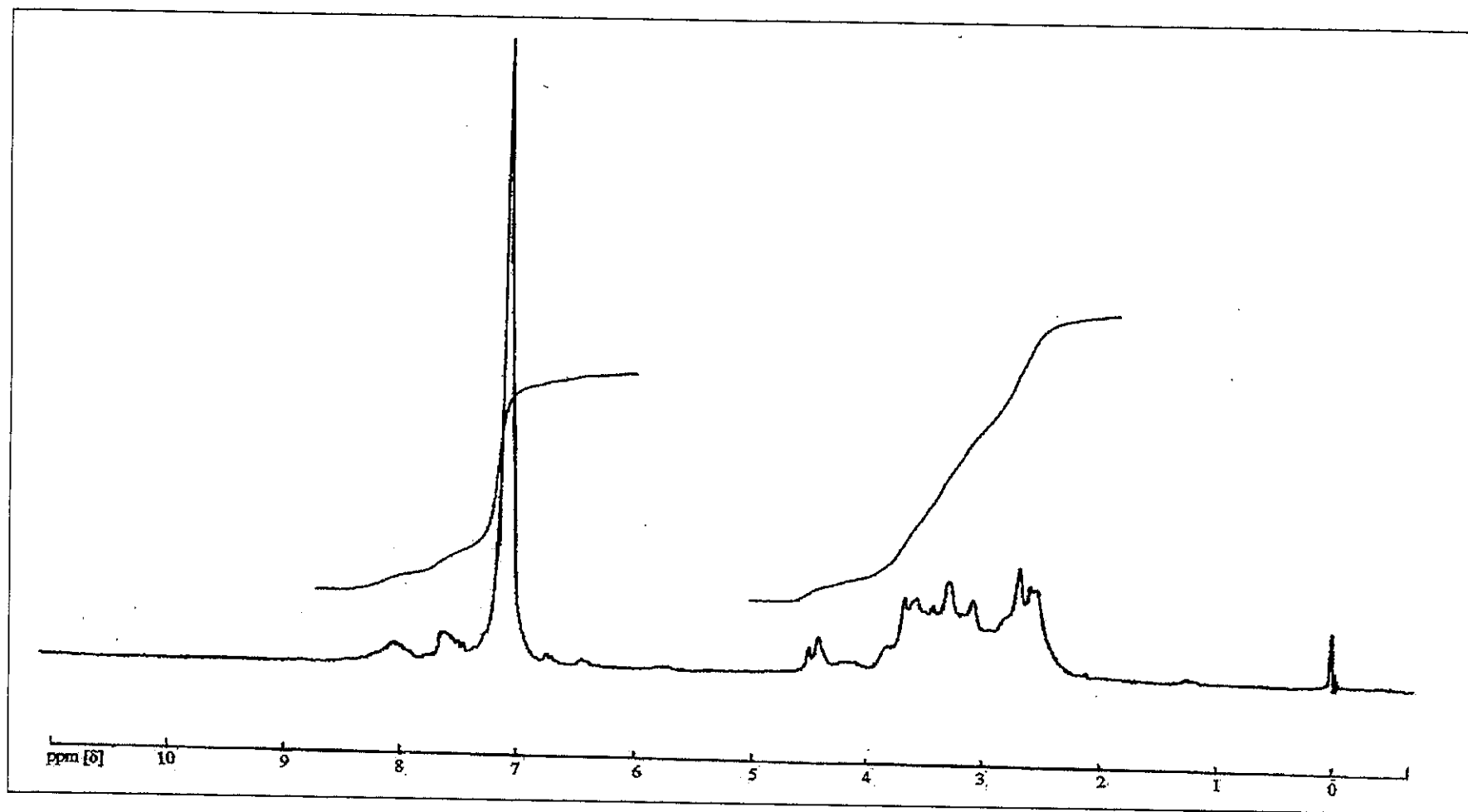


Figure 57 ^1H NMR spectrum (CDCl_3) of disodium complexes of macrocyclic ligand L^{12}

VITAE

Name Miss Wanida Wongratchasee

Birth Date 29 April 1976

Place of Birth Songkhla, Thailand

Education Attainment

Degree	Name of Institution	Year of Graduate
B. Sc. (Education)	Prince of Songkla University	1999

Scholarship Awards during Enrolment

The Higher Development Project : Postgraduate Education and Research Program in Chemistry, funded by The Royal Thai Government (PERCH).